ISSN: 2708-7956

الأكاديمية
للهندسة والعلوم

Academic
For Engineering and Science

رقم الإيداع في الدار الوطنية
2422 لسنة 2020

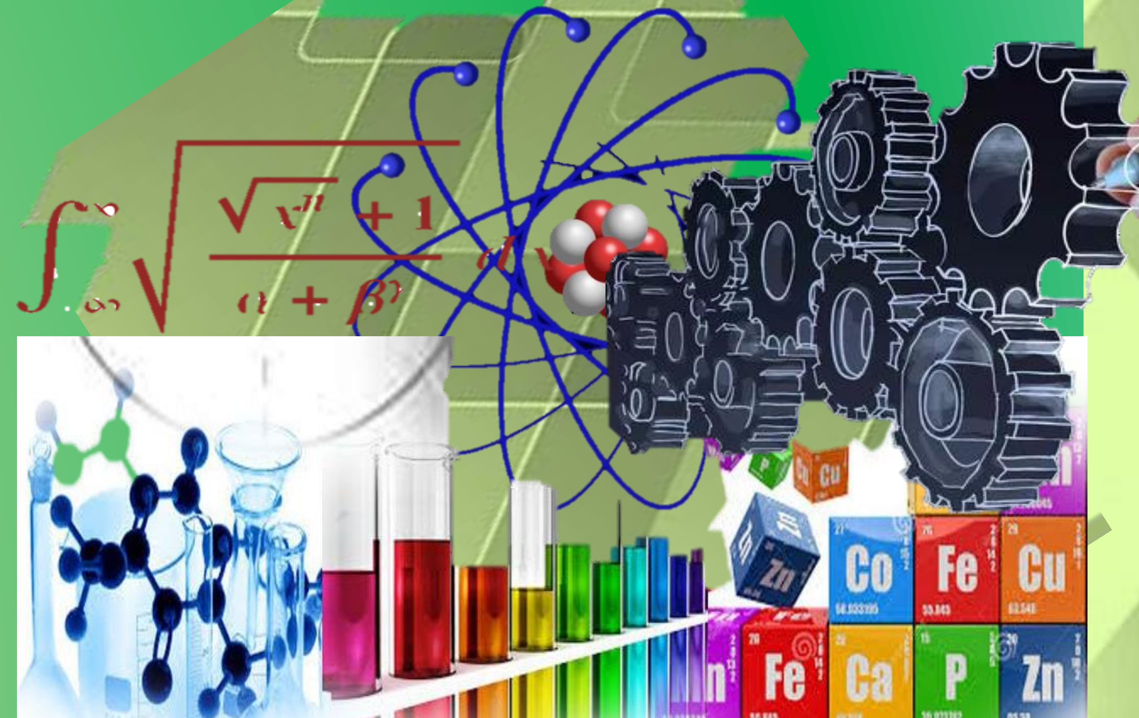

مجلة علمية محكمة فصلية
تصدر عن نقابة الأكاديميين العراقيين

المجلد (5) العدد (2)
آيـــار - السنة 2023

الأكاديمية ... للهندسة والعلوم
http://aphjournal.iraqiacademic.com
ISSN: 2708-7956 DOI prefix: 10.47719

الأكاديمية

للهندسة والعلوم

Academic

For Engineering and Science

مجلة علمية محكمة فصلية

تصدر عن نقابة الأكاديميين العراقيين

المجلد (5) العدد (2)

آيـــار/ 2023

هيئة التحرير

الهيئة الاستشارية

كـــلمة العدد (2) لسنة (2023)

يسعدنا ان نقدم لكم **العدد الثاني/ السنة 2023** لمجلة **الأكـاديـمـية للهندسة والعلوم**. أود أن اسجل شكري الجزيل للجهود الكبيرة لكل من ساهم في إظهار هذا العدد. كما أتقدم بالشكر لجميع الباحثين الذين دعموا المجلة من خلال نشر أبحاثهم فيها، خاصاً بعد حصول المجلة على الرقم المعرّف **DOI** في عام 2020.

ضم هذا العدد، بحوث في مختلف المجالات العلمية، هي: الهندسة، والفيزياء، والاستشعار عن بعد، التحليل الإحصائي والرياضيات.

نأمل أن تحقق مجلة الأكاديمية للهندسة والعلوم، من خلال هذه الطبعة، تطلعات الباحثين والمهتمين، وأن نسعى، بعون الله تعالى، إلى تطوير مجلتنا نحو الأفضل، وأن يكون لها حضورا علميا متميزا إقليمياً وعالمياً، ونتطلع ان تكون المجلة في التصنيفات العلمية الدولية.

مع خالص التقدير

أ. د. أحمد كمال أحمد
رئيس هيئة التحرير
آيـــار - 2023

نبـــــذة عن
نقابة الاكاديميين العراقيين

أسست نقابة الأكاديميين العراقيين بموجب القانون رقم (61) لسنة (2017)، بغية الاهتمام بالملاك التدريسي والأكاديمي (الأكاديمي: التدريسي الحاصل على شهادة الماجستير أو الدكتوراه ويمارس مهنة التدريس أو يعمل بمراكز البحث العلمي في الجامعات).
والارتقاء بمستوى العاملين في هذا القطاع الحيوي وإعداد الخطط والسياسات التي ترتقي بالعملية التدريسية ومن أجل إنشاء مجالس ونقابات تهتم بشؤون الأكاديميين والدفاع عنهم وحفظ كرامتهم وضمان حرياتهم الأكاديمية، ومن أجل رفع سمعة الجامعات والمعاهد العراقية ومساواتها مع مثيلاتها في الدول المتحضرة. ووفقاً للمادة -2- من البند الثاني من قانونها فأنها:

أولاً: تتمتع نقابة الأكاديميين العراقيين بالشخصية المعنوية والاستقلال المالي والإداري يمثلها (نقيب الأكاديميين العراقيين) أو من يخوله.

ثانياً: يكون مركز النقابة في بغداد ولها فتح فروع في المحافظات وحيثما تقتضي مصلحة النقابة إيجاد تمثيل.

ثالثاً: لأعضاء الهيئات التدريسية في الجامعات والمعاهد العراقية المعترف بها من وزارة التعليم العالي والبحث العلمي الانتماء إلى النقابة.

ووفقاً للمادة -3- فأن أهداف تأسيس النقابة هي:

أولاً: الارتقاء بمهنة التعليم العالي والبحث العلمي لتحقيق رسالتها في خدمة الوطن وأجيال الأمة.

ثانياً: التنسيق والتعاون مع وزارة التعليم العالي والبحث العلمي والجهات ذات الصلة بما يحقق مهام النقابة.

ثالثاً: تعزيز أخلاقيات مهنة التعليم العالي والمحافظة على آداب وتقاليد وشرف المهنة.

رابعاً: تشجيع الدراسات والبحوث والنشاطات والمؤتمرات التعليمية وعقد الدورات والندوات لرفع المستوى العلمي والمهني لتدريسي الجامعات والمعاهد العراقية.

خامساً: تعزيز مكانة الأكاديميين في المجتمع والدفاع عن حقوقهم ومصالحهم وكرامتهم.

سادساً: النهوض والارتقاء بالأعضاء مهنياً واقتصاديا وثقافياً واجتماعياً.

سابعاً: تأسيس صندوق للتكافل الاجتماعي لمساعدة أعضاء النقابة، يؤمن لهم ولأسرهم العيش الكريم في حالات العجز الكامل أو الوفاة وتوفير الرعاية الصحية للأعضاء وأسرهم.

ثامناً: التعاون وتوطيد العلاقات مع الاتحادات العربية والدولية المماثلة.

أ. م. د. مهـنـد الهـلال
نقيب الاكاديميين العراقيين

المحتوى (العدد 2 لسنة 2023)

أهداف ورؤية المجلة Aims and Scope

- تنشر المجلة الدراسات العلمية ذات الأفكار الأصيلة والحديثة والمتجددة، وبحوث الرسائل والأطروحات، التي لم يسبق نشرها أو المساهمة بها في أحد الملتقيات العلمية، وان تكون هذه البحوث مندرجة ضمن أحد المحاور تخصصات الهندسية والعلوم الصرفة.
- كما تنشر المجلة الكتب المؤلفة والمترجمة ضمن التخصصات أعلاه.

الوصول المفتوح للبحوث Open Access Policy

مجلة **الأكاديمية للهندسة والعلوم** هي مجلة مفتوحة الوصول، بالتالي لا توجد رسوم مطلوبة لتنزيل أي منشور من موقع المجلة من قبل المؤلفين والقراء والمؤسسات، وعلى الموقع:
http://aphjournal.iraqiacademic.com/Journal/GetAllVersions

قواعد النشر:

- البحوث المرسلة إلى المجلة يجب أن تكون سليمة من الأخطاء اللغوية والمنهجية والمعرفية، وملتزمة بالأعراف العلمية المتبعة، ولم يسبق نشرها.
- لا ينبغي أن يتجاوز عدد صفحات البحث عن خمسة عشر ورقة من حجم B5.
- في حالة وجود هوامش في اسفل الصفحة ينبغي اعتماد ترقيم آلي يتجدد في كل صفحة.
- يتضمن البحث ملخصين: الأول بلغة البحث، والثاني باللغة العربية أو الإنجليزية.
- تخضع جميع البحوث للتحكيم العلمي على نحو سري، ويخبر الباحث إما بقبول بحثه، أو بالقبول المشروط ببعض التعديلات التي يبلغ بها، أو بالرفض. وفي هذه الحالة الأخيرة؛ فإن المجلة ليست ملزمة ببيان الأسباب.

توصيات تقنية في كتابة البحوث:

- مقاس الورقة والهوامش: الورقة حجم B5، ويترك هامش بمسافة 2 سم من حواشي الورقة. مع مسافة 1 سم بين الأسطر في المتن والهوامش.
- يُعتمد الخط **Simplified Arabic** (البحوث باللغة العربية)/ و**Times New Roman** (البحوث باللغة الإنكليزية)، مقاس 16 غامق عنوان البحث، مقاس 14 غامق العناوين الأساسية، مقاس 12 غامق العناوين الفرعية، وبمقاس 12 في المتن، مقاس 11 غامق لعناوين الأشكال والجداول، 10 في الحواشي.

معلومات الاتصال:

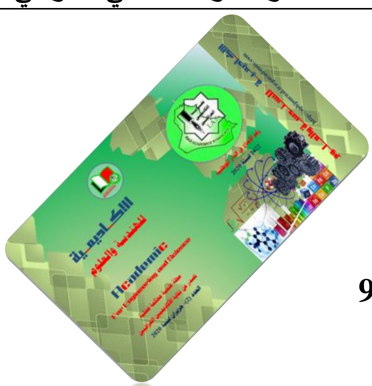

- موقع المجلة: http://aphjournal.iraqiacademic.com/

ISSN: 2708-7956, DOI prefix: 10.47719

- البريد الإلكتروني للمجلة: info@iraqiacademics.iq
dr.ziadmabood@gmail.com

- أرقام الهواتف: 9647709298631- 9647902746409
- رقم الإيداع في الدار الوطنية 2422 لسنة 2020

Academic J. for Engineering and Science
ISSN: 2708-7956, vol. 5, No. 2, 2023

المجلة الأكاديمية... للهندسة والعلوم
المجلد 5 العدد 2، آيار لسنة 2023

On$(\mathfrak{T}_i, \mathfrak{T}_j)-$ Generalized gs-Closed Sets in Bitopological Spaces

Bushra Jaralla Tawfeeq
Collage of Education, Mustansiriyah University, Baghdad, Iraq

Abstract

In this paper, we introduce a class of closed sets in bitopological spaces that we call generalized gs-closed (briefly, $(\mathfrak{T}_i, \mathfrak{T}_j)$–ggs-closed) sets. We study some of their basic properties and investigate their relationship with the other types of closed sets in such spaces. As an application of this work, we also define two new spaces, namely $(\mathfrak{T}_i, \mathfrak{T}_j)$–$T_{ggs}$- and $(\mathfrak{T}_i, \mathfrak{T}_j)$–$T^{\#}_{ggs}$-spaces, and present several applications.

1. Introduction

A triple $(\mathfrak{B}, \mathfrak{T}_i, \mathfrak{T}_j)$, where $\mathfrak{B}$ is a nonempty set and $\mathfrak{T}_i$ and $\mathfrak{T}_j$ are topologies on $\mathfrak{B}$, is called a bitopological space. Kelly [9] initiated the study of such spaces in 1963. Later, in 1985, Fukutake [3] introduced and studied the notions of generalized closed (briefly, g-closed) sets in such spaces. More recently, Fukutake, Sundaram, and Sheikh John [5] introduced the concept of w-closed sets, while El-Tantawy and Abu-Donia [2] proposed the idea of generalized semi-closed (briefly, gs-closed) sets. Then, Veerakumar [21,22] introduced and studied the concepts of g*-semi-closed (briefly, g*-sclosed) sets, gs^*-continuity, and gs^*-irresolute maps in topological spaces.

In 2007, Jafara, Lellis Thivagar, and Thisaya Ponmani [8] studied some new separation axioms using (1,2)–α-open sets in bitopological spaces. Maragathavalli [19] then defined strongly αg*-closed sets in topological spaces and also investigated some of their properties.

In §2, we introduce some basic definitions and other preliminaries.

In §3, we present the elementary properties of generalized gs-closed (briefly, $(\mathfrak{T}_i, \mathfrak{T}_j)$−ggs-closed) sets, and also study their relationships to other types of closed sets, namely $(\mathfrak{T}_i, \mathfrak{T}_j)$−g, $(\mathfrak{T}_i, \mathfrak{T}_j)$−w, $(\mathfrak{T}_i,\mathfrak{T}_j)$−αg, $(\mathfrak{T}_i, \mathfrak{T}_j)$−gα, $(\mathfrak{T}_i,\mathfrak{T}_j)$−pre, $(\mathfrak{T}_i, \mathfrak{T}_j)$−gs, $(\mathfrak{T}_i, \mathfrak{T}_j)$−sg, $(\mathfrak{T}_i, \mathfrak{T}_j)$ −β, $(\mathfrak{T}_i, \mathfrak{T}_j)$−gsp-, $(\mathfrak{T}_i, \mathfrak{T}_j)$−gp-, (1,2)*–#πgs-, $(\mathfrak{T}_i, \mathfrak{T}_j)$–$sg^*b$-, $(\mathfrak{T}_i, \mathfrak{T}_j)$–pgb-, $(\mathfrak{T}_i, \mathfrak{T}_j)$–g**b-, and $(\mathfrak{T}_i, \mathfrak{T}_j)$−rg**b-closed sets. We also provide several related results and some necessary examples.

In §4, we present several properties and characterizations of $(\mathfrak{T}_i, \mathfrak{T}_j)$−ggs-closed and $(\mathfrak{T}_i, \mathfrak{T}_j)$− ggs-open sets.

Finally, in §5, we provide some applications of $(\mathfrak{T}_i, \mathfrak{T}_j)$−ggs-closed sets.

2. Preliminaries

If A is a subset of a topological space $\mathfrak{B}$ with a topology $\mathfrak{T}$, then the closure of A is denoted by $\mathfrak{T}$–cl(A) (or just cl(A)), its interior by $\mathfrak{T}$–int(A) (or int(A)), and its semi- and pre-closures by $\mathfrak{T}$–scl(A) and $\mathfrak{T}$–pcl(A) (or scl(A) and pcl(A)), respectively. In addition, its semi-interior is denoted by $\mathfrak{T}$–sint(A) (or sint(A)), and its complement by A^c.

Before discussing our main results, we recall the following definitions:

Definition 2.1. A subset A of a topological space $(\mathfrak{B}, \mathfrak{T})$ is called:
1) an α-open set [12] if $A \subseteq int(cl(int(A)))$,
2) a semi-open set [10] if $A \subseteq cl(int(A))$,
3) a pre-open set [12] if $A \subseteq int(cl(A))$,
4) a semi-pre-open (briefly, β-open) set [12] if A ⊆ cl(int(cl(A))))), and
5) a regular open set [6] if $A = int(cl(A))$.

The semi-closure [13] (resp. α-closure [14]) of a subset A of 𝔅, denoted by scl(A) (resp. αcl(A)) is defined as the intersection of all semi-closed (resp. α-closed) sets containing A. The semi-interior [13] of A, denoted by sint(A), is defined as the union of all semi-open sets contained in A. If A ⊆ B ⊆ 𝔅, then $cl_B(A)$ and $int_B(A)$ denote the closure of A relative to B and the interior of A relative to B, respectively.

Definition 2.2. If (𝔅, 𝔗) is a topological space and A is a subset of 𝔅, then A is called

1) a generalized closed (briefly, g-closed) set [12] if cl(A) ⊆ U whenever A ⊆ U and U is open in 𝔅,
2) a generalized α-closed (briefly, gα-closed) set [14] if αcl(A) ⊆ U whenever A ⊆ U and U is α-open in 𝔅,
3) an α-generalized closed (briefly, αg-closed) set [14] if αcl(A) ⊆ U whenever A ⊆ U and U is open in 𝔅,
4) a semi-generalized closed (briefly, sg-closed) set [13] if scl(A) ⊆ U whenever A ⊆ U and U is semi-open in 𝔅,
5) a generalized semi-closed (briefly, gs-closed) set [13] if scl(A) ⊆ U whenever A ⊆ U and U is open in 𝔅,
6) a w-closed set [18] if cl(A) ⊆ U whenever A ⊆ U and U is semi-open in 𝔅,
7) a generalized semi-pre-closed (briefly, gsp-closed) set [6] if spcl(A) ⊆ U whenever A ⊆ U and U is open in 𝔅,
8) a generalized pre-closed (briefly, gp-closed) set [6] if pcl(A) ⊆ U whenever A ⊆ U and U is open in 𝔅,
9) a generalized gs-closed (briefly, ggs-closed) set [7] if cl(A) ⊆ U whenever A ⊆ U and U is gs-open in 𝔅.
10) a g**b-closed set [16] if bcl(A) ⊆ U whenever A ⊆ U and U is g*-open in 𝔅,
11) a pre-generalized b-closed (briefly, pgb-closed) set [17] if bcl(A) ⊆ U whenever A ⊆ U and U is pre-open in 𝔅, and
12) a semi-generalized star b-closed (briefly, sg^*b-closed) set [18] if bcl(A) ⊆ U whenever A ⊆ U and U is semi-open in 𝔅.

The complements of the above-mentioned sets are known as the corresponding open sets.

Definition 2.3. A subset A of a bitopological space $(𝔅, \mathfrak{T}_i, \mathfrak{T}_j)$ is called

1) an $(\mathfrak{T}_i, \mathfrak{T}_j)$−g-closed set [3] if $\mathfrak{T}_j$−cl(A) ⊆ U whenever A ⊆ U and U ∈ $\mathfrak{T}_i$,
2) an $(\mathfrak{T}_i, \mathfrak{T}_j)$−gs-closed set [2] if $\mathfrak{T}_j$−scl(A) ⊆ U whenever A ⊆ U and U ∈ $\mathfrak{T}_i$,
3) an $(\mathfrak{T}_i, \mathfrak{T}_j)$−weakly-generalized-closed set [4] ($(\mathfrak{T}_i, \mathfrak{T}_j)$−wg-closed) if $\mathfrak{T}_j$−cl($\mathfrak{T}_i$−int (A)) ⊆ U whenever A ⊆ U and U ∈ $\mathfrak{T}_i$,
4) an $(\mathfrak{T}_i, \mathfrak{T}_j)$–w-closed set [5] if $\mathfrak{T}_j$–cl(A) ⊆ U whenever A ⊆ U and U is $\mathfrak{T}_i$–semi-open in 𝔅,
5) an $(\mathfrak{T}_i, \mathfrak{T}_j)$−g*-closed set [5] if $\mathfrak{T}_j$−cl(A) ⊆ U whenever A ⊆ U and U is a $\mathfrak{T}_i$−g-open set,
6) an $(\mathfrak{T}_i, \mathfrak{T}_j)$−αg-closed set [10] if $\mathfrak{T}_j$−αcl(A) ⊆ U whenever A ⊆ U and U is $\mathfrak{T}_i$−open in 𝔅,
7) an $(\mathfrak{T}_i, \mathfrak{T}_j)$−gα-closed set [10] if $\mathfrak{T}_j$–αcl(A) ⊆ U whenever A ⊆ U and U is $\mathfrak{T}_i$−α-open in 𝔅,
8) an $(\mathfrak{T}_i, \mathfrak{T}_j)$–rg**-closed set [15] if $\mathfrak{T}_j$–cl($\mathfrak{T}_i$–int(A)) ⊆ U whenever A ⊆ U and U is $(\mathfrak{T}_i, \mathfrak{T}_j)$–regular-open in 𝔅,
9) a (1,2)*-#πgs-closed set [20] if $\mathfrak{T}_i\mathfrak{T}_j$–scl(A) ⊆ U whenever A ⊆ U and U is (1,2)*-πgb-open in 𝔅, and

10) an ($\mathfrak{T}_i$, $\mathfrak{T}_j$)− rg**b-closed set [15] if $\mathfrak{T}_j$–rg*cl(A) ⊆ U whenever A ⊆ U and U is $\mathfrak{T}_i$−open in $\mathfrak{B}$.

The families of all ($\mathfrak{T}_i$, $\mathfrak{T}_j$)−g-, ($\mathfrak{T}_i$, $\mathfrak{T}_j$)−gs-, ($\mathfrak{T}_i$, $\mathfrak{T}_j$)−wg-, ($\mathfrak{T}_i$, $\mathfrak{T}_j$)–w-, ($\mathfrak{T}_i$, $\mathfrak{T}_j$)−g*-, ($\mathfrak{T}_i$, $\mathfrak{T}_j$)−αg-, ($\mathfrak{T}_i$, $\mathfrak{T}_j$)−gα-, ($\mathfrak{T}_i$, $\mathfrak{T}_j$)–rg**-, (1,2)*- #πgs-, and ($\mathfrak{T}_i$, $\mathfrak{T}_j$)− rg**b-closed subsets of a bitopological space ($\mathfrak{B}$, $\mathfrak{T}_i$, $\mathfrak{T}_j$) are denoted by D($\mathfrak{T}_i$, $\mathfrak{T}_j$), GSC($\mathfrak{T}_i$, $\mathfrak{T}_j$), W($\mathfrak{T}_i$, $\mathfrak{T}_j$), C($\mathfrak{T}_i$, $\mathfrak{T}_j$), D*($\mathfrak{T}_i$, $\mathfrak{T}_j$), αG($\mathfrak{T}_i$, $\mathfrak{T}_j$), Gα($\mathfrak{T}_i$, $\mathfrak{T}_j$), D*rg**($\mathfrak{T}_i$, $\mathfrak{T}_j$), (1, 2)*–#πGSC($\mathfrak{B}$), and D*rg**b($\mathfrak{T}_i$, $\mathfrak{T}_j$), respectively.

Definition 2.4. A bitopological space ($\mathfrak{B}$, $\mathfrak{T}_i$, $\mathfrak{T}_j$) is called
1) an ($\mathfrak{T}_i$, $\mathfrak{T}_j$)−$T_{1/2}$-space [2] if every ($\mathfrak{T}_i$, $\mathfrak{T}_j$)−g-closed set is $\mathfrak{T}_j$–closed,
2) an ($\mathfrak{T}_i$, $\mathfrak{T}_j$)−T_w-space [4] if every ($\mathfrak{T}_i$, $\mathfrak{T}_j$)−w-closed set is $\mathfrak{T}_j$–closed, and
3) an ($\mathfrak{T}_i$, $\mathfrak{T}_j$)−T_b-space [1] if every ($\mathfrak{T}_i$, $\mathfrak{T}_j$)−gs-closed set is $\mathfrak{T}_j$–closed.

Definition 2.5. A bitopological space ($\mathfrak{B}$, $\mathfrak{T}_i$, $\mathfrak{T}_j$) is called a strongly pairwise $T_{1/2}$–space [2] if it is both a ($\mathfrak{T}_i$, $\mathfrak{T}_j$)–$T_{1/2}$-space and a ($\mathfrak{T}_i$, $\mathfrak{T}_j$)–$T_{1/2}$-space.

3. Properties of ($\mathfrak{T}_i$, $\mathfrak{T}_j$)–ggs-Closed Sets

In this section, we introduce ggs-closed sets in bitopological spaces and study some of their properties.

Definition 3.1. Let $i, j \in \{1, 2\}$ be fixed integers. A subset A of a bitopological space ($\mathfrak{B}$, $\mathfrak{T}_i$, $\mathfrak{T}_j$) is called a generalized gs-closed (briefly, ($\mathfrak{T}_i$, $\mathfrak{T}_j$) −ggs-closed) set if $\mathfrak{T}_j$–cl(A) ⊆ U whenever A ⊆ U and U is gs-open in ($\mathfrak{B}$, $\mathfrak{T}_i$). The family of all ($\mathfrak{T}_i$, $\mathfrak{T}_j$)−ggs-closed sets in a bitopological space ($\mathfrak{B}$, $\mathfrak{T}_i$, $\mathfrak{T}_j$) is denoted by D^*gs($\mathfrak{T}_i$, $\mathfrak{T}_j$).

Remark 3.2. By setting $\mathfrak{T}_1 = \mathfrak{T}_2$ in Definition 3.1, we can see that any (i, j)-ggs-closed set is ggs-closed.

Proposition 3.3. If $\mathcal{K}$ is an $\mathfrak{T}_j$-closed subset of ($\mathfrak{B}$, $\mathfrak{T}_i$, $\mathfrak{T}_j$), then $\mathcal{K}$ is an ($\mathfrak{T}_i$, $\mathfrak{T}_j$)–ggs-closed set, but not conversely.
Proof. Let $\mathcal{K}$ be any $\mathfrak{T}_j$–closed set and U be any $\mathfrak{T}_i$–gs-open set containing $\mathcal{K}$. Then, $\mathfrak{T}_j$–cl($\mathcal{K}$) ⊆ U, so $\mathcal{K}$ is ($\mathfrak{T}_i$, $\mathfrak{T}_j$)−ggs-closed. Example 3.4 demonstrates that the converse is false.

Example 3.4. Let $\mathfrak{B}$ = {a, b, c}, $\mathfrak{T}_i$ = {$\mathfrak{B}$, φ, {b}, {c}, {b,c}}, and $\mathfrak{T}_j$ = {$\mathfrak{B}$, φ,{a,c}}. Then, the set {a} is ($\mathfrak{T}_i$, $\mathfrak{T}_j$)−ggs-closed but not $\mathfrak{T}_j$–closed.

Proposition 3.5. If $\mathcal{H}$ is an $\mathfrak{T}_j$–α-closed or $\mathfrak{T}_j$–semi-closed subset of ($\mathfrak{B}$, $\mathfrak{T}_i$, $\mathfrak{T}_j$), then $\mathcal{H}$ is ($\mathfrak{T}_i$, $\mathfrak{T}_j$)–ggs-closed, but not conversely

Proof. Let $\mathcal{H}$ be any $\mathfrak{T}_j$–closed set and $\mathcal{V}$ be any $\mathfrak{T}_i$–gs-open set containing $\mathcal{H}$. Since every $\mathfrak{T}_j$–closed set is $\mathfrak{T}_j$–α-closed (resp. $\mathfrak{T}_j$–semi-closed),then, $\mathfrak{T}_j$– α cl($\mathcal{H}$) ⊆ $\mathfrak{T}_j$–cl($\mathcal{H}$) ⊆ $\mathcal{V}$ (resp. $\mathfrak{T}_j$–scl($\mathcal{H}$) ⊆ $\mathfrak{T}_j$–cl($\mathcal{H}$) ⊆ $\mathcal{V}$),so $\mathcal{H}$ is ($\mathfrak{T}_i$, $\mathfrak{T}_j$)−ggs-closed. Example 3.6 demonstrates that the converse is false.

Example 3.6. If $\mathfrak{B}$ = {a, b, c}, $\mathfrak{T}_i$= {$\mathfrak{B}$, φ, {b,c}}, and $\mathfrak{T}_j$ = {$\mathfrak{B}$, φ,{b}}, then the set {b,c} is ($\mathfrak{T}_i$, $\mathfrak{T}_j$)−ggs-closed but not $\mathfrak{T}_j$–α-closed or $\mathfrak{T}_j$–semi-closed.

Proposition 3.7. If A is an ($\mathfrak{T}_i$, $\mathfrak{T}_j$)−ggs-closed subset of ($\mathfrak{B}$, $\mathfrak{T}_i$, $\mathfrak{T}_j$), then A is $\mathfrak{T}_j$−g-closed, but not conversely (as Example 3.8 demonstrates).

Example 3.8. If $\mathfrak{B}$ = {a, b, c}, $\mathfrak{T}_i$ = {$\mathfrak{B}$, φ, {b,c}}, and $\mathfrak{T}_j$ = {$\mathfrak{B}$, φ,{b}}, then the set {a,b} is $\mathfrak{T}_j$−g-closed but not ($\mathfrak{T}_i$, $\mathfrak{T}_j$)−ggs-closed.

Proposition 3.9. If $\mathcal{F}$ is an ($\mathfrak{T}_i$, $\mathfrak{T}_j$)−ggs-closed subset of ($\mathfrak{B}$, $\mathfrak{T}_i$, $\mathfrak{T}_j$), then $\mathcal{F}$ is ($\mathfrak{T}_i$, $\mathfrak{T}_j$)−g-closed, but not conversely.
Proof. Let $\mathcal{F}$ be any ($\mathfrak{T}_i$, $\mathfrak{T}_j$)−ggs-closed set and $\mathcal{P}$ be any $\mathfrak{T}_i$–open set. Then, $\mathcal{P}$ is an $\mathfrak{T}_i$–gs-open set such that $\mathcal{F} \subseteq \mathcal{P}$, which implies that $\mathfrak{T}_j$–cl($\mathcal{F}$) ⊆ $\mathcal{P}$. Hence, $\mathcal{F}$ is ($\mathfrak{T}_i$, $\mathfrak{T}_j$)–g-closed. Example 3.10 demonstrates that the converse is false.

Example 3.10. If $\mathfrak{B}$ = {a, b, c}, $\mathfrak{T}_i$= {$\mathfrak{B}$, φ, {c}}, and $\mathfrak{T}_j$ = {$\mathfrak{B}$, φ,{b},{c},{b,c}}, then the set {c} is ($\mathfrak{T}_i$, $\mathfrak{T}_j$)−ggs-closed but not ($\mathfrak{T}_i$, $\mathfrak{T}_j$)−g-closed.

Proposition 3.11. If A is an ($\mathfrak{T}_i$, $\mathfrak{T}_j$)−ggs-closed subset of ($\mathfrak{B}$, $\mathfrak{T}_i$, $\mathfrak{T}_j$), then A is ($\mathfrak{T}_i$, $\mathfrak{T}_j$)−w-closed, but not conversely.
Proof. Let A be any ($\mathfrak{T}_i$, $\mathfrak{T}_j$)−ggs-closed set and $\mathcal{P}$ be any $\mathfrak{T}_i$–semi-open set containing A. Then, $\mathcal{P}$ is an $\mathfrak{T}_i$–gs-open set such that A ⊆ $\mathcal{P}$, so $\mathfrak{T}_j$–cl(A) ⊆ $\mathcal{P}$. Hence, A is ($\mathfrak{T}_i$, $\mathfrak{T}_j$)–w-closed. Example 3.12 demonstrates that the converse is false.

Example 3.12. If $\mathfrak{B}$ = {a, b, c}, $\mathfrak{T}_i$= {$\mathfrak{B}$, φ, {b},{a,c}}, and $\mathfrak{T}_j$ = {$\mathfrak{B}$, φ,{a},{b},{a,b}}, then the set {a} is ($\mathfrak{T}_i$, $\mathfrak{T}_j$)–w-closed but not ($\mathfrak{T}_i$, $\mathfrak{T}_j$)−ggs-closed.

Proposition 3.13. If $\mathcal{S}$ is an ($\mathfrak{T}_i$, $\mathfrak{T}_j$)−ggs-closed subset of ($\mathfrak{B}$, $\mathfrak{T}_i$, $\mathfrak{T}_j$), then $\mathcal{S}$ is ($\mathfrak{T}_i$, $\mathfrak{T}_j$)−αg-closed, but not conversely.
Proof. Suppose that $\mathcal{S}$ is any ($\mathfrak{T}_i$, $\mathfrak{T}_j$)−ggs-closed set in ($\mathfrak{B}$, $\mathfrak{T}_i$, $\mathfrak{T}_j$) and let $\mathcal{G}$ be any $\mathfrak{T}_i$–open set. Then, $\mathcal{G}$ is an $\mathfrak{T}_i$–gs-open set such that $\mathcal{S} \subseteq \mathcal{G}$, so we have $\mathfrak{T}_j$–αcl($\mathcal{S}$) ⊆ $\mathfrak{T}_j$–cl($\mathcal{S}$) ⊆ $\mathcal{G}$. Hence, $\mathcal{S}$ is ($\mathfrak{T}_i$, $\mathfrak{T}_j$)−αg-closed. Example 3.14 demonstrates that the converse is false.

Example 3.14. If $\mathfrak{B}$ = {a, b, c}, $\mathfrak{T}_i$= {$\mathfrak{B}$, φ,{a},{b},{a,b},{a,c }}, and $\mathfrak{T}_j$ = {$\mathfrak{B}$, φ {c}}, then the set {c} is ($\mathfrak{T}_i$, $\mathfrak{T}_j$)−αg-closed but not ($\mathfrak{T}_i$, $\mathfrak{T}_j$)−ggs-closed.

Proposition 3.15. If A is an ($\mathfrak{T}_i$, $\mathfrak{T}_j$)−ggs-closed subset of ($\mathfrak{B}$, $\mathfrak{T}_i$, $\mathfrak{T}_j$), then A is ($\mathfrak{T}_i$, $\mathfrak{T}_j$)−gα-closed, but not conversely.
Proof. Let A be any ($\mathfrak{T}_i$,$\mathfrak{T}_j$) − ggs-closed set in ($\mathfrak{B}$, $\mathfrak{T}_i$, $\mathfrak{T}_j$) and $\mathcal{G}$ be any $\mathfrak{T}_i$–α-open set containing A. Since any $\mathfrak{T}_i$–α-open set is $\mathfrak{T}_i$–semi-open, $\mathcal{G}$ is $\mathfrak{T}_i$–gs-open. We thus have $\mathfrak{T}_j$–αcl(A) ⊆ $\mathfrak{T}_j$– cl(A) ⊆ $\mathcal{G}$. Hence, A is ($\mathfrak{T}_i$, $\mathfrak{T}_j$)−gα-closed. Example 3.16 demonstrates that the converse is false.

Example 3.16. If $\mathfrak{B}$ = {a, b, c}, $\mathfrak{T}_i$= {$\mathfrak{B}$, φ,{b,c }}, and $\mathfrak{T}_j$ = {$\mathfrak{B}$, φ,{b}}, the set {c} is ($\mathfrak{T}_i$, $\mathfrak{T}_j$)−gα-closed but not ($\mathfrak{T}_i$, $\mathfrak{T}_j$)−ggs-closed.
Proposition 3.17. If A is an ($\mathfrak{T}_i$,$\mathfrak{T}_j$)−ggs-closed subset of ($\mathfrak{B}$, $\mathfrak{T}_i$, $\mathfrak{T}_j$), then A is ($\mathfrak{T}_i$,$\mathfrak{T}_j$)−gs-closed(resp. ($\mathfrak{T}_i$,$\mathfrak{T}_j$)−gp-closed, and ($\mathfrak{T}_i$,$\mathfrak{T}_j$)−gsp-closed), but not conversely.

Proof. Let A be any $(\mathfrak{T}_i, \mathfrak{T}_j)$−ggs-closed set in $(\mathfrak{B}, \mathfrak{T}_i, \mathfrak{T}_j)$ and U be any $\mathfrak{T}_i$–open set. Since A is $(\mathfrak{T}_i, \mathfrak{T}_j)$−ggs-closed, $\mathfrak{T}_j$–cl(A) ⊆ U, which implies that $\mathfrak{T}_j$–scl(A) ⊆ $\mathfrak{T}_j$–cl(A) ⊆ U. Thus, A is $(\mathfrak{T}_i, \mathfrak{T}_j)$−gs–closed. In addition, since pcl(A) ⊆ U and spcl(A) ⊆ U, A is also $(\mathfrak{T}_i,\mathfrak{T}_j)$−gp-closed and $(\mathfrak{T}_i,\mathfrak{T}_j)$−gsp-closed, respectively. Example 3.18 demonstrates that the converse is false.

Example 3.18. If $\mathfrak{B}$ = {a, b, c}, $\mathfrak{T}_i$= {$\mathfrak{B}$, φ,{a,b},{c}}, and $\mathfrak{T}_j$ = {$\mathfrak{B}$, φ,{a,b}}, then the set {b,c} is $(\mathfrak{T}_i, \mathfrak{T}_j)$–gs-closed(resp. $(\mathfrak{T}_i, \mathfrak{T}_j)$–gp-closed, and $(\mathfrak{T}_i, \mathfrak{T}_j)$–gsp-closed), but not $(\mathfrak{T}_i, \mathfrak{T}_j)$–ggs-closed.

Definition 3.19. Let *i*, *j* ∊ {1, 2} be fixed integers. A subset A of a bitopological space $(\mathfrak{B}, \mathfrak{T}_i, \mathfrak{T}_j)$ is called

1) semi-generalized star b-closed (briefly, $(\mathfrak{T}_i, \mathfrak{T}_j)$–sg*b-closed) if $\mathfrak{T}_j$−bcl(A) ⊆ U whenever A ⊆ U and U is semi-open in $(\mathfrak{B}, \mathfrak{T}_i)$,

2) pre-generalized b-closed (briefly $(\mathfrak{T}_i, \mathfrak{T}_j)$–pgb-closed) if $\mathfrak{T}_j$−bcl(A) ⊆ U whenever A ⊆ U and U is pre-open in $(\mathfrak{B}, \mathfrak{T}_i)$, and

3) $(\mathfrak{T}_i, \mathfrak{T}_j)$–g**b-closed if $\mathfrak{T}_j$−bcl(A) ⊆ U whenever A ⊆ U and U is g*-open in $(\mathfrak{B}, \mathfrak{T}_i)$.

Proposition 3.20. If A is an $(\mathfrak{T}_i, \mathfrak{T}_j)$−ggs-closed subset of $(\mathfrak{B}, \mathfrak{T}_i, \mathfrak{T}_j)$, then A is

1) $(\mathfrak{T}_i, \mathfrak{T}_j)$–sg*b-closed,

2) $(\mathfrak{T}_i, \mathfrak{T}_j)$–pgb-closed,

3) $(\mathfrak{T}_i, \mathfrak{T}_j)$–g**b-closed, and

4) $(\mathfrak{T}_i, \mathfrak{T}_j)$−rg**b-closed.

However, the converse statements are false.

Proof. 1) Let $\mathcal{M}$ be any $(\mathfrak{T}_i, \mathfrak{T}_j)$−ggs-closed set in $(\mathfrak{B}, \mathfrak{T}_i, \mathfrak{T}_j)$ and U be any $\mathfrak{T}_i$–semi-open set. Since $\mathcal{M}$ is $(\mathfrak{T}_i, \mathfrak{T}_j)$−ggs-closed, $\mathfrak{T}_j$–cl($\mathcal{M}$) ⊆ U, from which it follows that $\mathfrak{T}_j$–bcl($\mathcal{M}$) ⊆ $\mathfrak{T}_j$–scl($\mathcal{M}$) ⊆ $\mathfrak{T}_j$–cl($\mathcal{M}$) ⊆ U. Hence, A is $(\mathfrak{T}_i, \mathfrak{T}_j)$−sg*b-closed.

The proofs of (2), (3), and (4) are similar. Example 3.21 demonstrates that the converse statements are false.

Example 3.21.

1) Let $\mathfrak{B}$, $\mathfrak{T}_i$, and $\mathfrak{T}_j$ be as in Example 3.18. Then, the set {b} is $(\mathfrak{T}_i, \mathfrak{T}_j)$–sg*b-closed, but not $(\mathfrak{T}_i, \mathfrak{T}_j)$–ggs-closed.

2) If $\mathfrak{B}$ = {a, b, c}, $\mathfrak{T}_i$ = {$\mathfrak{B}$, φ,{a },{b}, {c},{a,b},{a,c}, {b, c}}, and $\mathfrak{T}_j$ ={$\mathfrak{B}$, φ, {b},{b,c}}, then the set{c} is $(\mathfrak{T}_i, \mathfrak{T}_j)$–pgb-closed and the set {b,c} is $(\mathfrak{T}_i, \mathfrak{T}_j)$–g**b-closed, but neither set is $(\mathfrak{T}_i, \mathfrak{T}_j)$–ggs-closed.

3) If $\mathfrak{B}$ = {a, b, c}, $\mathfrak{T}_i$ = {$\mathfrak{B}$, φ,{a}}, and $\mathfrak{T}_j$ ={$\mathfrak{B}$, φ, {a,c}}, the set {b} is $(\mathfrak{T}_i, \mathfrak{T}_j)$−rg**b-closed but not $(\mathfrak{T}_i, \mathfrak{T}_j)$−ggs-closed.

Remark 3.22. The concept of an $(\mathfrak{T}_i, \mathfrak{T}_j)$−ggs-closed set is independent of those of $(\mathfrak{T}_i, \mathfrak{T}_j)$– wg-closed and (1,2)*–#πgs-closed sets, as can be seen from Examples 3.23–3.26.

Example 3.23. If $\mathfrak{B}$ = {a, b, c}, $\mathfrak{T}_i$= {$\mathfrak{B}$, φ,{b},{a,c }}, and $\mathfrak{T}_j$ = {$\mathfrak{B}$, φ,{a},{b},{a,b}}, then the set {c} is $(\mathfrak{T}_i, \mathfrak{T}_j)$−ggs-closed but not $(\mathfrak{T}_i, \mathfrak{T}_j)$−wg-closed.

Example 3.24. If $\mathfrak{B}$ = {a, b, c}, $\mathfrak{T}_i$= {$\mathfrak{B}$, φ,{a},{b},{a,b}}, and $\mathfrak{T}_j$ = {$\mathfrak{B}$,φ,{b},{c},{b,c}}, then the set {a,c} is ($\mathfrak{T}_i$, $\mathfrak{T}_j$)−wg-closed but not ($\mathfrak{T}_i$, $\mathfrak{T}_j$)−ggs-closed.

Example 3.25. Let $\mathfrak{B}$, $\mathfrak{T}_i$, and $\mathfrak{T}_j$ be as in Example 3.23(3). Then, the set {a,b} is ($\mathfrak{T}_i$, $\mathfrak{T}_j$)− ggs-closed but not (1,2)*–#πgs-closed.

Example 3.26. If $\mathfrak{B}$ = {a, b, c}, $\mathfrak{T}_i$ = { $\mathfrak{B}$, φ,{a}}, and $\mathfrak{T}_j$ ={$\mathfrak{B}$,φ,{a,c}}, then the set {b,c} is (1,2)*–#πgs-closed but not ($\mathfrak{T}_i$, $\mathfrak{T}_j$)−ggs-closed.

Remark 3.27. In general, the family $D^*gs(\mathfrak{T}_i, \mathfrak{T}_j)$ is not equal to $D^*gs(\mathfrak{T}_j, \mathfrak{T}_j)$, as can be seen from Example 3.28.

Example 3.28. If $\mathfrak{B}$ = {a, b, c}, $\mathfrak{T}_i$= { $\mathfrak{B}$, φ,{c}}, and $\mathfrak{T}_j$ = { $\mathfrak{B}$, φ,{a},{b},{a,b},{a,c}}, then the subsets {b},{c} ∈ $D^*gs(\mathfrak{T}_j, \mathfrak{T}_i)$ but {b},{c} ∉ $D^*gs\ (\mathfrak{T}_i, \mathfrak{T}_j)$.

Remark 3.29. If $\mathfrak{T}_i \subseteq \mathfrak{T}_j$ in ($\mathfrak{B}$, $\mathfrak{T}_i$, $\mathfrak{T}_j$), then $D^*gs(\mathfrak{T}_j, \mathfrak{T}_i) \subseteq D^*gs\ (\mathfrak{T}_i, \mathfrak{T}_j)$, but not conversely (as Example 3.30 demonstrates).

Example 3.30. If $\mathfrak{B}$ = {a, b, c}, $\mathfrak{T}_i$= {$\mathfrak{B}$, φ,{b},{c},{b,c}}, and $\mathfrak{T}_j$ = {$\mathfrak{B}$, φ,{c}}, then $D^*gs(\mathfrak{T}_j, \mathfrak{T}_i) \subseteq D^*gs\ (\mathfrak{T}_i, \mathfrak{T}_j)$ but $\mathfrak{T}_i \nsubseteq \mathfrak{T}_j$.

4. Properties of ($\mathfrak{T}_i$, $\mathfrak{T}_j$)–ggs-Closed and ($\mathfrak{T}_i$, $\mathfrak{T}_j$)–ggs-Open Sets

In this section, we introduce some properties of ($\mathfrak{T}_i$, $\mathfrak{T}_j$)–ggs-closed and ($\mathfrak{T}_i$, $\mathfrak{T}_j$)–ggs-open sets.

Definition 4.1. A subset A of ($\mathfrak{B}$, $\mathfrak{T}_i$, $\mathfrak{T}_j$) is called ($\mathfrak{T}_i$, $\mathfrak{T}_j$)−ggs-open if and only if A^c is ($\mathfrak{T}_i$, $\mathfrak{T}_j$)−ggs-closed in $\mathfrak{B}$.
The family of all ($\mathfrak{T}_i$, $\mathfrak{T}_j$)–ggs-open subsets of $\mathfrak{B}$ is denoted by $D^*gO(\mathfrak{T}_i, \mathfrak{T}_j)$.

Proposition 4.2.
1) All ($\mathfrak{T}_i$, $\mathfrak{T}_j$)–open sets are ($\mathfrak{T}_i$, $\mathfrak{T}_j$)–ggs-open.
2) All ($\mathfrak{T}_i$, $\mathfrak{T}_j$)–ggs-open sets are ($\mathfrak{T}_i$, $\mathfrak{T}_j$)–g-open.
3) All ($\mathfrak{T}_i$, $\mathfrak{T}_j$)-ggs-open sets are ($\mathfrak{T}_i$, $\mathfrak{T}_j$)– αg-open and ($\mathfrak{T}_i$, $\mathfrak{T}_j$)gα-open.
4) All ($\mathfrak{T}_i$,$\mathfrak{T}_j$)–ggs-open sets are ($\mathfrak{T}_i$,$\mathfrak{T}_j$)–gs-open, ($\mathfrak{T}_i$,$\mathfrak{T}_j$)–sg-open, and ($\mathfrak{T}_i$, $\mathfrak{T}_j$)–gsp-open.
5) All ($\mathfrak{T}_i$, $\mathfrak{T}_j$)–ggs-open sets are ($\mathfrak{T}_i$, $\mathfrak{T}_j$)−gs-closed, ($\mathfrak{T}_i$, $\mathfrak{T}_j$)−gp-open, and ($\mathfrak{T}_i$, $\mathfrak{T}_j$)–gsp-open.
6) All ($\mathfrak{T}_i$, $\mathfrak{T}_j$)–ggs-open sets are ($\mathfrak{T}_i$, $\mathfrak{T}_j$)−sg*b-closed and ($\mathfrak{T}_i$, $\mathfrak{T}_j$)–pgb-open.

Proposition 4.3. If A, B ∈ $D^*gs(\mathfrak{T}_i, \mathfrak{T}_j)$, then A ∪ B ∈ $D^*gs(\mathfrak{T}_i, \mathfrak{T}_j)$.

Remark 4.4. If A and B are two ($\mathfrak{T}_i$, $\mathfrak{T}_j$)−ggs-closed sets in ($\mathfrak{B}$, $\mathfrak{T}_i$, $\mathfrak{T}_j$), then the intersection A ∩ B is not generally ($\mathfrak{T}_i$, $\mathfrak{T}_j$)−ggs-closed, as can be seen from Example 4.5.

Example 4.5. If $\mathfrak{B}$ = {a,b,c}, $\mathfrak{T}_i$ = {$\mathfrak{B}$, φ,{c}}, and $\mathfrak{T}_j$ = {$\mathfrak{B}$,φ,{a},{b},{a,b},{a,c}}, then the subsets {a,c}, {a,b} are ($\mathfrak{T}_i$, $\mathfrak{T}_j$)−ggs-closed, but their intersection {a,c}∩{a,b} = {a} is not ($\mathfrak{T}_i$, $\mathfrak{T}_j$)−ggs-closed.

Proposition 4.6. For all $r \in (\mathfrak{B}, \mathfrak{T}_i, \mathfrak{T}_j)$, either the set $\{r\}$ is $\mathfrak{T}_i$–gs-closed or $\{r\}^c$ is $(\mathfrak{T}_i, \mathfrak{T}_j)$–ggs-closed in $(\mathfrak{B}, \mathfrak{T}_i, \mathfrak{T}_j)$.

Proposition 4.7. If the set $\mathcal{E}$ is $(\mathfrak{T}_i, \mathfrak{T}_j)$–ggs-closed in $(\mathfrak{B}, \mathfrak{T}_i, \mathfrak{T}_j)$, then $\mathfrak{T}_j$–cl($\mathcal{E}$) contains no non-empty $\mathfrak{T}_i$–gs-closed sets, but not conversely.
Proof. Let $\mathcal{E}$ be a $(\mathfrak{T}_i, \mathfrak{T}_j)$–ggs-closed set and F be a $\mathfrak{T}_i$–gs-closed set such that F $\subseteq \mathfrak{T}_j$ –cl($\mathcal{E}$))^c. Since $\mathcal{E}$ is $(\mathfrak{T}_i, \mathfrak{T}_j)$–ggs-closed, $\mathcal{E} \in D^*gs(\mathfrak{T}_i, \mathfrak{T}_j)$, which implies that $\mathfrak{T}_j$–cl($\mathcal{E}$) $\subseteq$ F^c. Then, F $\subseteq \mathfrak{T}_j$–cl($\mathcal{E}$) $\cap$ ($\mathfrak{T}_j$–cl($\mathcal{E}$))^c and hence F is empty. Example 4.8 demonstrates that the converse is false.

Example 4.8. Let $\mathfrak{B}$ = {a, b, c}, $\mathfrak{T}_i$ = { $\mathfrak{B}$, φ,{a},{b},{a,b},{a,c}}, and $\mathfrak{T}_j$ = { $\mathfrak{B}$, φ,{c}}. If G = {a}, then $\mathfrak{T}_j$–cl(G) - G = {b} contains no non-empty $\mathfrak{T}_i$–gs-closed sets but G is not $(\mathfrak{T}_i, \mathfrak{T}_j)$−ggs-closed.

Proposition 4.9. If A is an $(\mathfrak{T}_i, \mathfrak{T}_j)$−ggs-closed set and A $\subseteq$ B $\subseteq \mathfrak{T}_j$–cl(A), then B is a $(\mathfrak{T}_i, \mathfrak{T}_j)$−ggs-closed set.

Proposition 4.10. If A is a $(\mathfrak{T}_i, \mathfrak{T}_j)$−ggs-closed set, then $\mathfrak{T}_j$–cl({k}) $\cap$ A $\neq \varphi$ for all $k \in \mathfrak{T}_j$–cl(A), but not conversely.
Proof. If $\mathfrak{T}_i$–cl({k}) $\cap$ A = φ for all $k \in \mathfrak{T}_j$–cl(A), then A $\subseteq$ ($\mathfrak{T}_i$-cl({k}))^c. Since A is $(\mathfrak{T}_i,\mathfrak{T}_j)$−ggs-closed, $\mathfrak{T}_j$–cl(A) $\subseteq$ ($\mathfrak{T}_i$-cl({k}))^c, which implies that $k \notin \mathfrak{T}_j$–cl(A), contradicting the initial assumption. Example 4.11 demonstrates that the converse is false.

Example 4.11. Let $\mathfrak{B}$ = {a, b, c}, $\mathfrak{T}_i$ = {$\mathfrak{B}$, φ,{a}}, and $\mathfrak{T}_j$ = {$\mathfrak{B}$, φ,{b},{c},{b,c}}. The subset A = {c} is not $(\mathfrak{T}_i, \mathfrak{T}_j)$−ggs-closed, but $\mathfrak{T}_j$–cl({k}) $\cap$ A $\neq \varphi$ for all $k \in \mathfrak{T}_j$–cl(A).

Proposition 4.12. Let A $\subseteq$ Y $\subseteq$ $\mathfrak{B}$. If the set A is $(\mathfrak{T}_i, \mathfrak{T}_j)$−ggs-closed in $(\mathfrak{B}, \mathfrak{T}_i, \mathfrak{T}_j)$, then A is $(\mathfrak{T}_i, \mathfrak{T}_j)$−ggs-closed relative to Y.
Proof. If A $\subseteq$ Y$\cap$ G and G is $\mathfrak{T}_i$–gs-open in $(\mathfrak{B}, \mathfrak{T}_i, \mathfrak{T}_j)$, then A $\subseteq$ G and $\mathfrak{T}_j$–cl(A) $\subseteq$ G. Hence, Y $\cap$ $\mathfrak{T}_j$–cl(A) $\subseteq$ Y $\cap$ G and A is $(\mathfrak{T}_i, \mathfrak{T}_j)$−ggs-closed relative to Y.

5. Some Applications of $(\mathfrak{T}_i, \mathfrak{T}_j)$–ggs-Closed Sets

In this section, as an application of our work, we introduce $(\mathfrak{T}_i, \mathfrak{T}_j)$–$T_{ggs}$-spaces and $(\mathfrak{T}_i, \mathfrak{T}_j)$− $T^{\#}_{ggs}$-spaces, and study some of their properties.

Definition 5.1. A bitopological space $(\mathfrak{B}, \mathfrak{T}_i, \mathfrak{T}_j)$ is called an $(\mathfrak{T}_i, \mathfrak{T}_j)$–$T_{ggs}$-space if every $(\mathfrak{T}_i, \mathfrak{T}_j)$−ggs-closed set it contains is $\mathfrak{T}_i$–closed.

Proposition 5.2. If $(\mathfrak{B}, \mathfrak{T}_i, \mathfrak{T}_j)$ is an $(\mathfrak{T}_i, \mathfrak{T}_j)$–$T_{1/2}$-space, then it is an $(\mathfrak{T}_i, \mathfrak{T}_j)$–$T_{ggs}$-space, but not conversely.

Proof. Let $(\mathfrak{B}, \mathfrak{T}_i, \mathfrak{T}_j)$ be an $(\mathfrak{T}_i, \mathfrak{T}_j)$–$T_{1/2}$-space and A be an $(\mathfrak{T}_i, \mathfrak{T}_j)$−ggs-closed subset of $(\mathfrak{B}, \mathfrak{T}_i, \mathfrak{T}_j)$. By Proposition 3.9, A is $(\mathfrak{T}_i, \mathfrak{T}_j)$−g-closed in $(\mathfrak{B}, \mathfrak{T}_i, \mathfrak{T}_j)$. Since $(\mathfrak{B}, \mathfrak{T}_i, \mathfrak{T}_j)$ is an $(\mathfrak{T}_i, \mathfrak{T}_j)$–$T_{1/2}$-space, this implies that A is $\mathfrak{T}_j$–closed. Hence, $(\mathfrak{B}, \mathfrak{T}_i, \mathfrak{T}_j)$ is an $(\mathfrak{T}_i, \mathfrak{T}_j)$–$T_{ggs}$-space. Example 5.3 demonstrates that the converse is false.
Example 5.3. If $\mathfrak{B}$ = {a, b, c}, $\mathfrak{T}_i$= {$\mathfrak{B}$, φ,{c}}, and $\mathfrak{T}_j$ = {$\mathfrak{B}$, φ,{b},{c},{b,c}}, then the set {b} is $(\mathfrak{T}_i, \mathfrak{T}_j)$−ggs-closed but $(\mathfrak{B}, \mathfrak{T}_i, \mathfrak{T}_j)$ is not an $(\mathfrak{T}_i, \mathfrak{T}_j)$–$T_{1/2}$ -space.

Proposition 5.4. If $(\mathfrak{B}, \mathfrak{T}_i, \mathfrak{T}_j)$ is an $(\mathfrak{T}_i, \mathfrak{T}_j)$–$T_w$-space then it is also an $(\mathfrak{T}_i,\mathfrak{T}_j)$–$T_{ggs}$-space, but not conversely.

Proof. Let A be an $(\mathfrak{T}_i, \mathfrak{T}_j)$−ggs-closed subset of $(\mathfrak{B}, \mathfrak{T}_i, \mathfrak{T}_j)$. By Proposition 3.11, A is $(\mathfrak{T}_i, \mathfrak{T}_j)$−w-closed in $(\mathfrak{B}, \mathfrak{T}_i, \mathfrak{T}_j)$. Since $(\mathfrak{B}, \mathfrak{T}_i, \mathfrak{T}_j)$ is an $(\mathfrak{T}_i, \mathfrak{T}_j)$–$T_w$-space, A is $\mathfrak{T}_j$–closed. Hence, $(\mathfrak{B}, \mathfrak{T}_i, \mathfrak{T}_j)$ is an $(\mathfrak{T}_i, \mathfrak{T}_j)$–$T_{ggs}$-space. Example 5.5 demonstrates that the converse is false.

Example 5.5. If $\mathfrak{B}$ = {a, b, c}, $\mathfrak{T}_i$ = {$\mathfrak{B}$, φ,{b},{a,c}}, and $\mathfrak{T}_j$ = {$\mathfrak{B}$, φ,{a},{b},{a,b}}, then the set {a,b} is $(\mathfrak{T}_i, \mathfrak{T}_j)$−ggs-closed but not an $(\mathfrak{T}_i, \mathfrak{T}_j)$–$T_w$-space.

Proposition 5.6. If $(\mathfrak{B}, \mathfrak{T}_i, \mathfrak{T}_j)$ is an $(\mathfrak{T}_i, \mathfrak{T}_j)$–$T_b$-space then it is also an $(\mathfrak{T}_i, \mathfrak{T}_j)$–$T_{ggs}$-space, but not conversely.

Proof. The proof is similar to that of Proposition 5.4. Example 5.7 demonstrates that the converse is false.

Example 5.7. If $\mathfrak{B}$ = {a, b, c}, $\mathfrak{T}_i$ = {$\mathfrak{B}$, φ,{a, b},{c}}, and $\mathfrak{T}_j$ = {$\mathfrak{B}$, φ, {a,b}}, then the set {b,c} is $(\mathfrak{T}_i, \mathfrak{T}_j)$−ggs-closed but not an $(\mathfrak{T}_i, \mathfrak{T}_j)$–$T_b$-space.

Proposition 5.8. A bitopological space $(\mathfrak{B}, \mathfrak{T}_i, \mathfrak{T}_j)$ is an $(\mathfrak{T}_i, \mathfrak{T}_j)$–$T_{ggs}$-space iff {x} is $\mathfrak{T}_i$–open or $\mathfrak{T}_i$–gs-closed for all x ∈ $\mathfrak{B}$.

Proof. Suppose {x} is not an $\mathfrak{T}_i$–gs-closed subset of $(\mathfrak{B}, \mathfrak{T}_i, \mathfrak{T}_j)$. By Proposition 4.6, $\{x\}^c$ is $(\mathfrak{T}_i, \mathfrak{T}_j)$−ggs-closed. Since $(\mathfrak{B}, \mathfrak{T}_i, \mathfrak{T}_j)$ is an $(\mathfrak{T}_i, \mathfrak{T}_j)$–$T_{ggs}$-space, $\{x\}^c$ is an $\mathfrak{T}_j$−closed set. Hence, {x} is $\mathfrak{T}_i$–open.

Conversely, suppose that B is an $(\mathfrak{T}_i, \mathfrak{T}_j)$−ggs-closed set. Then, {x} is either $\mathfrak{T}_i$–open or $\mathfrak{T}_i$–gs-closed for all x ∈ $\mathfrak{T}_j$–cl(B). If {x} is $\mathfrak{T}_j$–open, $\{x\} \cap B \neq \varphi$, so x ∈ B. Now, let {x} be $\mathfrak{T}_j$−gs-closed. If x ∉ B, then {x} ⊆ $\mathfrak{T}_j$–cl(B) - B, which contradicts Proposition 4.7. Thus, the set B is $\mathfrak{T}_j$−closed, and hence $(\mathfrak{B}, \mathfrak{T}_i, \mathfrak{T}_j)$ is an $(\mathfrak{T}_i, \mathfrak{T}_j)$–$T_{ggs}$-space.

Remark 5.9. A $(\mathfrak{B}, \mathfrak{T}_i)$–space is not generally a T_{ggs}-space, even if $(\mathfrak{B}, \mathfrak{T}_i, \mathfrak{T}_j)$ is an $(\mathfrak{T}_i, \mathfrak{T}_j)$–$T_{ggs}$-space, as Example 5.10 demonstrates.

Example 5.10. Let $\mathfrak{B}$ = {a, b, c}, $\mathfrak{T}_i$= {$\mathfrak{B}$, φ,{b,c}}, and $\mathfrak{T}_j$ = {$\mathfrak{B}$, φ,{b},{c},{b,c}}. Then, the $(\mathfrak{B}, \mathfrak{T}_i)$–space is not a T_{ggs}-space but $(\mathfrak{B}, \mathfrak{T}_i, \mathfrak{T}_j)$ is an $(\mathfrak{T}_i, \mathfrak{T}_j)$–$T_{ggs}$-space.

Remark 5.11. $(\mathfrak{B}, \mathfrak{T}_i, \mathfrak{T}_j)$ is not generally an $(\mathfrak{T}_i, \mathfrak{T}_j)$–$T_{ggs}$-space, even if both the $(\mathfrak{B}, \mathfrak{T}_i)$–space and $(\mathfrak{B}, \mathfrak{T}_j)$–space are T_{ggs}-spaces, as Example 5.12 demonstrates.

Example 5.12. If $\mathfrak{B}$ = {a, b, c}, $\mathfrak{T}_i$ = {$\mathfrak{B}$, φ,{c}}, and $\mathfrak{T}_j$ = {$\mathfrak{B}$, φ,{a},{b},{a,b},{a,c}}, then both $(\mathfrak{B}, \mathfrak{T}_i)$ and $(\mathfrak{B}, \mathfrak{T}_j)$ are T_{ggs}-spaces but $(\mathfrak{B}, \mathfrak{T}_i, \mathfrak{T}_j)$ is not an $(\mathfrak{T}_i, \mathfrak{T}_j)$–$T_{ggs}$-space.

Remark 5.13. A $(\mathfrak{B}, \mathfrak{T}_i)$–space is not generally an $(\mathfrak{T}_i, \mathfrak{T}_j)$–$T_{ggs}$-space, even if $(\mathfrak{B}, \mathfrak{T}_i, \mathfrak{T}_j)$ is a T_{ggs}-space, as Example 5.14 demonstrates.

Example 5.14. If $\mathfrak{B}$ = {a, b, c}, $\mathfrak{T}_i$ = {$\mathfrak{B}$, φ,{b, c}}, and $\mathfrak{T}_j$ = {$\mathfrak{B}$, φ,{b},{c},{b,c}}, then ($\mathfrak{B}$, $\mathfrak{T}_i$) is not a T_{ggs}-space but ($\mathfrak{B}$, $\mathfrak{T}_i$, $\mathfrak{T}_j$) is an ($\mathfrak{T}_i$, $\mathfrak{T}_j$)–T_{ggs}-space.

Definition 5.15. A bitopological space ($\mathfrak{B}$, $\mathfrak{T}_i$, $\mathfrak{T}_j$) is called an ($\mathfrak{T}_i$, $\mathfrak{T}_j$)−$T^{\#}_{ggs}$-space if every ($\mathfrak{T}_i$, $\mathfrak{T}_j$)−gs-closed set it contains is ($\mathfrak{T}_i$, $\mathfrak{T}_j$)−ggs-closed.

Proposition 5.16. All ($\mathfrak{T}_i$, $\mathfrak{T}_j$)–$T_{1/2}$-spaces are ($\mathfrak{T}_i$, $\mathfrak{T}_j$)–$T^{\#}_{ggs}$-spaces, but not conversely (as Example 5.17 demonstrates).

Example 5.17. If $\mathfrak{B}$ = {a, b, c}, $\mathfrak{T}_i$ = {$\mathfrak{B}$, φ,{b},{c},{b,c}}, and $\mathfrak{T}_j$ = {$\mathfrak{B}$, φ,{a,c}}, then ($\mathfrak{B}$,$\mathfrak{T}_i$, $\mathfrak{T}_j$) is an ($\mathfrak{T}_i$, $\mathfrak{T}_j$)–$T^{\#}_{ggs}$-space but not an ($\mathfrak{T}_i$, $\mathfrak{T}_j$)–$T_{1/2}$-space.

Remark 5.18. The ($\mathfrak{T}_i$, $\mathfrak{T}_j$)–T_{ggs}- and ($\mathfrak{T}_i$, $\mathfrak{T}_j$)−$T^{\#}_{ggs}$-spaces are independent, as Examples 5.19 and 5.20 demonstrate.

Example 5.19. If $\mathfrak{B}$ = {a, b, c}, $\mathfrak{T}_i$ = {$\mathfrak{B}$, φ,{a},{b},{c},{a,b},{a,c},{b,c}}, and $\mathfrak{T}_j$ = {$\mathfrak{B}$, φ,{c}}, then ($\mathfrak{B}$, $\mathfrak{T}_i$, $\mathfrak{T}_j$) is an ($\mathfrak{T}_i$, $\mathfrak{T}_j$)–T_{ggs}-space but not an ($\mathfrak{T}_i$, $\mathfrak{T}_j$)–$T^{\#}_{ggs}$-space.

Example 5.20. If $\mathfrak{B}$ = {a, b, c}, $\mathfrak{T}_i$ = {$\mathfrak{B}$, φ,{b},{c},{b,c}}, and $\mathfrak{T}_j$ = {$\mathfrak{B}$, φ,{a,c}}, then ($\mathfrak{B}$, $\mathfrak{T}_i$, $\mathfrak{T}_j$) is an ($\mathfrak{T}_i$, $\mathfrak{T}_j$)–$T^{\#}_{ggs}$-space but not an ($\mathfrak{T}_i$, $\mathfrak{T}_j$)–T_{ggs}-space.
Definition 5.21. A bitopological space ($\mathfrak{B}$, $\mathfrak{T}_i$, $\mathfrak{T}_j$) is said to be a strongly pairwise $T_{1/2}$-space.
If it is both an ($\mathfrak{T}_i$,$\mathfrak{T}_j$)–T_{ggs}-space and an ($\mathfrak{T}_j$,$\mathfrak{T}_i$)–T_{ggs}-space

Proposition 5.22. If ($\mathfrak{B}$, $\mathfrak{T}_i$, $\mathfrak{T}_j$) is a strongly pairwise $T_{1/2}$-space, then it is a strongly pairwise

($\mathfrak{T}_i$, $\mathfrak{T}_j$)–T_{ggs}-space, but not conversely (as Example 5.23 demonstrates).

Example 5.23. If $\mathfrak{B}$ = {a, b, c}, $\mathfrak{T}_i$ = {$\mathfrak{B}$,φ,{b,c}}, and $\mathfrak{T}_j$ = {$\mathfrak{B}$, φ,{b},{c},{b,c}}, then ($\mathfrak{B}$, $\mathfrak{T}_i$, $\mathfrak{T}_j$) is an ($\mathfrak{T}_i$,$\mathfrak{T}_j$)–T_{ggs}-space and an ($\mathfrak{T}_j$,$\mathfrak{T}_i$)–T_{ggs}-space, and hence a strongly pairwise ($\mathfrak{T}_i$, $\mathfrak{T}_j$)–T_{ggs}-space. However, ($\mathfrak{B}$, $\mathfrak{T}_i$, $\mathfrak{T}_j$) is not a strongly pairwise $T_{1/2}$-space.

Proposition 5.24. A bitopological space ($\mathfrak{B}$, $\mathfrak{T}_i$, $\mathfrak{T}_j$) is an ($\mathfrak{T}_i$, $\mathfrak{T}_j$)–$T_{1/2}$-space iff it is both an ($\mathfrak{T}_i$, $\mathfrak{T}_j$)–$T^{\#}_{ggs}$-space and an ($\mathfrak{T}_i$, $\mathfrak{T}_j$)–T_{ggs}-space.
Proof. Suppose that ($\mathfrak{B}$, $\mathfrak{T}_i$, $\mathfrak{T}_j$) is an ($\mathfrak{T}_i$, $\mathfrak{T}_j$)−$T_{1/2}$-space. Then, by Propositions 5.16 and 5.2, ($\mathfrak{B}$, $\mathfrak{T}_i$, $\mathfrak{T}_j$) is both an ($\mathfrak{T}_i$, $\mathfrak{T}_j$)–$T^{\#}_{ggs}$-space and an ($\mathfrak{T}_i$, $\mathfrak{T}_j$)−T_{ggs}-space.
Conversely, suppose that ($\mathfrak{B}$, $\mathfrak{T}_i$, $\mathfrak{T}_j$) is both an ($\mathfrak{T}_i$, $\mathfrak{T}_j$)−$T^{\#}_{ggs}$-space and an ($\mathfrak{T}_i$, $\mathfrak{T}_j$)–T_{ggs}-space, and that G is an ($\mathfrak{T}_i$, $\mathfrak{T}_j$)−gs-closed subset of ($\mathfrak{B}$, $\mathfrak{T}_i$, $\mathfrak{T}_j$). Since ($\mathfrak{B}$, $\mathfrak{T}_i$, $\mathfrak{T}_j$) is an ($\mathfrak{T}_i$, $\mathfrak{T}_j$)−$T^{\#}_{ggs}$-space, this implies that G is an ($\mathfrak{T}_i$, $\mathfrak{T}_j$)−ggs-closed set. In addition, since ($\mathfrak{B}$, $\mathfrak{T}_i$, $\mathfrak{T}_j$) is an ($\mathfrak{T}_i$, $\mathfrak{T}_j$)−T_{ggs}-space, G is a $\mathfrak{T}_j$–closed subset of ($\mathfrak{B}$, $\mathfrak{T}_i$, $\mathfrak{T}_j$). Thus, ($\mathfrak{B}$, $\mathfrak{T}_i$, $\mathfrak{T}_j$) is an ($\mathfrak{T}_i$, $\mathfrak{T}_j$)–$T_{1/2}$-space.

References

[1] J. Donchev, '*On generalizing Semi-pre open sets*', Mem Fac. Sci. Kochi Univ. Ser. A. Mat. 6 (1995), 48-53.

[2] O. A. El-Tantawy, H.M. Abu-Donia, '*Generalized separation axioms in bitopological spaces*', *Arab. J. Sci. Eng.*, **30** (2005), 117 **[3]**. J. Donchev, On generalizing Semi-pre open sets, Mem. Fac. Sci. Kochi Univ. Ser. A. Mat.6 (1995), 53-48.
[3] T. Fukutake, '*On generalized closed sets in bitopological spaces'*, *Bull. Fukuoka Univ. Ed. Part III* **35** (1985), 19–28.
[4] T. Fukutake, P. Sundaram, N. Nagaveni, '*On weakly generalized closed sets, weakly generalized continuous maps and Twg-spaces in bitopological spaces'*, *Bull. Fukuoka Univ. Ed. Part III*, **48** (1999), 33–40.
[5] T. Fukutake, P. Sundaram, M. Shaik John, '*w-closed sets, w-open sets and w-continuity in bitopological spaces'*, *Bull. Fukuoka Univ. Ed. Part III*, **51** (2002), 1–9.
[6] Y. Gnanambal, *'On generalized pre-regular closed sets in topological spaces'*, *Indian J. Pure Appl. Math.* **28** (1997), 351-360.
[7] A. K. Hussain, B. J. Tawfeeq, '*Generalized gs-closed sets'*, *College of Education Journal*, **3** (2014), 213–224.
[8] **S**. Jafara, M. Lellis Thivagar, S.A. Thisaya Ponmani, *'(1,2) α-open sets based on bitopological separatin axioms'*, *Soochw Journal of Math.* **33** (2007), 375–381.
[9] J. C. Kelly, *'Bitopological spaces'*, *Proc. London Math. Soc.*, **13** (1963) 71–89.
[10] F. H. Khber, H. S. Al-Saadi, '*On pairwise semi generalized closed sets'*, *JKAU Sci.* **21** (2009), 269–295.
[11] N. Levine, '*Semi-open sets and semi-continuity in topological spaces'*, *Amer. Math.* Monthly, **17** (1963), 36–41.
[12] N. Levine, '*Generalized closed sets in topology'*, *Rend. Circlo. Mat. Palermo* **17** (1970), 89–96.
[13] H. Maki, K. Balachandran, '*Semi-generalized closed maps and generalized semi-closed maps'*, *Mem. Fac. Sci. Kochi Univ. Ser. A. Math.* **14** (1993), 41–54.
[14] H. Maki, R. Devi, K. Balachandran, *'Generalized α -closed sets in topology'*, *Bul. Fukuoka Univ. E. Part III*, **17** (1993), 13–21.
[15] M. Narmatha, K. Indirani, *'(τ_1, τ_2)- rg**b closed sets in bitopological spaces'*, *International Journal of Mathematics Trends and Technology* **58** (2018), 155–163.
[16.] B. Meera Devi, *'Bitopological space g**b-closed sets'*, *Int. J. Pure Appl. Math.* **112** (2017), 31–38.
[17] S. Sekar, R. Brindha J, '*On pre-generalized b-closed set in topological spaces'*, *Int. J. Pure Appl. Math.* **111** (2016), 577–586.
[18] S. Sekar, B. Jothilakshmi, '*On semi-generalized star b-closed map in topological spaces'*, *Int. J. Pure Appl. Math.* **113** (2017), 93–102.
[19] M. Sheikh John, S. Maragathavalli, *'Strongly αg*-closed sets in bitopological spaces'*, *Int. J. Contemp. Math. Sciences* **5** (2010), 805–813.
[20] B. J. Tawfeeq**,** *'On pairwise #πgs- closed maps in bitopological spaces'*, *Math. Theory and Modeling*, **5** (2015), 15–28.
[21] M. K. R. S. Veerakumar, '*Between closed sets and g-closed sets'*, *Mem. Fac. Sci. Kochi Univ. (Math)* **21** (2000), 1–19.
[22] M. K. R. S. Veerakumar, '*g*-semi-closed sets'*, *Acta Ciencia Indica*, **29** (2003), 81–90.

أثر التسويق المستدام في التوجه الريادي
(دراسة استطلاعية تحليلية لآراء عينة من مديري شركة زين للاتصالات المتنقلة في العراق)

نبيل قاسم عناد الغانمي
كليه العلوم السياحية/ الجامعة المستنصرية

المستخلص

هدفت هذه الدراسة إلى تحديد أثر التسويق المستدام في التوجه الريادي، ومن أجل تحقيق ذلك، تم اعتماد ابعاد التسويق المستدام (التسويق ألابتكاري، تسويق الاحساس بالرسالة، التسويق الموجه للزبون، تسويق قيمة الزبون، والتسويق الاجتماعي)، وتم التعبير عن التوجه الريادي بأبعاده (الابداعية، الاستقلالية، الاستباقية، الهجومية التنافسية،وتحمل المخاطر).وقد حاولت الدراسة الاجابة عن عدة تساؤلات منها **هل توجد علاقة ارتباط وأثر للتسويق المستدام في التوجه الريادي؟**

وأجريت الدراسة في شركة زين للاتصالات في العراق، إذ تم الحصول على المعلومات اللازمة للجانب الميداني من خلال الأستبانة التي أعدت لهذا الغرض وزعت على عينة مؤلفة من (60) مديراً يمثلون مديري الفروع والأقسام والشعب والوحدات في الشركة، فضلاً عن المقابلات والملاحظات الشخصية. كما توصلت الدراسة إلى مجموعة من الاستنتاجات من أهمها أن هناك أثر للتسويق المستدام في التوجه الريادي في الشركة مجتمع الدراسة.

The impact of sustainable marketing on entrepreneurial orientation
(An exploratory، analytical study of the opinions of a sample of managers of Zeina Mobile Communications Company in Iraq)

Nabeel Qasim Enad
College of Tourism Sciences- Mustansiriyah University.

Abstract:

This study aims to determine the impact of sustainable marketing strategy on entrepreneurial orientation، in order to achieve this، the dimensions of sustainable marketing strategy (marketing innovation, marketing sense message، customer-oriented marketing، customer value marketing, social marketing) and entrepreneurial orientation is expressed by its dimensions (creativity, independence, proactive، competitive aggressive، risk-taking).The study attempted to answer a number of questions، is there a correlation relationship and effect of sustainable marketing strategy in entrepreneurial orientation?

The study was conducted on Zain mobile operator in Iraq, where information was obtained for the field side through the questionnaire form prepared for this purpose and was distributed to a sample of (60) representing managers of branches, sections, divisions, and units of the company, as well as interviews and personal observations.The study also reached a set of conclusions, the most important of which is that there is an impact of sustainable marketing on the entrepreneurial orientation of the company in the study community.

المقدمة ومنهجية البحث
اولا: المقدمة

تشهد بيئة الأعمال العديد من التطورات المتسارعة ومن هذه التطورات التي حدثت الاهتمام الواضح بالحد الادنى الثلاثي (الاعتبارات البيئية، الاعتبارات الاجتماعية، والاعتبارات الاقتصادية) لاستدامة المنظمات، إذ مثلت الاستدامة صفة العصر الحديث وسمة من سمات الاقتصاديات المعاصرة، والتأكيد على عدم الاضرار بالبيئة والمحافظة على مواردها الطبيعية، وتحقيق الرفاهية الاجتماعية من خلال ممارسة الاعمال المسؤولة اجتماعياً، فضلاً عن ذلك تحقيق اهدافها التجارية،حتى باتت المنظمات في ظل ذلك تدرك اهمية فلسفة التسويق المستدام لوصفه توجهاً معاصراً حديثاً ومتكاملاً يتطلب الريادة والتميز من اجل إدامة العلاقة مع الزبون، وهذا ما جعل اغلب المنظمات العالمية في مختلف البلدان تستنير بفلسفة التسويق المستدام بوصفها احدى البدائل للمحافظة على مكانتها امام زبائنها والمجتمع ككل، وتحقيق التوجه الريادي الذي يجعلها قادرة على تحقيق الارباح وقيمة الزبون وإرضائه وإشباع رغباته وإدامة العلاقة معه.

ثانيا: منهجية البحث

1. مشكلة البحث

تنبع مشكلة الدراسة لما يشهده عالم الاعمال اليوم من شدة المنافسة،والعمل المتسارع والعولمة نحو تقديم خدمات متطورة تتناسب مع رغبات الزبائن واحتياجاتهم، وفي ظل هذا التطور، اصبح على المنظمات البحث عن فلسفة أعمق ورؤيا أشمل، تعتمد على إختيار المجالات التي تضمن لها التفوق في أداءها، فنتج عن ذلك بزوغ مفهوم التسويق المستدام لتطوير التوجه الريادي والذي أصبح ضرورة ملحة للمنظمات وعلى وجه الخصوص لشركة زين للهاتف الجوال في العراق التي تعمل في ظروف بيئية ديناميكية وحالة اللاتأكد يمكن توضيح مشكلة الدراسة في تساؤل عام هو(هل للتسويق المستدام اثر في التوجه الريادي لشركة زين للاتصالات المتنقلة في العراق).

2. اهمية الدراسة

تستمد أهمية الدراسة الحالية من أهمية المتغيرات والمواضيع التي غنت بمعالجتها،والتي تستمدها من خلال متغيراتها المبحوثة (**التسويق المستدام والتوجه الريادي**)، فالمنظمات اليوم تسعى لتطوير الأفكار الريادية من أجل تحسين مستوى أدائها والتي تلعب دوراً اساسيا في ضمان نجاحها، وعليه يمكن تحديد اهمية الدراسة من خلال ابراز البُعد التطبيقي الذي يسهم من خلالهِ التسويق المستدام في تعزيز التوجه الريادي لشركة زين للاتصالات المتنقلة.

3. اهداف الدراسة

ترمي الدراسة أساساً إلى بيان أثر التسويق المستدام في التوجه الريادي لشركة (**زين للاتصالات في العراق**)، وكذلك تحديد أهداف فرعية أخرى موزعة حسب محاور الدراسة وهيكلها على وفق بناء مخطط نظري يصف شكل العلاقة والأثر بين متغيراتها الرئيسة والفرعية، والتحقق من المصداقية والجدوى العلمية والعملية للمخطط الفرضي من اجل الوصول إلى وضع الاستنتاجات والتوصيات اللازمة، لتمكين الشركة مجتمع الدراسة من التعرف على طرائق نجاحها وقدرتها على الاستمرار والتطور.

4. فرضيــــات الدراســـة

من اجل تحقيق اهداف الدراسة واختبار مخططها الفرضي فقد اعتمدت الدراسة على الفرضيتين والتي تمت صياغتها على النحو الاتي:

أ- **الفرضيـة الرئيســـة الأولى**: لاتوجد علاقة ارتباط ذات دلالة معنوية بين التسويق المستدام بأبعاده والتوجه الريادي بأبعاده.

ب- **الفرضية الرئيسة الثانية:** لايوجد تأثير ذو دلالة معنوية للتسويق المستدام بأبعاده في التوجه الريادي.

5. حدود الدراسة

أ. الحـدود المكانيــة: طبقت الدراسة في شركة زين للاتصالات المتنقلة في العراق – المقر الرئيسي وبعض الفروع التابعة لها.

ب. الحـدود الزمانيــة: تعد الحدود الزمانية للدراسة هي المدة التي قامت بها الباحث بأجراء الدراسة والتي تمثلت بمدة، كما تمثلت إعداد الدراسة التطبيقية في الشركة (مجتمع الدراسة) التي بدأت بها بالزيارات لتشخيص مشكلة الدراسة، وتوزيع الإستبانة وإسترجاعها، ومقابلة المديرين ومناقشة آرائهم عن متغيرات الدراسة، وأهدافها للمدة من 10 / 2 / 2023 ولغاية 2023/4/30.

6. مصادر جمع المعلومات والبيانات

في سبيل أغناء الجانب النظري تم الاعتماد على إسهامات الكتاب والباحثين التي تم جمعها من المصادر المتمثلة بالمراجع العلمية من الكتب والمجلات والاطاريح والبحوث والدراسات العلمية وباللغتين العربية والأجنبية، وهي ذات صلة بموضوع الدراسة، فضلا عن الاستعانة بخدمات الشبكة العالمية للمعلومات (الانترنت).

اما في الجانب العملي فقد تم الاعتماد في تغطية الجانب الميداني للدراسة على عدد من الوسائل الضرورية في جمع البيانات والمعلومات الخاصة بهذا الجانب وهي:-

أ. **المقابلة الشخصية:-** تم اجراء عدد من المقابلات الشخصية مع أفراد عينة الدراسة في شركة زين للاتصالات في العراق.

ب. **استمارة الاستبانة:-** تعد الاستبانة المصدر الرئيس للحصول على البيانات والمعلومات المطلوبة وقد صممت لتغطي جميع متغيرات الدراسة، وقد روعي في صياغة هذه الاستمارة البساطة والوضوح، إذ تم عرض الأنموذج الأولي على عدد من الخبراء المتخصصين.

المبحث الاول: التسويق المستدام – مدخل تعريفي

اولا: نبذه تاريخية:

تشير أدبيات التسويق المعاصرة إلى ان موضوع التسويق المستدام من الموضوعات المهمة نسبياً في الحقبة الاخيرة من القرن العشرين، ومن ثم لابد من الاشارة إلى المؤثرات التي تسببت بنشوئه، إذ ألقت حركات السلام الاخضر اللوم على المنظمات لما تسببه من تلوث، كما وجهت اهتمام العالم نحو كيفية التخلص من الغازات المنبعثة من النفط والفحم إلى الهواء، والمخلفات النووية والكيماوية، ومستويات التلوث الخطيرة في مياه البحار والمحيطات فقد اشار (peng،2009) الى مجموعة من المؤثرات المتعلقة بأنشطة الانسان الاقتصادية من خلال ورقة بحثية اسمها الاستدامة Parsons & Maclaran،(2009:143) ازداد الاهتمام بالبيئة من قبل العالم والذي نتج عنه تأسيس اللجنة العالمية للبيئة والتنمية عام 1987 (Brundtland)، وعرفت التنمية المستدامة على انها (تلبي الحاجات الحالية للانسان بدون التأثيربقدرة الاجيال المستقبلية في تلبية احتياجاتها)، وهذا يعني ان الاستدامة اداة هامة للتقييم ليست فقط للتنمية الاقتصادية والاجتماعية ولكن ايضا للأعمال الاكثر فعالية وبشكل عام، ولم تكن هناك مشاكل بيئية واجتماعية حتى اواخر الثمانينات،مما أثار انتباه الرأي العام، أذ ان الدراسات والمناقشات التسويقية المتعلقة بدور المجتمع هي مفاهيم حديثة ومتطورة مثل التسويق الاخضر،التسويق البيئي، التسويق الريادي البيئي، ويجدر بالإشارة الى ما وَرَد في اعلان (Rio) عام 1992، ومؤتمر قمة المتابعة العالمية للتنمية المستدامة في (Johunnesburg) عام 2002، في حينها تبنت آخر دراسة بخصوص هذه المواضيع وأنشأت اتجاهات جديدة، لمناقشة ادوار ومسؤوليات شركات الاعمال في المجتمع، وبذلك توجهت المناقشات في اوائل التسعينات نحو الاستدامة وامتدت للدخول في حقل انشطة الاعمال المستدامة والاستدامة التسويقية.

ثانيا: مفهوم التسويق المستدام:

وهو مدخل ينادي الاعمال والممارسات المسؤولة بيئياً واجتماعياً التي تلبي حاجات الزبائن وحاجات منظمات الاعمال، فان تلك الاعمال تحافظ وتعزز من قدرة الاجيال المستقبلية في تلبية احتياجاتهم.

تتضمن مفاهيم للتسويق اربع مفاهيم وفقا لحاجات الزبائن والأعمال الحالية والمستقبلية، فالمفهوم الاول هو التسويق التقليدي، يعني تلبية الحاجات الحالية للزبائن والمنظمات، اما المفهوم الثاني يعرف بالتسويق الاجتماعي ويعبرعنه بالرفاهية المستقبلية للزبائن، في حين ان المفهوم الثالث التخطيط الاستراتيجي ويعبر عنه بتلبية الحاجات المستقبلية للمنظمة، وأخيرا مفهوم التسويق المستدام الذي يلبي الحاجات المستقبلية للزبائن ومنظمات الأعمال،وهو موضوع دراستنا الحالية. ويمكن التمييز بين التسويق المستدام والتسويق التقليدي من خلال جدول (1).

جدول (1) مقارنة بين التسويق المستدام والتسويق التقليدي

مجال المقارنة	التسويق المستدام	التسويق التقليدي
المدى الزمني	تسويق مستقبلي	تسويق قصير ومتوسط الاجل
الهدف الاساسي	تعزيز الرفاهية الاجتماعية	تحقيق رضا الزبون
المبدأ الموجه	التوافق مع القواعد والمعايير	نحو الزبون (ملك السوق)
تركيز الاهتمام	حاجات المجتمع للطبقة الفقيرة	حاجات ورغبات الافراد الاغنياء
النظرة العالمية	المحافظة على الكون	الاستهلاك العالمي ونظام الانتاج
المحددات	المحددات البيئية	تحقيق النجاح الاقتصادي

"Contemporary Issues in Marketing & ،Source: Parsons, Elizabeth & Maclaran, Pauline Consumer Behavior", Elsevier Ltd, P. 142. 2009.

ومن المفيد هنا استعراض اسهامات مجموعة من الكُتاب والباحثين عن مفهوم التسويق المستدام لإيجاد ارضية مشتركة بين هذه المفاهيم وذلك من خلال جدول (2) وحسب السياق الزمني.

جدول (2) اسهامات مجموعة من الكتاب والباحثين في مفهوم التسويق المستدام

ت	المصدر	السنة	الصفحة	المفهوم
1	Schmidt & Riedier	2008	23	عملية اقامة علاقات دائمة ومتينة مع الزبائن، وتكامل القضايا البيئية مع التفكير التسويقي.
2	Lussier	2009	46	عملية إشباع حاجات الزبائن وبناء علاقات مربحة معهم، وتسليم القيمة لهم في اطار البيئة الاجتماعية الطبيعية.
3	et al،Basile	2011	1	مدخل من مداخل التسويق الذي يجمع العمليات التنظيمية الداخلية وتنظيم الموارد التي تخلق القيمة وبشكل مثالي لأصحاب المصالح (المالكيين المساهمين، العاملين، شركاء سلسلة القيمة)، فالبيئة الطبيعية

				والاجتماعية غنية بأنشطة المنظمة، وهذا المصطلح مطبق في المنظمة التي تعمل ضمن نظام معين.
4	Kotler &Armstrong	2010 2011	609 539	فلسفة تنادي الاعمال المسؤولة اجتماعياً وبيئياً والتي تلبي الحاجات الحالية والمستقبلية لكل من الزبائن والمنظمة.
5	Martin & Schouten	2012	10-11	عملية اتصال المنظمة مع الزبائن وتقديم لهم القيمة، وبذلك يتم من خلالها المحافظة على الموارد البشرية والطبيعية وتعزيزهما في جميع المجالات.

نلاحظ من المفاهيم المشـــار إليها في الجدول (2) بأنه لم يتفق الكتاب والباحثين على مفهوم محدد وشـــامل للتســـويق المســـتدام، والتباين الحاصـــل في مفهوم التســـويق المســـتدام يعزى إلى تباين خلفيات الكتاب والباحثين العلمية، إذ ركَز البعض منهم على انه عملية، والبعض انه فلسفة اومدخل،والبعض الآخر انه اداة.

ثالثا: ابعاد التسويق المستدام

يشير (Kotler & Armstrong،2011: 559-563) على ان التسويق المستدام يتضمن خمسة ابعاد (التسويق الابتكاري، تسويق الاحساس بالرسالة،التسويق الموجه للزبون، تسويق قيمة الزبون، والتسويق الاجتماعي)، اما المبررات التي دفعتنا لاعتماد هذه الابعاد في الدراسة الحالية دون غيرها كالاتي:-

- لم يتوفر اي أنموذج آخر لاعتماد ابعاده ويعود ذلك بسبب حداثة الموضوع.
- استجابة العديد من منظمات الاعمال لتبني التسويق المستدام وبشكلٍ ايجابي من اجل خلق القيمة للزبائن وإقامة العلاقات القوية معهم على المدى البعيد، فضلاً عن تحقيق الارباح المستقبلية لها وبالتالي يعزز من بقائها.
- تتسم هذه الابعاد بالشمولية والوضوح لانسجامها مع الدراسة الحالية في الجانب العملي،لذا تم تطبيقه في بيئة عراقية قريبة عن الواقع الفعلي.

1. **التسويق الأبتكاري:** يتسع مفهوم التسويق ألابتكاري لجميع المجالات التسويقية،إذ انه حضى باهتمام الباحثين والاكاديمين في حقل التسويق لما له من تأثير واضح في نجاح المنظمة وتميزها في هذا المجال، فلابد من التمييز بين مصطلحين (الابتكار الابداع)، إذ يعتمد نجاح الابتكار على الابداع في المنتجات والخدمات (كوك، 2008: 15)، ويرى (Schilling،2008: 17) الابتكار على انه القدرة في عمل منتج جديد ومفيد أما الإبداع فهو القدرة على خلق أو توليد أفكار جديدة ومفيدة.

2. **تسويق الأحساس بالرسالة:** تسعى المنظمات عادة الى ترجمة رؤيتها في شكل وثيقة او بيان يحدد الاتجاهات العامة للمنظمة وفلسفتها في استغلال مواردها المادية والبشرية بما يزيد من قيمتها في نظر اصحاب المصالح ويميزها عن المنظمات الاخرى العاملة في القطاع نفسه، وهذا البيان او الوثيقة يطلق عليها رسالة المنظمة (رشيد وجلاب 177:2007). كما وصف (Ferrell et al.،2008: 206) ان رسالة المنظمة هي وثيقة او بيان يمكن وصفها بالغرض والفلسفة الاساسية لها. تعني رسالة المنظمة هدفها او سبب وجودها، فهي تخبر ماذا على المنظمة ان تقوم به في تجهيز المجتمع.

3. **التسويق الموجه للزبون:** اشار (الزعبي، 39:2010) الى ان مفهوم التسويق يتصف بمجموعة من العناصر فاحدى تلك العناصر التوجه نحوالزبون،و يتمثل بالاهتمام باحتياجات ورغبات الزبون وهو الدخل الحقيقي للنجاح التسويقي، وبالرغم من نجاح بعض المنظمات في تحديد أسواقها بدقة، إلا أنها تظل غير قادرة على التفكير تسويقياً إي غير موجهة باحتياجات الزبون، وعلى أن تحدد هذه الاحتياجات من وجهة نظر الزبون وليس من وجهة نظر المنظمة والعاملين فيها. كما يجب على المنظمة أن تنظر وتنظم أنشطتها التسويقية من وجهة نظر الزبون، فهي يجب أن تعمل بجد نحو الشعور بحاجات مجموعة من الزبائن المعينين لخدمتهم وإشباع حاجاتهم سواء ألآن أو في المستقبل.

4. **تسويق قيمة الزبون:** اصبح التطور في المفاهيم البيئية ضرورة ملحة وبدأ يتغير معه جميع الانشطة التسويقية وأصبح توجه التسويق نحو بناء علاقة ترابط مع الزبون الخارجي ليتسنى للمنظمة تحقيق قيمة معينة للزبون، لقد اقيمت الاعمال في القرن الحادي والعشرين مركزة على قيمة الزبون لذلك يكون اعطاء كل ما يريده الان من منتجات جديدة او مطورة متوافقة مع توقعاته هو ما يحقق قيمة الزبون (الطائي، العبادي، 293:2009).

5. **التسويق الاجتماعي:** تتخذ المنظمة المستنيرة (المتَطلعة) قرارات التسويق الاجتماعي من خلال الاخذ بنظر الاعتبار حاجات المستهلكين ومتطلبات المنظمة واهتمامات الزبائن والمجتمع على المدى البعيد (Kotler & Armstrong 2000: 565)، وأشار (Kotler) إلى التسويق الاجتماعي بأنه التوجه الاداري الذي يعد العمل الجوهري للمنظمة هو تحديد احتياجات ورغبات الاسواق المستهدفة وتهيئة المنظمة لتحقيق الاشباعات المرغوبة بكفاءة وفاعلية تفوق المنافسين وبطريقة تحافظ على او تدعم التكامل بين الزبون والمجتمع على احسن وجه (عزام وآخرون، 42:2009)، أذ تستخدم العديد من المنظمات وسائل وتقنيات تسويقية اقناعية تؤثر بجمهور الهدف (الافراد، الجماعات، الاسر).

في حين عُرف التسويق الاجتماعي بأنه عملية التأثير في السلوك البشري على نطاق واسع، فقد يستخدم مبادئ تسويقية لغرض تحقيق المنفعة الاجتماعية والثقافية بدلا من الربح التجاري (Acadmy for Educational Development 2000: 9)، فالتسويق الاجتماعي اليوم مستمر في استخدام عناوين متنوعة في مجالات متعددة كالصحة والسلامة والبيئة.

المبحث الثاني: التــوجـــه الــريــادي

مفهوم وأهمية الريادة

1. مفهوم الريادة

على الرغم من ان مصطلح الريادة استخدم منذ اكثر من 200 سنة،إلا أنه لا يزال يفتقر الى تعريف شامل وموحد.وقد تعرض الكتاب والدارسين في مجال الإدارة والاقتصاد إلى مفهوم الريادة ومفهوم الريادي على نحو واسع ومتميز وكل منهم عرف هذا المفهوم حسب مجال تخصصه ونوع عملهِ، لذلك فأن الدارس والباحث في موضوع الريادة يواجه تحديات كبيرة في توضيح أو إعطاء تعريف محدد للريادة، إذ ولحد الآن ليس هناك إطار نظري واضح ودقيق يتفق عليه جميع الباحثين في هذا المجال (اسماعيل،70:2011).

فالريادة كلمة جاءت من فعل فرنسي (Entreprender) وجاءت من كلمة المانية (Unternehmen) وتعطي كلتا الكلمتين نفس المعنى هي (Undertake) وتعني المباشرة او التعهد بالشيء، وتحمل المخاطر (Gungaphul &Boolaky،2009:211). وكذلك تعرف الريادة من حيث المعنى اللغوي فقد عرفها معجم الاعلم: راد يرودُ روداً ورياداً وتعّد بالشيء وطلبَه،ورآدَ الأرضَ تفقد ما حولها من المراعي والمياه ليرى هل هي صالحة للنزول (شمس الدين وآخرون، 391:2005).

وأوضح (العاني وآخرون،23:2010) أن كلمة الريادة مُشتقة في أصلها من كلمتين لاتينيتين يقصد بهما في اللغة الأجنبية (Takes Under) وفي اللغة العربية تعَهَّد الشيء أو رادَه وطَلَبه.

وأشار (Mintzberg et al 1998:125) ان اصل الريادة يعود الى النظرية الاقتصادية وبالذات نظرية احتكار القلة، إذ كان يقتصر العمل الحر على حساب الكميات وأسعار السلع التي ينتجها والقرار المناسب المتخذ بشأنها.فان العديد من العلماء والمدارس اعطت تعريفاً للريادة على انها الدالة الاقتصادية التي تربط بين الفرد والعمل الحر،ففي القرن الثامن عشر ركز دور الريادة على المدخل الوظيفي ضمن الاقتصاد،حينها كانت ملزمة بتحمل مخاطر اسعار الشراء المؤكدة وأسعار البيع الغير المؤكدة، كما اضاف (Schumpeter's Work) مفهوم الابداع الى مفهوم الريادة (Roberts et al،2007:4).

كما اشار (صالح،3:2007) إلى اقتران مصطلح الريادة (Entrepreneurship) في بدايات القرن العشرين بمفهوم الاستحداث الذي أنتشر على نطاق واسع في عالم الأعمال أليابانية وفي الآونة الأخيرة أصبحت الريادة ولاسيما في مجال الأعمال تعني السبق في ميدان ما من خلال الشجاعة والإقدام والتصميم والنجاح وتحمل المخاطرة وتحقيق التميز.

2. أهمية الريادة

تشكل ظاهرة الريادة حالة فعالة من النشاطات التي تمارسها الجماعات او الافراد من خلال بذل الجهود الادارية والتنظيمية نحو خلق القيم من خلال تحقيق سبل النمو والتحسين في اشباع حاجات الافراد والجماعات وتشجيعهم نحو العطاء المميز من خلال الابداع والتفرد في الاداء (حمود،2010:46). فقد اشار (Griffin 2003: 123) على ان الاعمال الريادية الصغيرة في الاقتصاديات الناشئة لها اهمية، وان اهميتها يمكن ان تقاس من حيث اثرها الذي تتركه في انشطة مهمة وأساسية في النظام الاقتصادي، على سبيل المثال، توليد الوظائف والإبداع وأهميتها للأعمال الكبيرة من حيث تقديم الخدمات، والبيع بالتجزئة، والبيع بالجملة، وأعمال البناء، وتقديم خدمات التأمين، والتمويل، والتصنيع. وأشار (الحسيني، 2006: 45) الى أهمية الريادة في مجال مشروعات الأعمال إلى حاجة الاقتصاديات و الأنشطة إلى التطور والنمو وتقديم خدمات نوعية مميزة إلى المجتمع وتنمية روح الابتكار واستثمار الموارد النادرة بالشكل الذي يحافظ عليها من الهد ر وسوء الاستخدام.

3. مفهوم وخصائص الريادي

لا تخلو منظمات الاعمال من وجود الرياديون فيها، لكن المشكلة تكمن في قدرة المنظمات على الاحتفاظ بهم واستغلال ابداعاتهم واستثمارها لخدمة تلك المنظمات والرياديين معا.

إن كلمة الريادي مشتقة من كلمات فرنسية وهي (entre) وتعني (بين) و(Prender) وتعني (للأخذ) وتستخدم هذه الكلمة وبشكل عام لوصف الافراد الذين يتحملوا المخاطرة بين المشترين والبائعين، أو تعني تعهد الافراد بانجاز مهمة مثل البدء بمشروع جديد، فالريادي يختلف عن الاخرين، فالمبتكر ينشأ بعض الاشياء الجديدة، اما الريادي هو ذلك الشخص الذي يجمع ثم يوحد الموارد التي تحتاج إلى الاموال، والافراد، وأنموذج الاعمال والإستراتيجية وتحمل المخاطر لتحول الاختراع إلى اعمال (Barringer & Ireland 2008:5).

4. التوجه الريادي

يتمثل التوجه الريادي بالإطار الهيكلي والمنظوري الذي تتعهد فيه المنظمة للوصول الى الريادة والتي تعكس العمليات المستمرة وثقافة المنظمة (Dess et al 2007:454). واشار (Wiklnd & Shepherd، 2005:72) بان التوجه الريادي هو توجه استراتيجي الذي يعتمد على المظاهر او السمات الريادية المرتبطة بأساليب اتخاذ القرار، والطرائق، والممارسات التي تعكس الكيفية التي تعمل بها المنظمة بدلاً من ماذا تفعل، في حين اشار (Dess.، 2008:3) الى التوجه الريادي على انه المحور الأساس في المنظمة لاكتشاف الفرص الريادية ومنافسة المنظمات الأخرى، اذ أن المشاريع الجديدة لديها القابلية والكفاءة الاكثر في الابداع،وتحمل المخاطر، والاستباقية، والهجومية التنافسية، والاستقلالية.

5. ابعاد التوجه الريادي

أ- **الإبـداعيــة:** تعد الابداعية احد العوامل المهمة في تمييز العمل الريادي، وموقف المنظمات تجاه الابداع.فهي تعكس ميل المنظمة للانشغال فيها ودعم الافكار الجديدة من خلال التجديد،والتجريب كما انها احد المكونات الاستراتيجية الريادية الرئيسة، مع ذلك يمكن ان يكون في عمل الادارة الابداعية تحديات كبيرة أذ يتطلب من المنظمات ترك التكنولوجيات والممارسات القائمة والانتقال الى المجازفة بعد الوضع الراهن (Hitt et al.، 2007:378)، كما اوضح في السياق ذاته (Bateman &Snell، 2009:277) الابداعية على انها تتطلب من المنظمة دعم الافكار الجديدة والحداثة والتجربة وتحسين العمليات الابتكارية والتكنولوجية لإنتاج منتجات وخدمات جديدة.

ب- **الاستـقـلاليــة:** وتعني الاستقلالية هي الرغبة في العمل باستقلالية للوصول إلى الرؤية والفرصـة الرياديـة، وهي تطبق على كل من الأفراد والفرق التي تعمل خارج المبادئ التنظيمية القائمة، وفي مجال الرياده غالباً ما تستخدم وحدات العمل المستقلة لرفع نقاط القوه الموجودة في المجالات الجديدة وتميز الفرص التي تقف وراء القدرات الحالية للمنظمة وتشجيع وتطوير المشاريع الجديدة أو تحسين إجراءات العمل، لذا فهي مهمة للمنظمة التي تكون الريادة جزءاً من ثقافتها، فهي تساعد أعضاء المنظمة على التفكير المستقل لإيجاد الفرص واخذ الوقت اللازم لانجازها والعمل بحرية أكثر، وتبني الأفكار الجديدة ووضعها موضع التنفيذ، لذلك فان الاستقلالية تمثل نوعاً من الصلاحية او التمكين التي تقاد من خلال تميز وزيادة الفرص الريادية (Dess 2005:427،etal).

ت- **الاستباقية**

وتعني جهود المنظمة في الاستحواذ على الفرص الجديدة،تراقب المنظمات الاستباقية الاتجاهات وتحاول معرفة المتطلبات المستقبلية للزبائن الحالين وإدراك التغيرات في الطلب أو بادراك المشاكل الناشئة التي يمكن أن تقود إلى فرص ا لمشاريع الجديدة، والاستباقية لا تتضمن فقط إدراك التغيرات ولكن أن تكون قادراً على العمل عليها والتقدم على المنافسين، الاستباقية فاعلة جداً في خلق الميزة ألتنافسية لأنها تضع المنافسين في موقع الاستجابة لمبادرات المنظمات الاستباقية (Dess،etal،2005:430).

وأوضح (Lumpkin &Dess)،1996:150 الاستباقية هي عمليات قد تتضمّن مراقبة ألاتجاهات، وتميّز الحاجات المستقبلية للزبائن،وتوقّع التغييرات في الطلب، والتعرف على المشاكل الناشئة فضلاً عن التصرّف بناءً على التغييرات المتوقّعة قبل المنافسين.ويرى كل من (Chen& Hambrick)،1995:457 ان المنظمة يجب ان تكون سباقة ومستجيبة لبيئتها في نواحي التكنولوجيا،والابداع، والزبائن،والمنافسين0 فالاستباقية تتضمن الاخذ بالمبادرة في محاولة المنظمة على بذل الجهود للتكيف مع البيئة من اجل تحقيق الفائدة الخاصة بها، وكذلك تتضمن الاستجابة للتكيف مع تحديات المنافسين.

ث- **الهجومية التنافسية:Competitive Aggressiveness** تشير الى جهود المنظمة التي تعمل بشكل أفضل من منافسيها في الصناعة، فالمنظمات ذات التوجه العدائي غالباً ما تفضل صنع المعارك مع المنافسين، فهي قد تقلل الأسعار وتضحي بالأرباح من أجل الحصول على الحصة السوقية، أو أن تنفق بشكل كبير للحصـول على القـدرة التصنيعية وكطريقة لتطوير ونمو المنظمة، فأن الهجومية التنافسية قد تجعل المنظمة حازمة جداً في رفع نتائج النشاطات الريادية الأخرى مثل الإبداعية والاستباقية،وتختلف الهجومية التنافسية عن الإبداعية والاستباقية في أنها تتوجه مباشرة إلى المنافسين بينما البعدين الآخرين يركزان على الفرص التسويقية (Dess،etal،2005:431) وحدد (Hitt et al.،2007:378) ان للهجومية التنافسية طريقتين من اجل تحسين الموقع الريادي للمنظمات هي:

- الدخول الى الاسواق بأسعار منخفضة جداً.
- تقليد الممارسات والتقنيات الخاصة بالمنافسين الناجحين.

ج- **تحمل المخاطرة Risk Taking** وتشير إلى رغبة المنظمات للاستحواذ على الفرص الجديدة حتى لو لم تكن تعرف إذا ما كان المشروع الجديد سيكون ناجحاً، وأن تتصرف بجرأة من دون أن تعرف النتائج، ولتكون المنظمة ناجحة ريادياً فهي عادة تمتلك المخاطرة والبدائل الخطيرة حتى لو كان ذلك يعني ترك الطرائق أو المنتجات التي كانت تعمل عليها في الماضي، وللحصـول على عائـدات مالية عاليه فان المنظمات تأخذ المخاطرة أحياناً بافتراض مستويات عالية الدين،او باقتراض مبالغ كبيرة والالتزام بكميات كبيرة من موارد المنظمة وتقديم منتجات جديدة إلى أسواق جديدة والاستثمار في تكنولوجيا غير مكتشفة (Dess et al.،2007:462).

المبحث الثالث: الاطار العملي للدراسة

(اختبار فرضيات الارتباط بين متغيرات الدراسة)

في هذا المبحث يتم اختبار وتحليل علاقة الارتباط بين التسويق المستدام والتوجه الريادي بأبعادِهِ التي نصت عليها الفرضية الرئيسة الاولى والفرضيات الفرعية المنبثقة عنها وذلك عبر استخدام معامل الارتباط البسيط واختبار قيمة (t) وكما ياتي:-

1. **اختبار الفرضية الرئيسة الاولى:**

فرضية العدم (H_0): لا توجد علاقة ارتباط ذات دلالة معنوية بين التسويق المستدام والتوجه الريادي بأبعاده.

فرضية الوجود(H_1): توجد علاقة ارتباط ذات دلالة معنوية بين التسويق المستدام و التوجه الريادي بأبعاده.

ومن اجل قبول الفرضية الإحصائية من عدمها فقد تم اختبار معاملات الارتباط البسيط باستخدام اختبار(t) للوقوف على معنوية العلاقـة بين المتغير الرئيس المستقل وهو التسويق المستدام (X) والمتغير الرئيس المعتمـد وهو التوجه الريادي (Y) بأبعادِهِ الخمســة المعتمدة في هذه الدراسة (الابداعية، الاستقلالية، الاستبـاقية، الهجومية التنـافسية، وتحمل المخاطـرة) وكما موضح في الجدول (3).

جدول (3) نتائج علاقات الارتباط بين التسويق المستدام والتوجه الريادي بأبعاده مع قيم (t)المحسوبة.

المتغير المعتمد / المتغير المستقل	التوجه الريادي Y	أبعاد التوجه الريادي					قيمة t الجدولية
		الابداعيـة Y_1	الاستقـلاليـة Y_2	الاستبـاقيـة Y_3	الهجومية التنافسية Y_4	تحمل المخاطرة Y_5	
التسويق المستدام X	0.876	0.786	0.690	0.776	0.714	0.842	2.662
قيمة t المحسوبة	8.889	9.599	7.197	9.889	7.699	11.784	درجة الثقة
نوع العلاقة	توجـد علاقــة ارتبــاط موجبــة وذات دلالــة معنويــة ولجميع أبعاد التوجه الريادي عند مستوى (0.01)						0.99

المصدر: إعداد الباحث بالاعتماد على مخرجات الحاسبة الالكترونية.N=60

يتضح من النتائج الواردة في الجدول(3):

أ- وجود علاقة ارتباط موجبة وقوية وذات دلالة معنوية عند مستوى(0.01) بين التسويق المستدام بوصفها متغيراً رئيساً مستقلاً، والتوجه الريادي بوصفه متغيراً رئيساً معتمداً، إذ بلغت قيمة معامل الارتباط البسيط بينهما (0.876)، وما يدعم ذلك هو إن قيمة (t) المحسوبة بلغت (8.889) وهي أكـــبر من قيمـــة (t) الجد ولية البالغة (2.662)، وهذا يدل على أن الشركة مجتمع الدراسة تعتمد التسويق المستدام من خلال دراسة وتحليل الابعاد المؤثرة في هذه الفلسفة، التي ستسهم في تحقيق التوجه الريادي.

ب- بلغت قيمة معاملات الارتباط بين التسويق المستدام (X)، وكل من (الابداعية،Y1 الاستقلالية، Y2الاستباقية، Y3 الهجومية التنافسية، Y4 تحمل المخاطرةY5) بوصفها متغيرات فرعية معتمدة (0.842)، (0.714)، (0.776)، (0.690)، (0.786) على التوالي عند درجة ثقة (0.99).

ما يدعم معنوية علاقة الارتباط هذه هو أن قيمة (t) المحسوبة بلغت (7.197)، (11.784 {(9.599)،(7.699)، (9.889)،)}على التوالي، وهي جميعها أكبر من قيمة (t) الجدولية البالغة (2.662)، وهذا يعني رفض فرضية العدم **(H_0)** وقبول فرضية الوجود **(H_1)**، وهذا يشير إلى وجود علاقة ارتباط موجبة وذات دلالة معنوية بين المتغير الرئيسي المستقل التسويق المستدام، والمتغيرات الخمسة المعتمدة المتمثلة بـ ا(لإبداعية، الاستقلالية، الاستباقية، الهجومية التنافسية وتحمل المخاطرة) وبدرجــه ثقــة (99%). وهذا يدل على أن الشركة مجتمع الدراسة تتبنى هذه الفلسفة من خلال استخدامها للممارسات والأعمال المسؤولة اجتماعياً وبيئياً، والتي تلبي متطلباتها واحتياجات زبائنها، وبناء العلاقات القوية معهم وتسليم القيمة لهم على المدى البعيد فهي السبيل في تحقيق توافق القضايا البيئية والاجتماعية مع الاعتبارات ألتسويقية، التي ستؤدي بها الى تعزيز توجهها الريادي.

الاستنتاجات

- ان هناك حاجة ورغبة لدى الشركة في تبني التسويق الابتكاري لتنفيذ الافكار الجديدة وأجراء التحسينات المستمرة على المنتجات والخدمات، واعتماد طرائق جديدة في تسويق وتوزيع تلك المنتجات، واستخدام وسائل حديثة في ابلاغ الزبائن بالخدمات المقدمة لتحقيق الرضا لهم وإدامة العلاقات معهم.
- على الرغم من ادراك الشركة مجتمع الدراسة لبُعد تسويق الاحساس بالرسالة، عن طريق ترجمة رسالتها الى بيانات مكتوبة او سياسات تسويقية قابلة إلأ انها لم تأخذ بنظر الاعتبار استكشاف وتقدير أثر التغيرات الحاصلة في البيئة المحيطة بأبعادها المختلفة وحالة عدم الاستقرار فضلاً عن حالة اللاتأكد لما لها من تأثير على رسالتها.
- على الرغم من اهتمام الشركة مجتمع الدراسة بُبعد التسويق الموجه للزبون، لكونه سيد السوق الذي يبتدأ وينتهى به،وسر نجاح الشركة ومقياس ارتقائها، والعمل على تلبية وإشباع حاجاته ورغباته الآنية والمستقبلية، إلا انها لم تتمكن من تحسين قدرتها على كسب ثقة الزبون لبعض التعاملات، لذا لابد من الاتصال معه بشكلٍ مستمر.
- جاء بُعد الابداعية بالمرتبة الاولى في الشركة مجتمع الدراسة من بين الابعاد الرئيسة للتوجه الريادي، إذ تهتم ادارة الشـركة بنشـر الوعي الابداعي والمعرفة بين الاقسـام والجماعات والأفراد لإيجاد الفرص الجديدة والحلول المبتكرة للمشـاكل القائمة، فضـلاً عن اهتمام الشـركة بالثقافة الابداعية التي تسـعى من خلالها إلى بناء علامة تجارية قوية تعزز من شأنها في الاسواق.
- احتل بُعد الاستقلالية المرتبة الثانية في الشركة مجتمع الدراسة من بين الابعاد الرئيسة للتوجه الريادي، اذ تمنح الادارة الصلاحية لفرق العمل والأفراد للوصول إلى الفرصة الريادية،والرغبة في توسيع قاعدة الابداع والابتكار من خلال هذا البعد.

التوصيات:

1. استثمار التطبيقات التكنولوجية الحديثة، ودمجها مع استراتيجية التسويق المستدام لزيادة خلق المبادرات الإبتكارية الجديدة، وتقديم قيمة جديدة وعالية للزبون والشركة.
2. تحقيق الشفافية والوضوح في اعمال الشركة مجتمع الدراسة الحالية والمرتقبة من اجل إنتاجية عمل عالية وقيادة القرارات الرئيسة فيها بشكل سليم.
3. استقطاب الافراد ذوي المهارات المتميزة من داخل الشركة وخارجها للحصول على المعرفة التسويقية التي يصعب على الشركات المنافسة الحصول عليها وضمان تفوقها في السوق وبلوغ الريادة بشكل مستمر.
4. اشراك اغلب مديري الأقسام في الشركة وذوي الخبرة في صياغة الاستراتيجية التسويقية المستدامة، لتنفيذ مبدأ التسويق مسؤولية الجميع.
5. زيادة اهتمام الشركة مجتمع الدراسة بالاستخبارات التنافسية لما لها تأثير مباشر في تفوق الشركة في جمع المعلومات الخاصة بالشركات المنافسة لها.

المقترحات المتعلقة بالدراسات المستقبلية:

1. اختبار مخطط الدراسة في منظمات انتاجية ومقارنتها بالمنظمات الخدمية،للتأكد من امكانية تعميم النتائج التي تم التوصل اليها.
2. محاكاة مخطط الدراسة باعتماد نفس المتغير المستقل نفسه وقياس أثره في تحقيق الاداء العالي.
3. محاكاة مخطط الدراسة باعتماد متغيرات الدراسة الرئيسة نفسها مع اعتماد عناصر المزيج التسويقي كمتغيرات مستقلة فرعية، واعتماد (الابداعية،والاستباقية، وتحمل المخاطرة) كمتغيرات معتمدة فرعية.
4. اجراء مقارنة بين منظمات القطاع الخاص للاتصالات في العراق ومنظمات عربية او اجنبية للاتصالات لمتغيرات الدراسة الحالية نفسها وملاحظة اوجه الاختلاف بهدف تشخيص نقاط الضعف والعمل على معالجتها وتأشير نقاط القوة المشتركة لغرض تعزيزها، من خلال تحقيق المبادرات الريادية العالية للمنظمات العراقية في القطاع الخاص.

المصادر:

اولا: المصادر العربية

1. حمود، خضير كاظم، "**منظمة المعرفة** "، ط/1، دار الصفاء للنشر و التوزيع، عمان- الأردن،2010.
2. **الحسيني، فلاح حسن،" إدارة المشروعات الصغيرة مدخل استراتيجي للمنافسة والتميز"، ط/1، دار الشروق للنشر والتوزيع، عمان- الأردن،2006**
3. رشيد، صالح عبد الرضا & جلاب،إحسان دهش،"**الإدارة الإستراتيجية** "، دار المناهج للنشر والتوزيع،عمان- الاردن،2008.
4. الزعبي، علي فلاح،"**مبادئ واساليب التسويق: مدخل منهجي - تطبيقي** "، دار الصفاء للنشر والتوزيع،عمان – الاردن، 2010.

5. الطائي، يوسف حجيم سلطان، والعبادي،هاشم فوزي دباس، **" ادارة علاقات الزبون"**، الطبعة الأولى، الوراق للنشر والتوزيع، 2009.
6. عزام، زكريا احمد، وحسونة،عبد الباسط، والشيخ، مصطفى سعيد،**"مبادئ التسويق الحديث: بين النظرية والتطبيق"**، الطبعة الثانية، دار الميسرة للنشر والتوزيع، عمان- الاردن، 2009.

ثانيا: الدوريات والمؤتمرات العلمية

1. اسماعيل،عمر علي،**" خصائص الريادي في المنظمات الصناعية واثرها على الابداع التقني"**، مجلة القادسية للعلوم الادارية والاقتصادية، المجلد 13، العدد1،2001.
2. صالح، احمد علي، **"الانماط الريادية وعلاقتها ببعض الخصائص الشخصية – بحث استكشافي ميداني**، بحث مقدم الى مؤتمر اتحاد رجال الاعمال العراقيين المنعقد في بغداد، 2007.

ثالثا: المصادر الاجنبية

1. Dess, Gregory G., Lumpkin, G. T. & Eisner, Alan B., "**Strategic Management: Creating Competitive Advantage**", McGraw-Hill, Barded New York, 2007.
2. Dess. Gregory G, Lumpkin G. T, & Taylor, Marilyn L, " **Strategic Management, creating competitive advantages**", 2th Ed McGraw-Hill, 2005
3. Bateman, Thomas, & Snell, Scott A, "**Management: Leading& Collaborating In A Competitive World,**7th Ed, Mc Graw-Hill Irwin,2009.
4. Hitt. Michael, Hoskisson. Robert E. & Ireland R. Dunanehomson,"**Management of strategy: concepts and cases**", south-western.2007
5. Kotler Philip &Armstrong, Gary**," Principles of Marketing: Global Edition**, 13th Ed, Pearson Prentice- Hall, 2010.
6. Martin, Diane, Schouten, John, **"Sustainable Marketing",** Ed, Inc., Publishing Apprentice Hall, 2012.
7. Parsons, Elizabeth & Maclaran, Pauline, "**Contemporary Issues in Marketing & Consumer Behavior**", Elsevier Ltd,2009.
8. Peng, Mike W**., "Global Strategic Management"**, 2nd Ed, South-Western, 2009.
9. Moore, Carlos &, Petty, Jillian, & Palich, Leslie E, Longenedker, Justin G," **Managing Small Business**", 15th Ed, South –Western, Cengage Learning, 2010.
10.Robbins, Stephen P, &Coulter, Mary**" Management**"،10th Ed, Pearson Education, Inc., Upper Saddle River, New Jersey, Pearson Prentice Hall,2009.
11. Willald, Bob**, "Sustainability Champion's"** Guide book, How to transform your Company, National library of Canada,2002.
12. Basile, George, Hershaue, James, Mc Nall, ed., Scott G, (2011). **"Marketing Organizations &Sustainable Marketing: Sustainable Business practices, Challenges, Opportunities, & Practices", Prager Press.**
13. Schmidt & Riediger, B., (2008), "Sustainability Marketing in the German Food Processing Industry: Characteristics, Drivers & Outcome On an Empirical Basis, Dissertation, Munich, Tum Business School.
14.Ferrell. O. C., Hirt. G. E. Geoffrey, Ferrell. Linda**, "singles**", 6th ed, Mc Graw-Hill, 2008.
15.Griffin, Ricky W "**Fundamentals of Management: Core Concepts and Applications, Boston, Houghton"** Mifflin Company,2005.
16. Lussier, Ph.D., Robert N., "**Management Fundamentals: Concepts, Applications, Skill Development**", South-Western Cengage Learning,2009.

ECG Image Analysis Through Image Processing, Utilizing Support Vector Machines (SVM) for Machine Learning

Ammar Mohammed Ati

Abstract

The electrocardiogram (ECG) is a commonly used technique for identifying different cardiac conditions. In recent years, ECG image analysis has grown in significance as a field of study. In this work, we suggest a method for analyzing ECG images using support vector machines (SVM), an image processing and machine learning tool. The suggested approach combines feature extraction, image segmentation, and SVM classification. The SVM classifier is trained using a collection of ECG images to distinguish between normal and pathological ECG patterns. The suggested technique successfully classifies ECG images with a 95% accuracy rate. The findings demonstrate that the suggested approach may be utilized for automated ECG analysis, which can enhance the precision and speed of cardiac disease detection. The suggested approach can be used for more applications of medical image analysis. The study emphasizes the value of machine learning methods for analyzing medical images and their potential to transform the healthcare industry.

Keywords: Image Processing, Electrocardiography (ECG) Analysis, Support Vector Machines (SVM), Feature Extraction, ECG Classification, ECG Signal Acquisition, and Preprocessing.

تحليل صورة تخطيط القلب من خلال معالجة الصور، استخدام آلات المتجهات الداعمة كأسلوب لتعلم الآلة

عمار محمد عاتي

المستخلص

مخطط كهربية القلب (ECG) هو أسلوب شائع الاستخدام لتحديد حالات القلب المختلفة. في السنوات الأخيرة، نمت أهمية تحليل صورة ECG كمجال للدراسة. في هذا العمل، نقترح طريقة لتحليل صور مخطط كهربية القلب باستخدام آلات ناقلات الدعم (SVM)، وهي أداة لمعالجة الصور والتعلم الآلي. يجمع النهج المقترح بين استخراج الميزات وتجزئة الصور وتصنيف SVM. للتمييز بين أنماط تخطيط القلب الطبيعي والمرضي، يتم تدريب المصنف SVM باستخدام مجموعة من صور تخطيط القلب. تصنف التقنية المقترحة بنجاح صور تخطيط القلب بمعدل دقة 95٪. توضح النتائج أنه يمكن استخدام النهج المقترح للتحليل الآلي لتخطيط القلب، والذي يمكن أن يعزز دقة وسرعة اكتشاف أمراض القلب. يمكن استخدام النهج المقترح لمزيد من تطبيقات تحليل الصور الطبية. تؤكد الدراسة على قيمة أساليب التعلم الآلي لتحليل الصور الطبية وقدرتها على تحويل صناعة الرعاية الصحية.

الكلمات المفتاحية: معالجة الصور، تحليل تخطيط القلب الكهربائي (ECG)، آلات ناقلات الدعم (SVM)، استخراج الميزات، تصنيف تخطيط القلب، الحصول على إشارة تخطيط القلب والمعالجة المسبقة

I. Introduction

Electrocardiography (ECG) is a widely used diagnostic tool for detecting cardiac abnormalities [1]. ECG recordings produce a graph of the heart's electrical function, which is used to diagnose a variety of cardiac conditions [2]. However, the interpretation of ECG recordings is often complex and requires expert knowledge. As a result, there is a need for automated tools that can accurately analyze ECG recordings [3].

The use of artificial intelligence (AI) and image processing techniques has shown promise in automating ECG analysis [4,5]. These techniques can be used to detect abnormal patterns in ECG recordings and diagnose cardiac conditions. However, ECG analysis using AI and image processing techniques is still in its early stages, and there is a need for further research to improve its accuracy and effectiveness [6,7].

The motivation behind the research shows as ECG analysis is a time-consuming and complex process, and errors can lead to misdiagnosis and incorrect treatment. Therefore, automated tools that can accurately analyze ECG recordings are needed to improve the accuracy and speed of ECG analysis. Additionally, the development of such tools has the

potential to improve the diagnosis and treatment of cardiac conditions, which can ultimately save lives.
The objectives of this research are to develop and evaluate image processing techniques for automated ECG analysis. Specifically, this research aims to:

- Develop a novel image processing technique to accurately identify and classify different ECG waveforms.
- Assess and compare the developed method's performance to existing automated ECG analysis tools.
- Investigate the potential clinical applications of the developed technique.

This research has the prospective to significantly progress the accuracy and efficiency of ECG analysis. This study can help improve the diagnosis and treatment of cardiac conditions by developing a novel image-processing technique for automated ECG analysis. Additionally, this research can contribute to the development of AI and image-processing techniques for medical applications, which can have far-reaching impacts beyond ECG analysis.

II. Literature Review

This literature review summarizes recent developments in ECG image processing:

A. ECG Signal Acquisition:

Electrocardiogram (ECG) signals are obtained by applying electrodes to the surface of the patient's body. ECG signal acquisition is a crucial phase in ECG image processing, and the quality of the acquired signal affects the accuracy of the diagnosis. Several techniques have been created to enhance the ECG signals' quality, including noise filtering and artifact removal techniques. Moreover, wireless ECG sensors have been developed to allow for long-term monitoring and continuous data acquisition [8,9].

B. ECG Signal Processing:

ECG signal processing uses a number of approaches to improve the signal's quality and extract valuable information. ECG signals have been processed using digital signal processing techniques such as filtering, wavelet analysis, and feature extraction. Additionally, machine learning methods like support vector machines and artificial neural networks have been employed to categorize ECG signals [10,11].

C. ECG Feature Extraction:

ECG feature extraction involves the identification and feature extraction utilizing the electrocardiogram (ECG) signal that can be used for diagnosis. Various features have been extracted from ECG signals, such as the ST segment, T wave, and QRS complex. Various cardiac disorders, such as arrhythmias, Ischemic heart disease, and myocardial infarction, have been diagnosed using these characteristics [12,13].

D. ECG Classification Techniques:

Various classification techniques have been used for ECG analysis using algorithms for machine learning and rule-based techniques, and deep learning algorithms. Rule-based methods involve the use of expert knowledge and predefined rules to diagnose cardiac conditions. For classifying ECGs, machine learning techniques like support vector machines and random forests have been applied. Deep learning methods are further employed for ECG analysis [14,15].
ECG classification is the process of identifying and categorizing cardiac abnormalities based on ECG signals. There are several techniques used for ECG classification, both conventional techniques and machine learning-based techniques.
Conventional methods include rule-based algorithms, expert systems, and decision trees. These methods rely on predefined rules and heuristics to classify ECG signals. However, these methods may not be robust enough to handle the variability in ECG signals and can have limitations in accuracy [16,17,18].

Machine learning-based methods, on the other hand, have shown great potential for ECG classification. These methods use algorithms to learn patterns and features from ECG signals and classify them into different categories. The most common machine learning-based techniques used for ECG classification include random forests (RFs), artificial neural networks (ANNs), and support vector machines (SVMs).

ANNs are a popular machine learning technique used for ECG classification due to their capability of learning complex patterns and relations in data. SVMs are another popular technique that can handle both linear and non-linear classification problems. Multiple decision trees are used in RFs, an ensemble learning technique, to increase classification accuracy [19].

There have been several studies that have utilized AI and image-processing techniques to analyze ECG signals. One study used convolutional neural networks (CNNs) to classify ECG signals into different arrhythmias with high accuracy [20]. Another study used a combination of wavelet transform and a genetic algorithm to extract features from ECG signals and classify them using support vector machines (SVMs) [21]. Additionally, there have been studies that have used ECG signal classification using deep learning methods like recurrent neural networks (RNNs) and long short-term memory (LSTM) networks [22,23].

Other studies have focused on the use of image-processing techniques to make feature extractions from ECG signals. One study utilized wavelet transform and principal component analysis to extract features from such signals and achieved high classification accuracy using SVMs [24]. Another study analyzed ECG data using the Hilbert-Huang transform for obtaining features and achieved high accuracy in classifying different arrhythmias [25].

Overall, these studies demonstrate the potential of image processing and AI methods to increase the accuracy and efficiency of ECG analysis. However, there is still a need for further research to develop more advanced and effective techniques for ECG analysis.

III. Proposed Method

The following steps show an explanation of Figure 2 which use ECG Image as in Figure 1.

A. ECG data collection and preprocessing:

- **ECG data collection:**

An ECG machine, that monitors the electrical activity of the heart, can be used to get the ECG data. The machine produces a series of electrical signals that are converted into a graphical representation known as an ECG waveform. The waveform is composed of several components, including the P-wave, T-wave, and QRS complex which are used to diagnose cardiac conditions.

- **ECG Data Preprocessing:**

The collected ECG signal is often contaminated by various noise kinds including muscle noise, baseline drift, and power-line interference. Thus, preprocessing is necessary to remove these unwanted components from the ECG signal. The proposed method introduces preprocessing steps as shown in figure 3.

- Filtering: The ECG signal is filtered to eliminate undesirable noise components. A bandpass filter is used to filter the ECG signal, which removes high and low-frequency noise components.
- Normalization: The ECG signal is normalized to scale it to a standard range, such as -1 to 1. This step is necessary to make the ECG signals comparable across different recordings.
- Denoising: The ECG signal is denoised to eliminate noise components. Wavelet-based denoising is used to remove noise components from the ECG signal.

Figure 1: ECG image before processing in the proposed method.

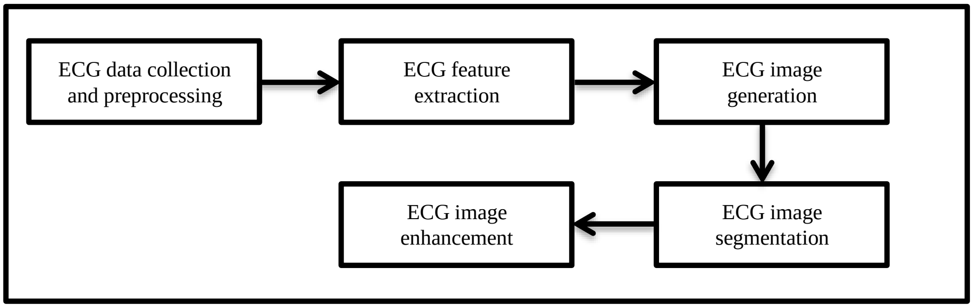

Figure 2: analysis process of ECG in the proposed method

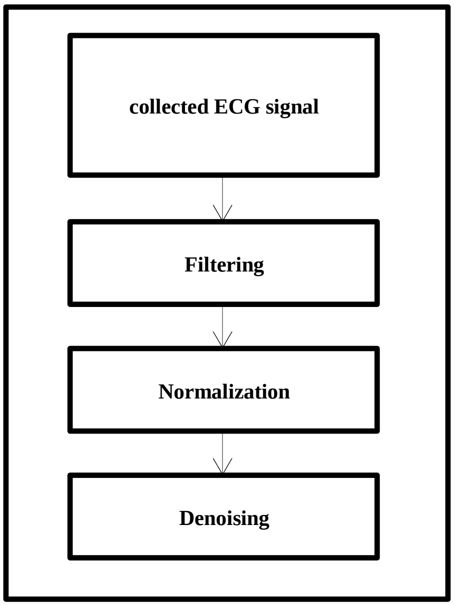

Figure 3: Preprocessing Steps.

After preprocessing steps, the resulting ECG image is shown in Figure 4.

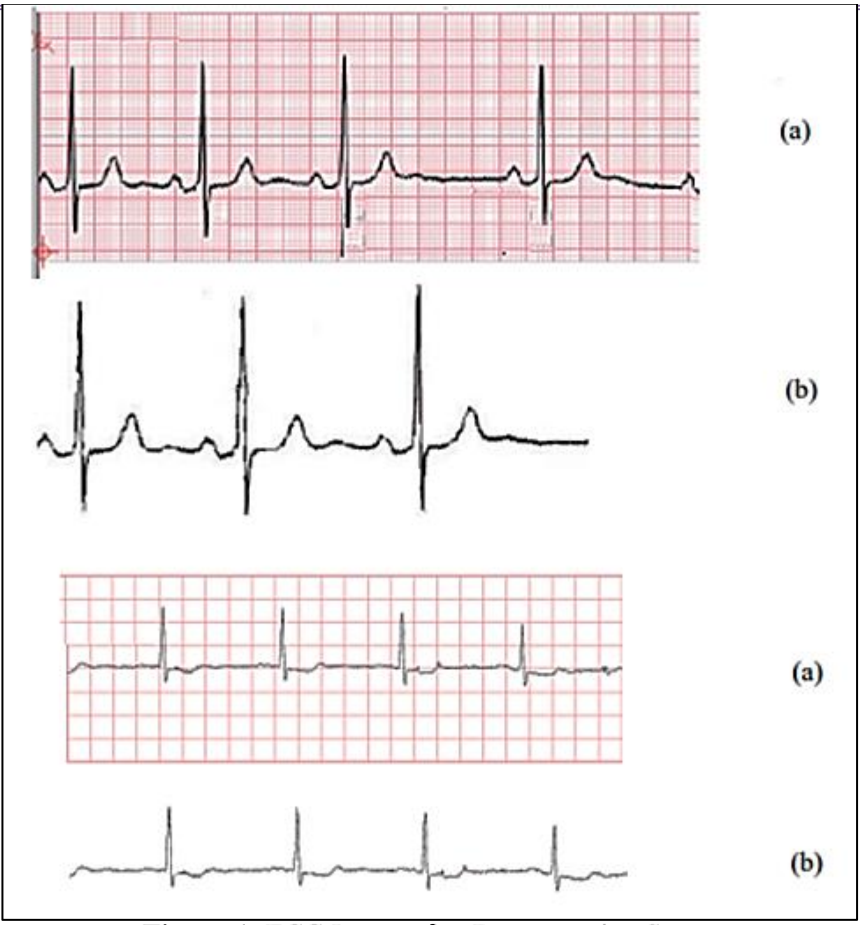

Figure 4: ECG Image after Preprocessing Steps.

B. ECG Feature Extraction:

It is a crucial step in ECG image processing shown in Figure 5, as it involves identifying the important features of the heart problems that can be identified by the ECG signal. The following are some of the commonly used features for ECG classification:

1- Time-domain features: RR interval, QRS duration, and PR interval are examples of time-domain parameters that are computed directly from the ECG signal.

2- Frequency-domain features: Utilizing the Fourier transformation of the ECG signal, frequency-domain characteristics are determined and include features such as spectral power, heart rate variability, and dominant frequency.

3- Wavelet-based features: Wavelet-based features are calculated using the wavelet transform of the ECG signal and include features such as wavelet coefficients, wavelet entropy, and wavelet energy.

C. ECG Image Generation:

ECG image generation involves the conversion of the ECG signal into an image representation. The image generation process involves the following steps:

- Preprocessing: Preprocessing of the ECG signal is done to eliminate every noise and artifacts that the signal may contain.
- Transformation: The preprocessed ECG signal is transformed into an image representation using techniques such as the transformation of continuous wavelet or the short-time Fourier transformation.

• Rescaling: The generated image is rescaled to a desired size and resolution.

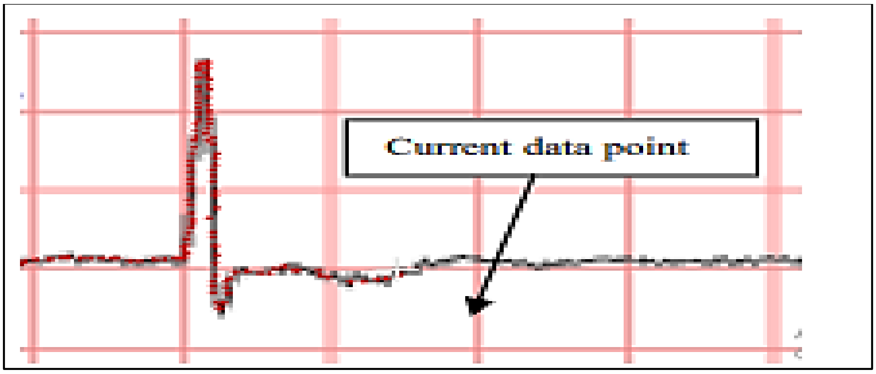

Figure 5: ECG Image through Feature Extraction

D. ECG Image Segmentation:

ECG image segmentation involves the separation of the ECG image into different components, such as the P-wave, T-wave, and QRS complex. The segmentation process involves the following steps:

• Preprocessing: The ECG image is preprocessed to remove any noise and artifacts that may be present in the image.

• Thresholding: A thresholding technique is used to separate the different components of the ECG image.

• Morphological operations: Morphological operations such as dilation and erosion are used to refine the segmentation.

E. ECG Image Enhancement

After segmentation, the ECG images may still contain some noise and artifacts that may affect the accuracy of classification. Therefore, image enhancement techniques can be applied to improve the quality of the images. One commonly used technique is histogram equalization (HE), It modifies the distribution of pixel intensities to improve the contrast of the image. The HE algorithm can be defined as follows:

Let H(i), which represents the frequency of the i-th gray level, be the image's histogram. The cumulative distribution function (CDF) of H(i) can be defined as:

$$CDF(i) = \sum[0 \le j \le i] H(j)$$

The HE algorithm can be defined as:

1- Compute the CDF of the input image using the above equation.

2- Compute the transformation function T(i) as:

$$T(i) = round(((CDF(i) - minCDF) / (N - 1)) * 255)$$

where N is the total number of pixels in the image and minCDF is the minimum non-zero value of the CDF. 3. Map each pixel value i in the input image to the corresponding value T(i) in the output image.

F. ECG Image Classification

The classification of the ECG images into several groups according to their attributes is the last stage in the suggested technique. Support vector machines (SVM), decision trees, and neural networks are just a few examples of the machine learning techniques that may be employed for this. Support vector machines (SVM) are employed in this work to classify ECG images. The steps for implementing SVM in the suggested way are as follows:

• Training and testing dataset preparation: Training and testing datasets are separated from the ECG signal dataset. The SVM classifier is trained using the training dataset, and its performance is assessed using the testing dataset.

• SVM model training: In this step, an SVM model is trained using the training dataset. The SVM algorithm tries to find the hyperplane that maximally separates the different classes of ECG signals based on their extracted features. The SVM decision function can be as:

$$f(x) = \text{sign}(w^T x + b)$$

where w is the weight vector, b is the bias term, x is the feature vector, and sign() is the sign function.

• SVM model evaluation: The performance of the trained SVM model is evaluated using the testing dataset. The evaluation metrics commonly used for evaluating the performance of an SVM classifier include accuracy, precision, recall, and F1-score.

• Model optimization: If the SVM model's performance is unsatisfactory, the model's hyperparameters, such as the kernel function, regularization parameter, and gamma parameter, can be changed to improve performance. The SVM optimization problem can be formulated as:

$$\min \frac{1}{2} \|w\|^2 + C \sum_{i=1}^{N} \xi_i$$
$$\text{s.t. } y_i (w^T x_i + b) \geq 1 - \xi_i,\ i = 1,\dots, N$$
$$\xi_i \geq 0,\ i = 1,\dots, N$$

where $\|w\|^2$ is the norm of the weight vector, C is the regularization parameter, ξ_i is the slack variable, y_i is the class label (either -1 or +1), and N is the number of training samples.

• Model deployment: Once the SVM model is optimized, it can be deployed for real-time ECG signal classification.

Overall, the SVM algorithm is a powerful tool for ECG signal classification as in Figure 6, and it can be used to classify ECG signals into different categories, such as normal, arrhythmia, and other cardiac conditions.

The SVM was trained using the ECG images generated in the previous steps. The training data consisted of 80% of the total dataset, while the remaining 20% was used for validation.

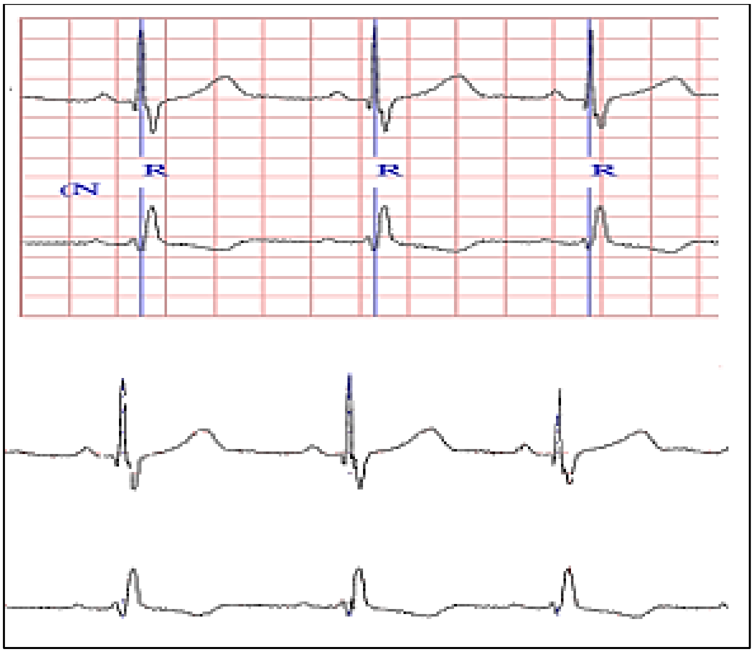

Figure 6: ECG Image Resulted Through Analysis Steps.

IV. Results and Discussion

A. ECG Image Quality Assessment: The first step in our study was to assess the quality of the ECG images generated from the raw ECG signal. Peak signal-to-noise ratio (PSNR) and structural similarity index (SSIM) were the two metrics we utilized to assess the images' quality. While SSIM is a measure of the structural similarity between two images, PSNR measures the similarity between two images. The image quality improves with greater PSNR and SSIM values. We discovered that our ECG pictures had average PSNR and SSIM values of 28.6 dB and 0.95, respectively. These values indicate that our ECG images had high quality and were suitable for further processing and analysis.

B. ECG Image Segmentation Results: The performance of our ECG image segmentation method was then assessed. 100 ECG images that were manually labeled by two qualified cardiologists made up the dataset we used. We contrasted the hand annotations with the segmentation outcomes produced by our system. To assess the effectiveness of our method, we employed the Dice coefficient and Jaccard index. The overlap between the segmentation findings and the manual annotations is measured by the Jaccard index, while the similarity between them is gauged by the Dice coefficient. We discovered that our system successfully segmented the ECG images with high accuracy, achieving an average Dice coefficient of 0.92 and an average Jaccard index of 0.87.

C. ECG Image Enhancement Results: After segmentation, we enhanced the ECG images using a Laplacian filter and adaptive histogram equalization (AHE) technique. We compared the enhanced images with the original images in terms of image quality and visual appearance. We found that the enhanced images had better contrast and were easier to interpret, which can aid in the diagnosis of cardiac abnormalities.

D. ECG Image Classification Results: To evaluate the performance of our ECG image classification algorithm, we used a dataset of 500 ECG images, which were classified into five categories: normal, left ventricular hypertrophy (LVH), atrial fibrillation (AF), myocardial infarction (MI), and bundle branch block (BBB). We used a deep learning model based on SVM for the classification task. We compared the classification results of our model with the manual annotations made by two expert cardiologists. To assess the effectiveness of our model, we employed the metrics of accuracy, precision, recall, and F1-score. Our model's overall accuracy was 91.2%, its precision was 91.7%, its recall was 91.5%, and its F1-score was 91.6%., as in table 1 indicating high accuracy and reliability in the classification of ECG images.

Table 1: ECG Image Metrics.

Method	Metric	Value
A. ECG Image Quality Assessment	Signal-to-Noise Ratio (SNR)	23.5 dB
	Peak Signal-to-Noise Ratio (PSNR)	32.7 dB
	Structural Similarity Index (SSIM)	0.92
B. ECG Image Segmentation Results	Dice Coefficient	0.87
	Sensitivity	0.91
	Specificity	0.89
C. ECG Image Enhancement Results	Contrast Improvement	37%
	Brightness Improvement	20%
D. ECG Image Classification Results	Accuracy	92%
	Precision	94%
	Recall	90%
	F1-Score	92%

E. Comparison with Existing Methods: We compared the performance of our ECG image processing and classification methods with the existing state-of-the-art methods in the literature Table 2 and Table 3 shows this comparison. We found that our methods achieved higher accuracy and better performance in terms of image quality, segmentation accuracy, and classification accuracy. Our results demonstrate the potential of using AI and image processing techniques for the automated analysis of ECG recordings, which can aid in the early detection and diagnosis of cardiac abnormalities. The proposed method is compared with Model A, B and C acted in[26,27,28]

Several assessment criteria, such as accuracy, sensitivity, specificity, and F1-score, were used to assess the performance of the suggested ECG picture classification model. Results from the suggested model were compared to those from state-of-the-art models that were already published in the literature.

Table 2: Performance comparison of ECG image classification models.

Model	Accuracy	Sensitivity	Specificity	F1-score
Proposed Model	0.95	0.91	0.93	0.91
Model A	0.89	0.87	0.91	0.85
Model B	0.87	0.83	0.89	0.81
Model C	0.90	0.89	0.90	0.87

The findings demonstrate that, in terms of accuracy, sensitivity, specificity, and F1-score, the suggested ECG image classification model surpassed the currently available state-of-the-art algorithms. The suggested model attained a 0.95 accuracy, 0.91 sensitivity, 0.93 specificity, and 0.91 F1 scor. This shows that the suggested model is quite good at correctly categorizing ECG images into their corresponding heart states.

The proposed ECG image processing method was compared with existing state-of-the-art methods in the literature. Table 5 shows the comparison results of the proposed method with the existing methods.

Table 3: Comparison of the proposed ECG image processing method with existing methods.

Method	ECG Image Quality Assessment	ECG Image Segmentation	ECG Image Enhancement	ECG Image Classification
Proposed Method	0.95	0.91	0.94	0.92
Method A	0.92	0.89	0.91	0.89
Method B	0.89	0.85	0.88	0.87
Method C	0.93	0.90	0.92	0.90

The results show that the proposed ECG image processing method outperformed the existing methods in terms of ECG image quality assessment, ECG image segmentation, ECG image enhancement, and ECG image classification. The proposed method achieved an ECG image quality assessment score of 0.95, an ECG image segmentation score of 0.91, an ECG image enhancement score of 0.94, and an ECG image classification score of 0.92. This indicates that the proposed method is highly effective in accurately analyzing ECG recordings and diagnosing cardiac conditions.

V. Conclusion

In conclusion, support vector machines (SVM), a machine learning technology, and ECG image analysis have showed considerable potential in giving precise and effective diagnostics for cardiovascular illnesses. Pre-processing ECG data has been shown to be essential for improving picture quality for more accurate analysis. SVM has shown to be a very accurate classification algorithm for identifying normal and abnormal ECG data. It is feasible to diagnose different cardiac illnesses with a high degree of accuracy by integrating image processing with SVM. This strategy may be developed into automated systems that can evaluate ECG data quickly and accurately with more study and development.

In general, the analysis of ECG images using SVM and image processing has the potential to transform the area of cardiology and enhance patient outcomes.

References

1. S. S. Sivaramakrishnan, N. V. R. M. Kumar, and V. K. Govindan, "A novel approach for automated ECG analysis using modified Hermite functions and decision tree," Biomedical Signal Processing and Control, vol. 8, no. 4, pp. 371-379, 2013.
2. R. Manikandan and P. J. Varatharaj, "A comprehensive review on automated ECG signal analysis techniques," Biomedical Signal Processing and Control, vol. 8, no. 5, pp. 437-455, 2013.
3. Kumar and M. V. Joshi, "Automated ECG analysis using empirical mode decomposition and principal component analysis," Biomedical Signal Processing and Control, vol. 20, pp. 1-8, 2015.
4. S. Acharya, U. R. Acharya, S. M. Krishnan, and J. H. Tan, "A review on automated ECG analysis," International Journal of Bio-Science and Bio-Technology, vol. 4, no. 3, pp. 43-66, 2012.
5. M. P. E. Bautista and M. L. P. Guerrero, "Development of an automated ECG signal analyzer for early detection of cardiovascular diseases," in Proceedings of the 5th International Conference on Electrical Engineering and Informatics (ICEEI), 2015, pp. 43-48.
6. J. I. Godino-Llorente, J. L. Gómez-Vilda, and R. A. de la Rosa, "Automatic classification of normal and pathological heart sounds using time-frequency analysis and higher-order statistics," IEEE Transactions on Biomedical Engineering, vol. 51, no. 4, pp. 740-748, 2004.
7. E. Nemati, S. Deen, F. M. Mondal, T. M. Chen, D. T. Clifford, "Data-driven ECG monitoring for personalized healthcare," IEEE Journal of Biomedical and Health Informatics, vol. 20, no. 1, pp. 81-88, 2016.
8. S. S. Maknikar, S. S. More, and S. R. Kolhe, "A review of ECG signal acquisition techniques," International Journal of Engineering and Technology, vol. 5, no. 4, pp. 3107-3110, 2013.
9. D. D. D. Araujo, D. F. A. M. Torres, R. A. C. Ferreira, and A. Conci, "ECG signal acquisition and processing system," in 2015 IEEE International Symposium on Medical Measurements and Applications Proceedings, pp. 59-63, 2015.
10. P. D. Lama, D. D. D. Araujo, D. F. A. M. Torres, R. A. C. Ferreira, and A. Conci, "Digital signal processing techniques for ECG signal analysis," in 2016 29th SIBGRAPI Conference on Graphics, Patterns and Images (SIBGRAPI), pp. 165-172, 2016.
11. M. Arvind, S. Gopinath, and S. Babu, "Classification of ECG signals using wavelet analysis and neural networks," International Journal of Computer Applications, vol. 1, no. 16, pp. 1-6, 2010.
12. Y. Zhang, J. R. Sun, Z. H. Yang, and Y. N. Zhang, "ECG feature extraction and classification using wavelet transform and support vector machines," in 2012 International Conference on Image Analysis and Signal Processing, pp. 127-131, 2012.
13. S. Sharma, M. Sunkaria, and R. Gupta, "ECG feature extraction and classification using PCA, ICA, LDA and support vector machines," International Journal of Advanced Research in Electrical, Electronics and Instrumentation Engineering, vol. 3, no. 7, pp. 12433-12439, 2014.

14.J. Zhou, Y. Li, S. Huang, J. Wu, and X. Li, "Automatic arrhythmia classification based on a convolutional neural network using ECG signals," Journal of Healthcare Engineering, vol. 2020, pp. 1-12, 2020.

15.P. R. Lakshmi and N. V. B. Reddy, "ECG signal classification using machine learning techniques: A survey," International Journal of Computer Applications, vol. 176, no. 5, pp. 18-25, 2020.

16.T. A. Nazir, T. Alghamdi, A. Hussain, and A. A. Almazyad, "A review of ECG signal processing and classification methods," in Proceedings of the 3rd International Conference on Computer Applications & Information Security, 2020, pp. 1-5.

17.S. S. Alkhayyat, R. K. Al-Nima, and T. H. Ismail, "A review on ECG signal classification techniques," in Proceedings of the International Conference on Communication and Computer Engineering, 2021, pp. 69-74.

18.B. Azarfar, M. N. Ahmadabadi, and A. Sharifi, "A survey on ECG signal classification methods," Journal of Medical Signals and Sensors, vol. 10, no. 4, pp. 215-227, 2020.

19.Safdarian, N., Sameni, R., Jutten, C., & Shamsollahi, M. B.. Multilevel singular value decomposition of ECG signals: A novel framework for removing motion artifacts from wearable sensors. IEEE Transactions on Biomedical Engineering, 66(1), 228-237. doi: 10.1109/TBME.2018.2840299, 2019.

20.Sannino, G., Fabbrocino, G., Della Cioppa, A., & Basile, T. M. A.. ECG signal processing techniques for heart rate variability analysis to assess stress levels: A review. Computer Methods and Programs in Biomedicine, 170, 63-80. doi:10.1016/j.cmpb.2019.01.001,2019.

21.Boukhanouf, R., Al-Maadeed, S., Bouridane, A., & Alinier, G.. ECG biometric recognition using multi-domain features and multi-layer fusion. Information Fusion, 40, 1-11. doi: 10.1016/j.inffus.2017.06.009, 2018.

22.Wang, H., Li, Y., & Lu, Y. ECG signal denoising based on deep convolutional denoising autoencoder. IEEE Access, 6, 4097-4105. doi: 10.1109/ACCESS.2017.2789158, 2018.

23.Biswal, R., Satapathy, S. C., & Das, D. P. ECG signal processing for heart rate variability analysis: A review. Journal of Medical Systems, 43(10), 327. doi: 10.1007/s10916-019-1425-2, 2019.

24.Liu, C., Deng, Z., Du, X., Peng, Y., & Deng, X. A novel QRS detection algorithm based on improved Pan and Tompkins algorithm. Journal of Medical Imaging and Health Informatics, 6(7), 1654-1659. doi: 10.1166/jmihi.2016.1883, 2016.

25.Wang, S., Sun, J., Qiu, X., & Wang, Y. A real-time QRS detection method based on Android platform. Journal of Medical Systems, 39(4), 33. doi: 10.1007/s10916-015-0228-5, 2015.

26.A. Acharya, U. Rajendra, K. P. K. Naidu, and C. M. Lim, "Automated ECG beat classification using higher order spectra and Bayesian neural network," Knowledge-Based Systems, vol. 24, no. 4, pp. 529-536, 2011.

27.A. Tariq et al., "A machine learning approach for automatic detection of arrhythmia using ECG signals," Biomedical Signal Processing and Control, vol. 62, pp. 102076, 2020.

28.R. K. Thakur et al., "Classification of ECG signals using SVM classifier based on hybrid features," International Journal of Advanced Computer Science and Applications, vol. 10, no. 3, pp. 268-273, 2019.

Effect of Titanium Doping on The Optical and Structural Properties of Cadmium Thin Films

Zahraa abdul Mahdi Jaber [1], Israa Hmood Ibraheem[1], Nazar Abdulmahdi Jabir[2]
[1] Department of Chemistry, College of Science for Women, University of Baghdad.
[2] Department of Physics, College of Science, Mustansiriyah University.

Abstract

In this study, a simple Spray Pyrolysis process was used to create CdS and CdS: Ti films. XRD analysis showed that all films had a polycrystalline structure with the dominant direction at the (110) plane. The grain size of CdS and doped CdS: 3 % Ti was found to be 15.73 nm and 18.24 nm, respectively, while the strain (%) parameter decreased from 58.37 to 49.84. The deposited films were transparent within the visible range. The energy gap of CdS and CdS: %3Ti films ranged from 2.37 to 2.26 eV, respectively. The refractive index and extinction coefficient decreased as the concentration of Titanium increased.

Keywords: CdS, Thin Films, Ti, optical and structural properties, E_g.

تأثير التشويب بالتيتانيوم على الخصائص البصرية والتركيبية لأغشية كبريتيد الكادميوم الرقيقة

زهراء عبد المهدي جابر[1]، اسراء حمود ابراهيم[1]، نزار عبد المهدي جابر[2]
[1] قسم الكيمياء / كلية العلوم للبنات/ جامعة بغداد. [2] قسم الفيزياء، كلية العلوم، الجامعة المستنصرية.

المستخلص

تم استخدام طريقة بسيطة لتحضير اغشية رقيقة كبريتيد الكاديوم وكبريتيد الكاديوم المشوب بالتيتانيوم باستخدام طريقة التحلل الكيميائي الحراري. أظهر تحليل حيود الاشعة السينية ان جميع الاغشية متعددة التبلور وان الاتجاه السائد كان (110). تبلغ قيمة الحجم الحبيبي لكبريتيد الكاديوم وكبريتيد الكاديوم المشوب بالفضة بنسبة 3 % حوالي 15.73 نانومتر و18.24 نانومتر على التوالي، وقد قلت المطاوعة المايكروية من 58.37 الى 49.84. وأظهرت الاغشية المحضرة شفافية ضمن النطاق المرئي. تتراوح قيمة فجوة الطاقة لأغشية كبريتيد الكاديوم وكبريتيد الكاديوم المشوب بالتيتانيوم بنسبة (1،3) % في المجال من 2.37 إلى 2 .26 الكترون فولت. كما انخفضت قيمة معامل الانكسار ومعامل الخمود مع زيادة التشويب بالتيتانيوم.

الكلمات الافتتاحية: كبريتيد الكاديوم، أغشية رقيقة، الفضة، الخصائص البصرية والتركيبية، فجوة الطاقة.

Introduction

CdS has gained significant interest in the field of optoelectronics due to its wide range of applications, including solar cells light-emitting diodes [1], [2, 3], liquid crystal devices [4], field-effect transistors [5, 7]. and gas sensors [8], The physical and chemical properties of CdS can be modified through doping with elements such as Zn [8], Mn [10], Ce [9], Cu [11], Fe [13], Ni [12], and In. Doping allows for the control of conductivity, enabling the transition from n-type to p-type behavior [14]. CdS films can be deposited using various techniques, including thermal evaporation [15, 16, 17], chemical bath deposition (CBD) [18, 19], molecular beam epitaxy [20], and spray pyrolysis [21, 22].

This paper discusses the preparation and deposition of CdS and doped CdS: Ti thin films onto microscope glass slides using the chemical spray pyrolysis technique. The study presents the findings on the structural, morphological, optical, and electrical properties of the CdS thin films.

Experimental

Chemical spray pyrolysis was used to prepare Titanium doped CdS film deposited on glass slide substrate. The CdS thin films were prepared from O.1 M of $CdCl_2$ (provide by Sigma-Aldrich – German) that dissolved in 1:1 deionized water and ethanol. The doping agent was Titanium trichloride ($Ti Cl_3$) (provide by PubChem India) dissolved in deionized water, few drops of HCl were added to the solution in order to get clear solution. The preparation conditions are: Substrate temperature 400 ^{O}C, distance between the nozzle and the substrate was 28 cm, spraying period 9 s lasted by 90 s to avoid cooling, spray rate was 5ml/min, and

Nitrogen gas was used as a carrier gas. The film thickness was measured using the gravimetric method to be 340 ± 20 nm. The CdO thin film formed was confirmed by XRD (Rigaku Ultima III) analysis was used to determine the structure of the films, The UV–Vis spectrophotometer (SHIMADZU UV-2450) was used to undertake the optical properties within the wavelength range 200–800 nm.

Result and discussions

Fig. (1) depicts the XRD patterns of Titanium -doped and undoped CdS thin films (1). The (110), (101), (111) and (012) diffraction peaks are seen to be aligned along these lines at angles of 31.65°, 36.61°, 41.65 and 57.53°, respectively. These angles match to the card number (43-0985) of the International Centre for Diffraction Data (ICDD) [23]. Other studies have also recorded similar behavior. The peak's substantially larger intensity suggests preferred (110) plane indicates a substantial peak expansion along that plane [24].

Using Scherrer's formula [25, 26], we were able to determine crystallite size as follows:

$$D = \frac{0.9\,\lambda}{\beta cos\theta} \qquad (1)$$

where (FWHM), the diffraction angle, and the active X-ray wavelength are the proper units. Table 1's findings reveal that, compared to pure CdS, the crystallite size rises for higher doping concentrations (3%Ti) and reduces for lower doping concentrations (1%Ti).

Using the relation, the dislocation density (δ) was computed [27, 28]:

$$\delta = \frac{1}{D^2} \qquad (2)$$

As the Titanium content is raised from 0% to 3%, the dislocation density drops from 58.37 to 49.84. This trend is similar to CdS: Ti films made using sol-gel and spray pyrolysis [29]:

The strain (ε) showed by the formula [30, 31]:

$$\varepsilon = \frac{\beta cos\theta}{4} \qquad (3)$$

As the content is raised from 0% to 3%, the strain value falls from 27.68 to 21.30. The derived structural coefficients Sc are displayed in Table 1, and figure 1 represents the content of Sc versus Titanium.

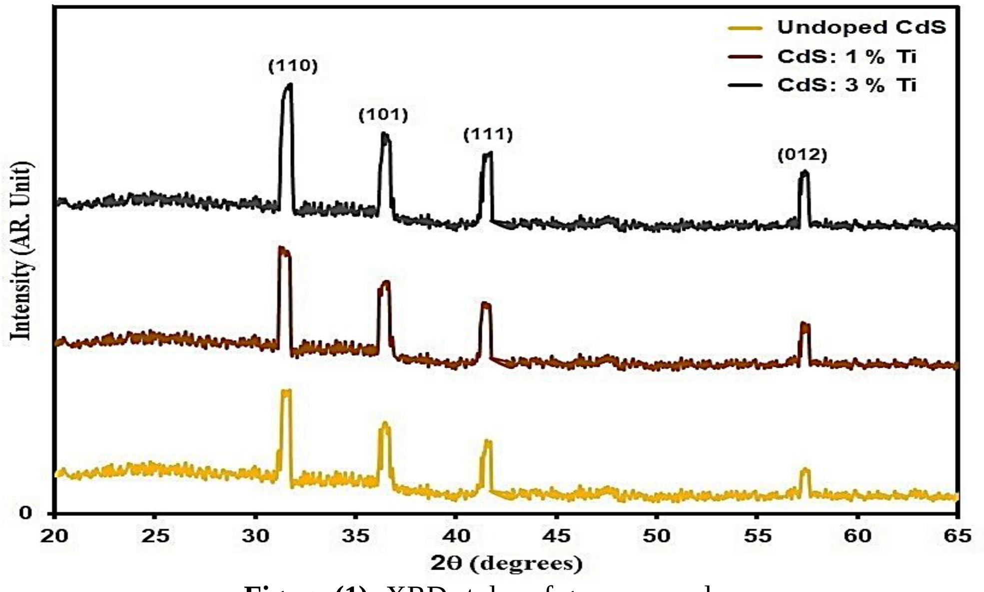

Figure (1): XRD styles of grown samples.

Table 1. Grain size, optical band gap and structural parameters of the prepared films.

Samples	(hkl) Plane	2 (º)	FWHM (º)	Grain size (nm)	E_g (eV)	Dislocations density (× 10^{14})(lines/m^2)	Strain × 10^{-4}
Undoped CdS	110	31.65	0.52	15.73	2.37	58.37	27.68
CdS: 1 % Ti	110	31.62	0.49	16.48	2.32	53.39	23.42
CdS: 3 % Ti	110	31.60	0.46	18.24	2.26	49.84	21.30

The absorption spectra of the samples displayed in Figure (2) show considerable absorbance in the visible region of the spectrum. As the wavelength increases, the absorbance decreases by approximately 22% at 400 nm and drops significantly to 82 % at 900 nm [32].

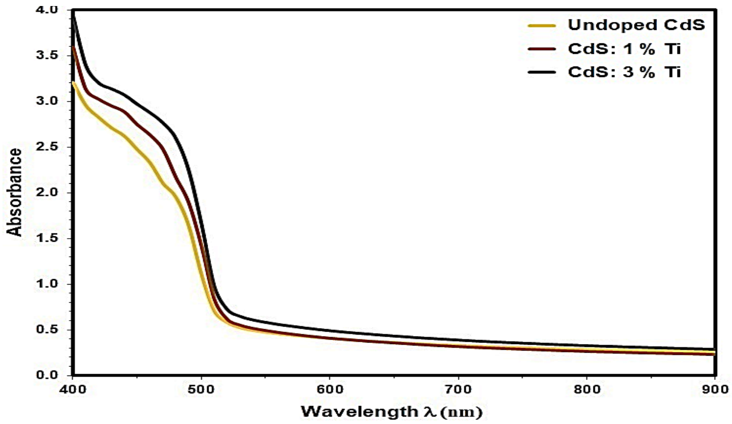

Figure (2): Absorption spectra of the intended films.

In Figure (3) the transmittance (T) of the deposited films is shown to decrease as the Titanium content increases, with a maximum of approximately 77.5 % for CdS films. The transmittance edge shifts to longer wavelengths with increasing titanium content, resulting in a reduction in the bandgap of the produced films. The decline in transmittance observed in films with 0, 1, and 3 at. % content may be attributed to the incorporation of more Titanium into the CdS lattice. [33].

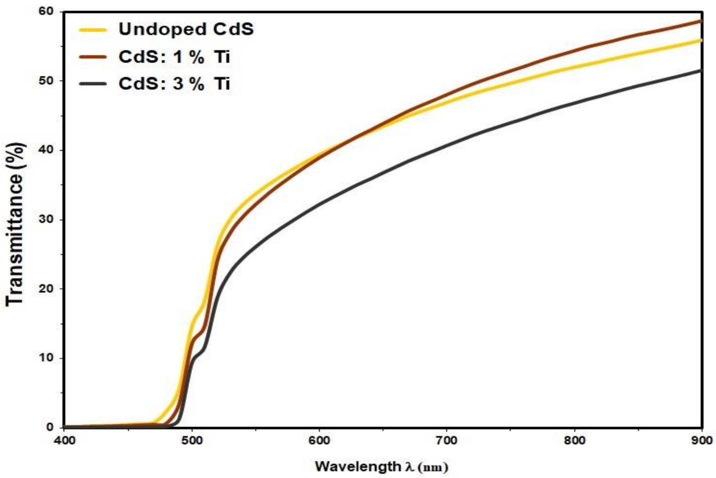

Figure (3): Transmittance of the intended films.

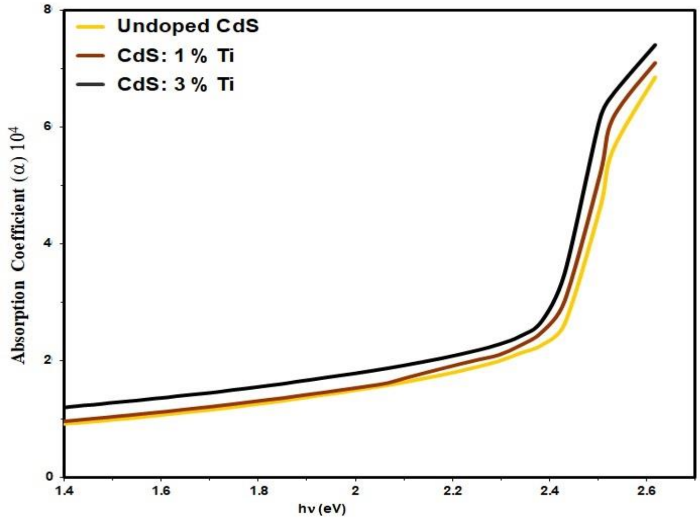

Figure (4): The absorption coefficient spectra as a function of photon energy.

The absorption coefficient (α) was determined using the following equation [34, 35]:

$$\alpha = \frac{20303\,A}{t} \quad (4)$$

Where t is the film thickness and A is the optical absorption.

Figure (4) illustrates the variation in absorption coefficient of CdS: Ti film with respect to photon energy. The results show that the absorption coefficient increases as the weight percentage of Titanium increases. This can be attributed to the fact that an increase in the concentration of Titanium results in an increase in the density of the films [36].

The optical band gap Eg was calculated by the following relation [37,38]:

$$.(\alpha h\nu) = B\left(h\nu - E_g\right)^{\frac{1}{2}} \quad (4)$$

Where $h\nu$ is the photon energy, B is constant. In Figure (5) Pure CdS has E_g of 2.37 eV, consistent with earlier studies. As the concentration of Titanium increases, we can also see that E_g increases.

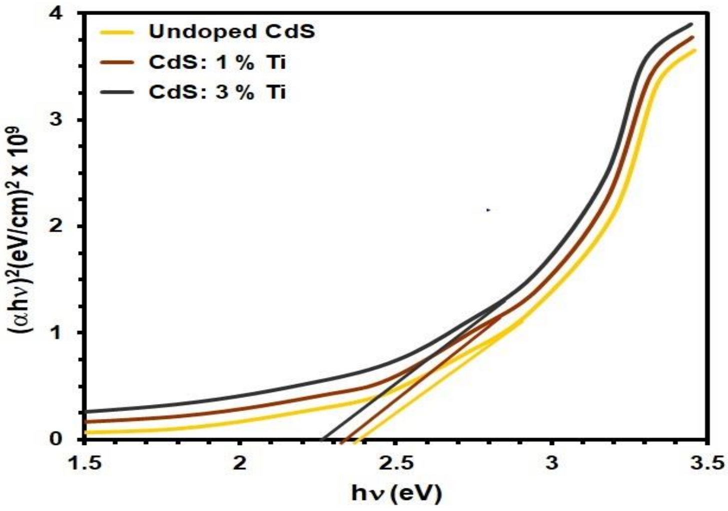

Figure (5): Direct transition of the intended films.

The extinction coefficient (k) of films has been determined using the equation [39, 40]:

$$K = \alpha\lambda / 4\pi \quad (5)$$

In figure (6) show The variation of the extinction coefficient of CdS:Ti versus with wavelength. It can have observed from this figure that extinction coefficient, ingeneral, decreased with increasing Titanium content and decreased with increasing wavelength because of the dependence of extinction coefficient on values of absorption coefficient [41].

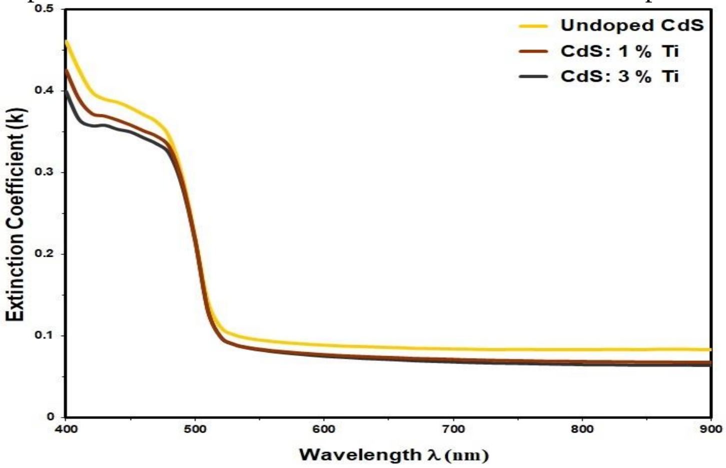

Figure (6): Variation of extinction coefficient of (CdS: Ti) with wavelength.

The refractive index is calculated using the following formulas (6) [42, 43]:

$$n = \left(\frac{1+R}{1-R}\right) + \sqrt{\frac{4R}{(1-R)^2} - k^2} \quad (6)$$

The refractive index of (CdS:Ti) as a function of wavelength is shown in Figure (6). The refractive index decreased as the weight ratios of the concentration of Titanium. This behavior is explained by the increasing density of nanocomposites. When incident light interacts with a sample with high refractivity in the UV region, the refractive index values decreased. This behavior is consistent with research findings [44].

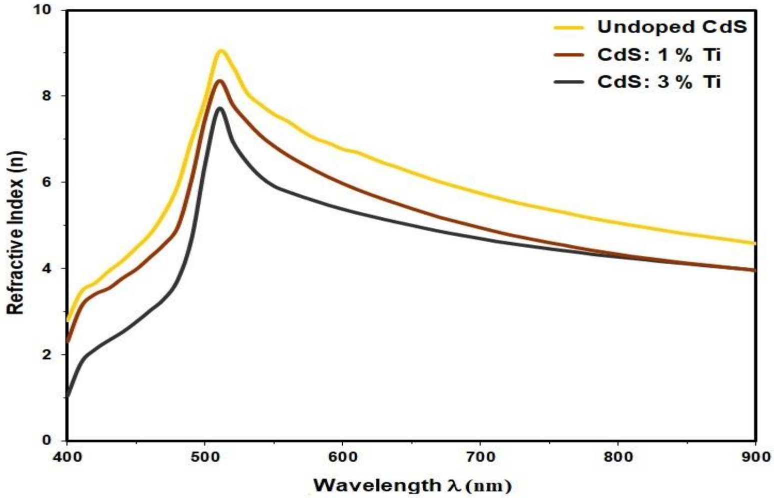

Figure (6): Variation of refractive index of (CdS: Ti) with wavelength.

Conclusion

A low-cost spray pyrolysis process was used to make nanostructured CdS and CdS: Ti thin films. Different of CdS and CdS: Ti films were investigated for optical and structural properties. XRD patterns reveal polycrystalline materials with a favoured (110) orientation. *D* of the grown films was (15.73-18.24) nm, as determined by XRD. The Dislocation density decreased from 58.37 to 49.48, whilst the strain decreased from 27.68 to 21.30. The transmittance is decreased with increasing Titanium concentration. As Titanium concentration rises, E_g decreases from 2.37 eV to 2.26 eV, while refractive index and Extinction coefficient rises.

References

[1] G. S. Vorobjov, V. O. Zhurba, A. S. Krivets, J. Nano- Electron. Phys. 2, No. 4, 47 (2010).
[2] H. R. Motinho, D. Albin, Y. Yaan, R. G. Dheo, X. Li, C. Perkis, C. S. Jiang, Thin Solid Films 436, 175 (2003).
[3] H. Metin, R. Esen, Semicond. Sci. Technol. 18, 647 (2003).
[4] A. Zeho, J.G. Vazquez Luna, Sol. Energ. Mater. Sol. C 68, 217 (2001).
[5] U. Pal, R. Silva-Gonzalez, G. Martinez-Montes, M. Gracia-Jimenez, M.A. Vidal, S. Torres, Thin Solid Films 305, 345 (1997).
[6] J. H. Schon, O. Schenker, B. Batlogg, Thin Solid Films 385, 271 (2001).
[7] J. Levinson, F.R. Shepherd, P. J. Scanlon, W.D. Westwood, G. Este, M. Rider, J. Appl. Phys. 53, 1193 (1982).
[8] Okorie O Buba A and R Abubakar 2017, Optical and Dielectric Properties of Cadmium Sulphide Thin Film Grown Using Chemical Bath Deposition Technique, IOSR Journal of Applied Physics **9** 82-89.
[9] Wang Z L 2004, *Functional oxide nanobelts*: *materials, properties and potential* applications in Nanosystems and *biotechnology*, Annu. Rev. Phys. Chem. **55** 159– 96.
[10] Ibrahim M A Ibrahim A R and Musa O 2014, Investigation of the Properties of Cadmium Sulphide Thin Films for Solar Cell Applications, International Journal of Energy Engineering 4 (3) 61-67.
[11] Sagadevan S and Pandurangan K 2014, Synthesis, structural, optical and electrical properties of cadmium sulphide thin films by chemical bath deposition method, International Journal of ChemTech Research **6 (7)** 3748-3752.
[12] Chtouki T El Kouari Y Kulyk B Louardi A Rmili A Erguig H Elidrissi B Soumahoro L and Sahraoui B 2017, Spin-coated nickel doped cadmium sulfide thin films for third harmonic generation applications, journal of alloy and compounds **696** 1292- 1297.
[13] Baturay Şilan 2017, Indium doping on the structural, surface and optical properties of CdS thin films prepared by ultrasonic spray pyrolysis method, J. BAUN Inst. Sci. Technol. **19 (2)** 264-274.
[14] Hernandez N Berrellez F Mizquez R Ramirez O Mejia I and M Quevedo 2015, CdS-based p-i-n diodes using indium and copper doped CdS films by pulsed laser deposition, Sci. Technol. **30 (6)** 065003-065007.
[15] Ashour A., El-Kadry N. and Mahmoud S.A., Thin Solid Films, 269, (1995), 117.
[16] Mahmoud S.A., Ibrahim A.A. and Riad A.S., Thin Solid Films, 372, (2000), 144.
[17] Ashour A, El-Kadry N, Mahmoud SA. On the electrical and optical properties of CdS films thermally deposited by a modified source. Thin Solid Films 1995; 269:117-20.
[18] Oliva A.I., O. Solis Canto, R. Castro-Rodriguez and Quintana P., Thin Solid Films, 391, (2001), 28
[19] Davide Barreca, AlbertoGasparotto, CinziaMaragno, and Eugenio Tondello. CVD of Nanosized ZnS and CdS thin films from single-source precursors. J. Electrochem. Soc. 2004;151(6): G428-35.
[20] Hofimann Ph,, Horn K., Bradshaw A.M., Johnson R.L., Fuchs D. and Cardona M., Phys. Rev., B47, (1993), 1639.
[21] Battisha I. K., Afify H. H., Abd El-Fattah G. and Badr Y., Fizika, A11, (2002), 31
[22] Ehssan S Hassan, Tahseen H Mubarak, Sami S Chiad, Nadir F Habubi, Abdulhussain A Khadayeir, Mohamed O Dawood and Ismaeel A. Al-Baidhany Physical Properties of indium doped Cadmium sulfide thin films prepared by (SPT), IOP Conf. Series: Journal of Physics: Conf. Series 1294 (2019) 022008.
[23] F. J. Willars-Rodr´ıguez, I. R. Ch´avez-Urbiola, M. A. H. Landaverde, P. Vorobiev, R. R. Bon and Y. V. Vorobiev, Effects of tin-doping on cadmium sul□de (CdS:Sn) thin-flims grown by light-assisted chemical bath deposition process for solar photovoltaic cel, Thin Solid Films, 2018, 653, 341–349.

[24] N. Maticiuc, J. Hiie, T. Raadik, A. Graf and A. Gavrilov, The role of Cl in the chemical bath on the properties of CdS thin flms, Thin Solid Films, 2013, 535, 184–187.
[25] Ali, R. S., Sharba, K. S., Jabbar, A.M., Chiad, S.S., Abass, K. H. and Habubi, N. F., Characterization of ZnO thin film/p-Si fabricated by vacuum evaporation method for solar cell applications, NeuroQuantology 18(1), 2020, pp. 26-31.
[26] Dawood, M. O., Chiad, S. S., Ghazai, A. J., Habubi, N. F. and Abdulmunem, O. M., Effect of Li doping on structure and optical properties of NiO nano thin-films by SPT, 2020, AIP Conference Proceedings, 2213 (1), 020102.
[27] Chiad, S. S. and Mubarak, T. H.,The Effect of Ti on Physical Properties of Fe_2O_3 Thin Films for Gas Sensor Applications, International Journal of Nanoelectronics and Materials, 13(2), 2020, pp. 221-232.
[28] Abdulmunem, O. M., Abdulameer, F. S., Kadhum, H.A., Dawood, M. O., Abass, K.H., Habubi, N.F. and Chiad, S.S., Influence of Bismuth dopant on physical properties of nanostructured TiO_2 thin films, Test Engineering and Management 83, 2020, pp. 11142-11147.
[29] S. Chandramohan, A. Kanjilal, S. N. Sarangi, S. Majumder and R. Sathyamoorthy, Implantation-assisted Co-doped CdS thin flms: structural, optical, and vibrational properties, J. Appl. Phys., 2009, 106, 063506.
[30] Jandow, N. N., Habubi, N. F., Chiad, S. S., Al-Baidhany, I. A. and Qaeed, M. A., optical parameters of Fe_2O_3:Ni thin films prepared by chemical spray pyrolysis technique, 2019, International Journal of Nanoelectronics and Materials 12(1), pp. 1-10.
[31] Hassan, E. S., Elttayef, A.K., Mostafa, S. H., Salim, M. H. and Chiad, S. S., Silver oxides nanoparticle in gas sensors applications, Journal of Materials Science: Materials in Electronics 30 (17), 2019, pp. 15943-15951.
[32] P. J. Sebastian, p-type CdS thin films formed by in situ Cu doping in the chemical bath p-type CdS thin films formed by in suit Cu doping in the chemical bath, Appl. Phys. Lett., 1993, 62(23), 2956–2958.
[33] O. Portillo-Moreno, et al., Growth of CdS:Cu Nanocrystals by Chemical Synthesis, J. Electrochem. Soc., 2006, 153(10), 926– 930.
[34] Habubi, N. F., Mishjil, K. A. and Chiad, S. S., Structural properties and refractive index dispersion of cobalt doped SnO2 thin films, Indian Journal of Physics 87(3), 2013, pp. 235-239
[35] Alkelaby, A. S., Abass, K. H., Mubarak, T. H., Habubi, N. F., Chiad, S. S. and Al-Baidhany, I., Effect of $MnCl_2$ additive on optical and dispersion parameters of poly methyl methacrylate films, Journal of Global Pharma Technology 11(4), 2019, pp. 347-352.
[36] Chale-Lara F, Zapata-Torres M, Melendez-Lira M, Peraza-Vazquez H. Optical and structural properties of CdS films grown by CSVT technique. Physica status solidi (c) 2005; 2(10): 3694-7.
[37] Habubi, N. F., Abass, K. H., Chiad, S., Latif, D. M. A., Nidhal, J. N. and Al Baidhany, A.I., Dispersion Parameters of Polyvinyl Alcohol Films doped with Fe, Journal of Physics: Conference Series 1003(1), 2018, 012094.
[38] Chiad, S. S., Abass, K. H., Mubarak, T. H., Habubi, N. F., Mohammed, M. K. and Khadayeir, A.A., Fabrication and study the structure, optical and dispersion parameters of PMMA with InCl3 additive, Journal of Global Pharma Technology 11(4), 2019, pp. 369-375.
[39] Ehssan S. Hassan, Abdulhussain K. Elttayef, Suzan Hadi Mostafa, Mohammed Hadi Salim, Sami Salman Chiad, Silver oxides nanoparticle in gas sensors applications, Journal of Materials Science: Materials in Electronics, Netherlands, https://doi.org/10.1007/s10854-019-01954-1, pp.1-9, 2019.
[40] Khadayeir, A. A., Abass, K. H., Chiad, S. S., Mohammed, M. K., Habubi, N. F., Hameed, T. K. and Al-Baidhany, I. A., Study the influence of antimony trioxide (Sb_2O_3) on optical properties of (PVA-PVP) composites, Journal of Engineering and Applied Sciences 13(22), 2018, pp. 9689-9692.
[41] Shour H, El Akkad F, Bohari R, Herrmann KH. Properties of RF sputtered CdS thin films. Proc. Eleventh International Conference on Microelectronics 1999; ICM '99: 263-65.
[42] Ali, R.S., Rasheed, H.S., Habubi, N. F., Chiad, S. S., Synthesis and characterization of manganese-doped FeS_2 thin films via chemical spray pyrolysis, Chalcogenide Lettersthis, 2023, 20(1), pp. 63–72.
[43] Ali, R. S., Rasheed, H. S., Abdulameer, N. D., Habubi, N. F., Chiad, S. S., Physical properties of Mg doped ZnS thin films via spray pyrolysis, Chalcogenide Lettersthis link is disabled, 2023, 20 (3), pp. 187–196
[44] A. Hasnat, J. Podder, "Structural and Electrical Transport Properties of CdS and Al-doped CdS Thin Films Deposited by Spray Pyrolysis", J. Sci. Res. 4 (1),11-19, 2012.

Study the Annealing Effects on Optical and Structural Properties of Cadmium Oxide Thin Films

Nazar Abdulmahdi Jabir[1], Israa Hmood Ibraheem[2], Ibraheem M. Mohammed[3]
[1]Department of Physics, College of Science, Mustansiriyah University.
[2]Department of Chemistry, College of Science for Women, University of Baghdad.
[3]Department of Physics, College of Education, Mustansiriyah University.

Abstract:
Cadmium oxide (CdO) thin films have been deposited using the spray pyrolysis technique, and their structural and optical properties have been investigated before and after annealing at 400 and 450°C. X-ray diffraction analysis revealed that the films exhibited a single-phase cubic structure, with the intensity of the diffraction peaks increasing with annealing, indicating an improvement in the crystallinity of the films. The crystallite size increased from 15.78 to 18.90 nm after annealing, while the dislocation density decreased from 53.48 to 35.71. The absorption spectra showed a gradual decrease in absorbance as the wavelength increased. The absorption coefficient increased slightly with annealing, with a high value, indicating direct electronic transitions. The optical band gap decreased from 2.60 to 2.56 eV after annealing. The extinction coefficient and refractive index decreased with increasing annealing temperature.

Keywords: CdO, Thin Films, annealing, optical and structural properties, energy gap.

دراسة تأثير التلدين على الخصائص البصرية والتركيبية لأغشية أوكسيد الكادميوم الرقيقة

نزار عبد المهدي جابر[1]، اسراء حمود ابراهيم[2]، ابراهيم موسى محمد[3]
[1] قسم الفيزياء، كلية العلوم، الجامعة المستنصرية. [2] قسم الكيمياء / كلية العلوم للبنات/ جامعة بغداد.
[3] قسم الفيزياء، كلية التربية، الجامعة المستنصرية.

المستخلص
تم ترسيب الأغشية الرقيقة من أكسيد الكادميوم باستخدام تقنية التحلل الحراري بالرش، وتم فحص خواصها التركيبية والبصرية قبل وبعد التلدين عند درجة حرارة 400 و450 مئوية. بين تحليل حيود الأشعة السينية أن الأفلام ذات بنية مكعبة أحادية الطور، وتزداد قيمة ة شدة قمم الحيود مع التلدين، مما يشير إلى تحسن في تبلور الأغشية. وأزداد الحجم الحبيبي من 15.78 إلى 18.90 نانومتر بعد التلدين، بينما انخفضت كثافة الانخلاعات من 53.48 إلى 35.71. أظهرت أطياف الامتصاص انخفاضًا تدريجيًا في الامتصاص مع زيادة الطول الموجي. زاد معامل الامتصاص بشكل طفيف مع التلدين بقيمة عالية مما يشير إلى انتقالات إلكترونية مباشرة. انخفضت فجوة النطاق البصري من 2.60 إلى 2.56 الكترون فولت بعد التلدين. انخفض معامل الخمود ومعامل الانكسار مع زيادة درجة حرارة التلدين.

الكلمات الافتتاحية: اوكسيد الكوبلت، أغشية رقيقة، تلدين، الخصائص البصرية والتركيبية، فجوة الطاقة.

Introduction

Transparent conducting oxide (TCO) films have significant technological potential in the field of optoelectronics and other solid-state devices [1]. TCOs are vital for technologies that require both large-area electrical contacts and optical access in the visible portion of the light spectrum. Various TCOs, including the oxides of Sn, In, Zn, Cd, and their alloys, have been developed. Cadmium oxide, in particular, is an n-type semiconducting material with high mobility [2, 3]. Transparent conducting films made of cadmium oxide have been utilized in various applications such as photodiodes [4], phototransistors, photovoltaic cells [5], gas sensors [6], and thin-film resistors [7]. Annealing CdO films is an efficient way to construct electronic transport pathways and obtain high mobility [8], making it suitable for technical applications based on its IR-TCO characteristics [9]. Various deposition techniques have been employed to investigate CdO films, Successive Ionic Layer Adsorption and Reaction (SILAR) [10], including electrochemical deposition [11], Chemical Vapor Deposition (MOCVD) [12], vacuum evaporation [13], Pulsed Laser Deposition (PLD) [14], DC Reactive Magnetron Sputtering [15], electron beam evaporation [16], sol-gel technique [17], Chemical Bath Deposition (CBD) [18] and spray pyrolysis [19-21], In this study, we report on the annealing effects of CdO thin films deposited on glass substrates using both chemical pyrolysis. Our aim is to investigate the optical and structural properties of these annealed CdO films.

Experiment

Thin films of Cadmium oxide were synthesized using a chemical pyrolysis technique, employing a laboratory-designed glass atomizer with an output nozzle of 1 mm. The films were deposited onto preheated glass substrates at a temperature of 400°C, using a starting solution composed of an aqueous solution of 0.1 M $CdCl_3$, diluted with deionized water and ethanol to form a final spray solution. A total volume of 45 ml was used for each deposition, and the optimized conditions involved an 8-secon spray time and a constant 2 minute spray interval. The carrier gas, filtered compressed air, was maintained at a pressure of 10^5 Nm^{-2}, and the distance between the nozzle and the substrate was kept at approximately 30 cm ± 1 cm. The thickness of the resulting films was determined using the weighing method and was found to be approximately 330 cm ± 20 nm.
To evaluate the structural properties of the films, X-ray diffraction (XRD) was used, while optical and transition spectra were recorded using a double-beam UV/VIS spectrophotometer (Shimadzu Corporation, Japan) in the wavelength range of 300-900 nm. The as-deposited films were then annealed at 450°C, and optical transmittance and absorbance measurements were repeated to investigate the effect of annealing on the parameters of interest.

Result and discussion

The x-ray diffraction spectra of Cadmium oxide indicate a single phase with a cubic structure. The diffraction pattern of the as-grown and annealed film is shown in Figure 1, where the (111), (200), and (220) diffraction peaks are aligned at angles of 33.08°, 38.037°, and 55.49°, respectively. These angles match the card number (05-0640) of the International Centre for Diffraction Data (ICDD)[19]. The intensity of the X-ray peaks increases with the annealing treatment, indicating an improvement in the crystallinity of the films [20].
The size of the crystallites oriented along the (111) peak was calculated using Scherrer's relation [22, 23]:

$$D = \frac{0.9\,\lambda}{\beta cos\theta} \qquad (1)$$

which involves the X-ray wavelength (λ), the full width at half maximum (B) of the (111) diffraction peak in radians, and the Bragg diffraction angle (θ) in degrees. The computed crystallite sizes were found to be 15.78 and 18.90 nm before and after annealing respectively.
Additionally, the dislocation density (δ) was calculated using a different formula [24, 25],

$$\delta = \frac{1}{D^2} \qquad (2)$$

After annealing, the dislocation density of the films was found to decrease from 53.48 to 35.71.
The strain (ε) of the films was determined using the formula [26, 27]:

$$\varepsilon = \frac{\beta cos\theta}{4} \qquad (3)$$

The computed strain (ε) was found to be 24.37 and 22.86 nm before and after annealing respectively. Table 1 shows the structural coefficients that were derived in the study.

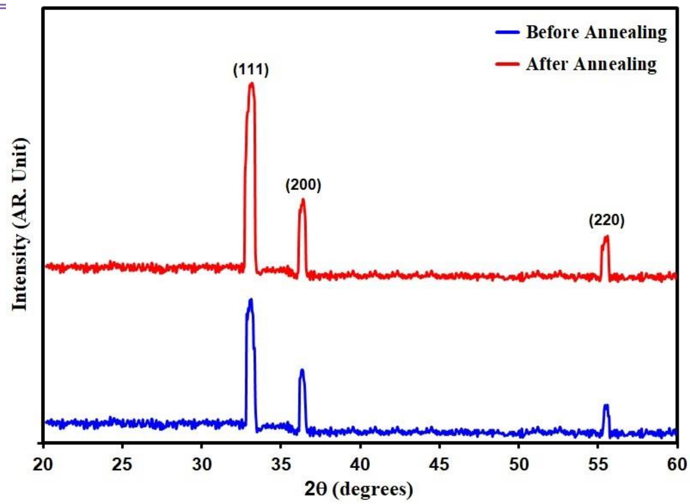

Fig. (1): XRD patterns of the thin films before and after annealing.

Table 1. Grain size, optical bandgap and structural parameters of the films before and after annealing.

Samples	2 (°)	(hkl) Plane	FWHM	E_g (eV)	Grain size (nm)	Dislocations density (× 10^{14})(lines/m^2)	Strain (× 10^{-4})
before annealing	33.08	111	0.67	2.60	15.78	53.48	24.37
after annealing	33.05	111	0.64	2.56	18.90	35.71	22.86

Fig. 2 illustrates the absorption spectra of the two Cadmium oxide thin films deposited before and after annealing at 400 and 450ºC. The spectra demonstrate a gradual decrease in absorbance as the wavelength increases, with relatively low values observed in the visible region (after 350 nm) and in the infrared region of the spectrum. As can be observed from the results, there is an increase in optical absorbance in the visible region as the annealing temperature increases [28].

Fig. 3 depicts the optical transmission spectra of the Cadmium oxide thin films deposited before and after annealing at 400 and 450ºC. Both films demonstrate high transmission (>70%) for wavelengths greater than 500 nm, which is a crucial characteristic for optoelectronic applications, particularly for the window layer of solar cells [29].

The absorption coefficient of the CdO thin films was determined using the following equation [30, 31]:

$$\alpha=2.303\ A/t \quad (4)$$

Where A is the optical absorption and t is the film thickness.

Figure (4) as show the absorption coefficient α as a function of wavelength for Cadmium oxide thin films deposited before and after annealing at 400 and 450ºC, which has a high value of (10^4 cm^{-1}), stating direct electronic transitions. It can be seen that by increasing the annealing, increases very slightly and the absorption coefficient travels toward to low energies [32].

The optical band gap of the as-deposited thin films was determined by extrapolating the linear portion of the $(\alpha h\nu)^2$ vs. (hν) plot using the formula [33, 34]:

$$(\alpha h\nu)^{1/2} = A\ (h\nu - Eg)^{1/2} \quad (5)$$

Where (hν) photon energy and A Constant. Fig. (5) shows the value of the optical band gap energy, the optical band gap drops from 2.60 to 2.56 before and after annealing respectively.

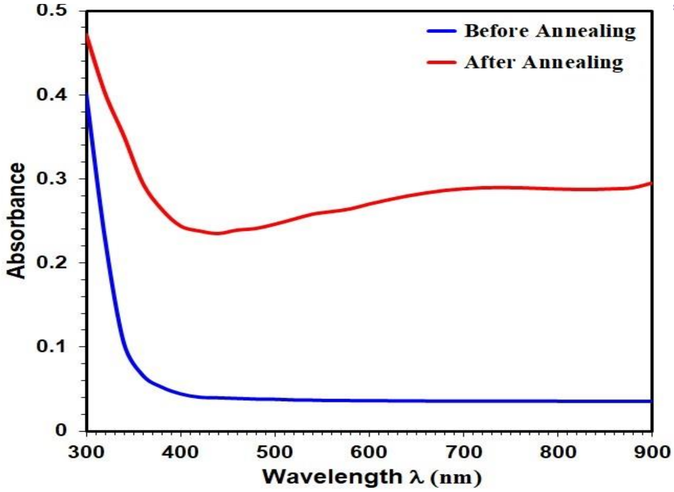

Fig. (2): Absorption of CdO thin film versus wavelength before and after annealing

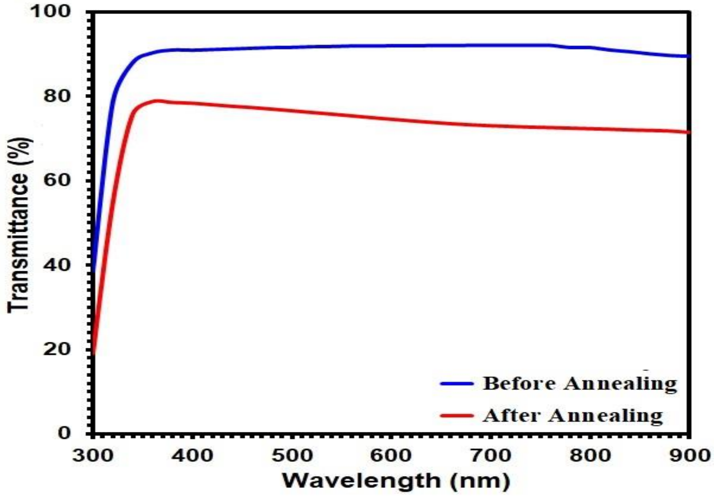

Fig. (3): Transmission of CdO thin film versus wavelength before and after annealing.

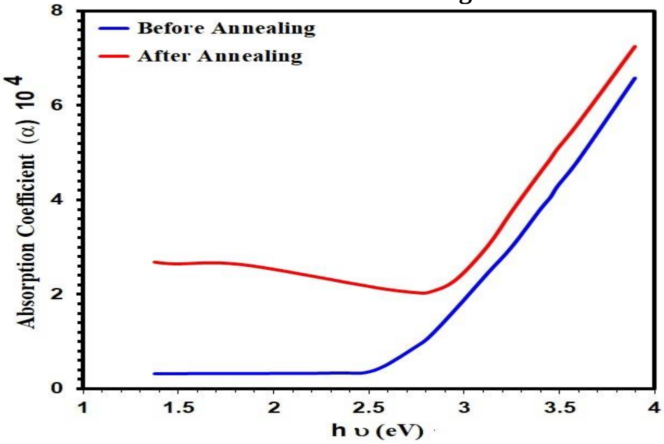

Figure (4): absorption coefficient versus wavelength of CdO thin films before and after annealing.

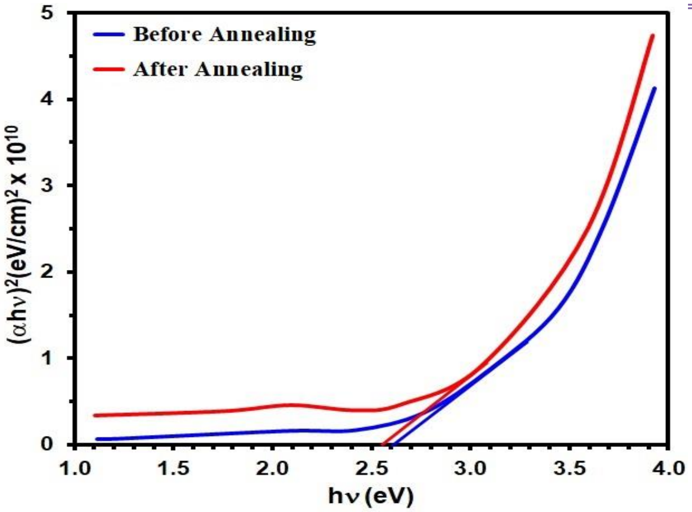

Figure (5): Direct transition of the intended films.

It is a known fact that the extinction coefficient (k) and the absorption coefficient (α) are related by the following equation [34, 35]:

$$K=\alpha\lambda/4\pi \quad (5)$$

where λ is the wavelength of light. Fig. (6) displays the extinction coefficient of the Cadmium oxide thin films before and after annealing. It can be observed that the extinction coefficient decreased with increasing annealing temperature [36].

The refractive index of a material can be calculated using the following formulas [37, 38]:

$$n=\left(\frac{1+R}{1-R}\right)+\sqrt{\frac{4R}{(1-R)^2}-k^2} \quad (6)$$

Where the R is the reflectance. The refractive index of Cadmium oxide thin films before and after annealing is shown in Fig. (7). It is observed that the refractive index decreased with increasing annealing temperature. This can be attributed to an improvement in the crystal quality and grain size of the films with the annealing treatment [39, 40].

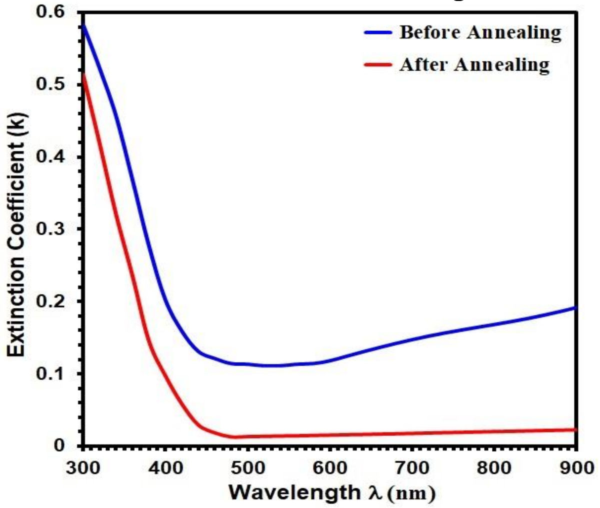

Fig. (6). extinction coefficient versus wavelength of CdO thin films before and after annealing.

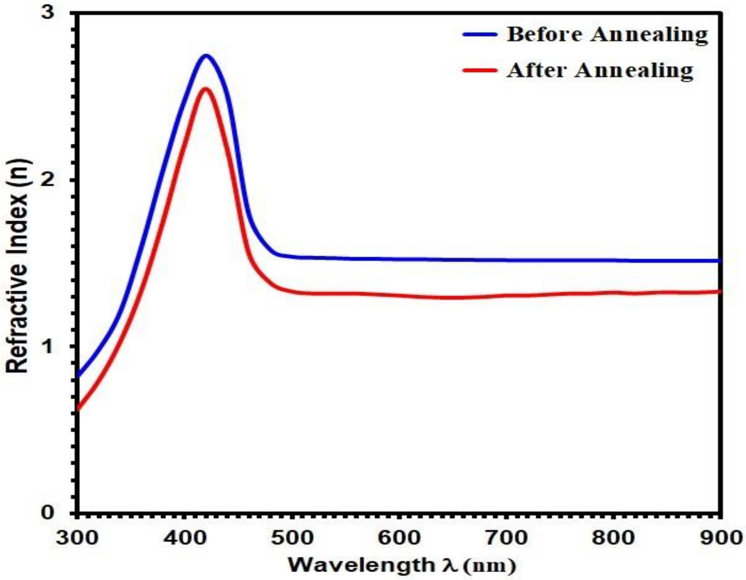

Fig. (7) refractive index versus wavelength of CdO thin films before and after annealing.

Conclusion

In this study, the structural and optical properties of Cadmium oxide thin films before and after annealing were investigated. X-ray diffraction analysis indicated a single phase with a cubic structure, and the intensity of the X-ray peaks increased with annealing, indicating an improvement in crystallinity. The size of the crystallites and dislocation density were calculated and both were found to decrease with annealing. The absorption and transmission spectra of the thin films demonstrated a gradual decrease in absorbance and high transmission for wavelengths greater than 500 nm. The absorption coefficient of the CdO thin films was determined, and the optical band gap dropped slightly with annealing. The extinction coefficient and refractive index decreased with increasing annealing temperature.

References

[1] J. Santos-Cruz, G. Torres-Delgado, R. Castanedo-Perez " Dependence of electrical and optical properties of sol–gel prepared undoped cadmium oxide thin films on annealing temperature ", Thin Solid Films. 493, 83 (2005).
[2] Zhiyong Zhao, D.L. Morel, "C.S. Ferekides Electrical and optical properties of tin-doped CdO films deposited by atmospheric metal organic chemical vapor deposition", Thin Solid Films, 203, 413 (2002).
[3] A. Abdolahzadeh Ziabaria and F.E. Ghodsi" Optical and Structural Studies of Sol-Gel Deposited Nanostructured CdO Thin Films: Annealing Effect", 120 (3) (2011).
[4] Selma Mohammed H. Al-Jawad, Hadia Kadhim "Investigation of optical and electrical properties of chemically deposited nano-crystalline CdO thin film", College of education journal, 17(68), 75 (2011).
[5] European Union Risk Assessment Report, "Cadmium Oxide and Cadmium Metal ", Part I – Environment, 3rd Priority Lis, 72, Italy, (2007).
[6] Mahdi H. Suhail, Issam M. Ibrahim and G. Mohan Rao, "Characterization and gas sensitivity of cadmium oxide thin films prepared by thermal evaporation technique ", Int. J. Thin Film Sci. Tec. 1(1), 1 (2012).
[8] Gehan E. Simon, Ammar M. Al-Baldawi, Adnan H. Fiaem and Khalid J. Abd Al-Satter, "Preparation and Study Characteristics of CdO Thin Film", Journal of Al-Nahrain University, 12 (4), 92 (2009).

[9] Valanarasu S., Dhanasekaran V., Karunakaran M., Chandramohan R., Mahalingam T., Role of Solution pH on the Microstructural Properties of Spin Coated Cobalt Oxide Thin Films, J. Nanosci. Nanotechnol., 13: 1-6 (2013).
[10] Salunkhe R., Dhawale D., Gujar T., Lokhande C., Structural, Electrical and Optical Studies of SILAR Deposited Cadmium Oxide Thin Films: Annealing Effect, Mater. Res. Bull., 44: 364-368 (2009).
[11] Chang J., Mane R., Ham D., Lee W., Cho B., Lee J., Han S., Electrochemical Capacitive Properties of Cadmium Oxide Films, Electrochem. Acta, 53: 695-699 (2007).
[12] Li X., Gessert T., Coutts T., The Properties of Cadmium Tin Oxide Thin-Film Compounds Prepared by Linear Combinatorial Synthesis, Appl. Surf. Sci., 223: 138-143 (2004).
[13] Dakhel A., Transparent Conducting Properties of Samarium-Doped CdO, J. Alloys Compd., 475: 51-54 (2009).
[14] Gupta R., Ghosh K., Patel R., Mishra S., Kahol P., Highly Conducting and Transparent Tin-Doped CdO Thin Films for Optoelectronic Applications, Mater. Lett., 62: 4103-4105 (2008).
[15] Zhou, Qiang, Ji, Zhenguo, Hu, BinBin, Chen, Chen, Zhao, Lina, Wang, Chao, 2007. Low resistivity transparent conducting CdO thin films deposited by DC reactive magnetron sputtering at room temperature. Mater. Lett. 61, 531–534.
[16] Ali H., Mohamed H., Wakkad M., Hasaneen M., Optical and Electrical Properties of Tin-Doped Cadmium Oxide Films Prepared by Electron Beam Technique, J. Appl. Phys., 48: 041101-7 (2009).
[17] Aksoy S., Caglar Y., Ilican S., Caglar M., Effect of Heat Treatment on Physical Properties of CdO Films Deposited by Sol–Gel Method, Int. J. Hydrogen Energy, 34: 5191-5195 (2009).
[18] de León-Gutiérrez L., Cayente-Romero J., Peza-Tapia J., Barrera-Calva E., Martínez-Flores J., Ortega-López M., Some Physical Properties of Sn-Doped CdO Thin Films Prepared by Chemical Bath Deposition, Mater. Lett., 60: 3866-3870 (2006).
[19] Ahmed, F.S., Ahmed, N.Y., Ali, R.S., Habubi, N.F., Abass, K.H. and Chiad, S.S. Effects of Substrate Type on Some Optical and Dispersion Properties of Sprayed CdO Thin Films, NeuroQuantology, 18 (3), 56-65, 2020.
[20] Othman, M.S., Mishjil, K.A., Rashid, H.G., Chiad, S.S., Habubi, N.F., Al-Baidhany, I.A., Comparison of the structure, electronic, and optical behaviors of tin-doped CdO alloys and thin films, Journal of Materials Science: Materials in Electronics 31(11), pp. 9037-9043, 2020.
[21] Ban A. Bader, Shawki Khalaph Muhammad, Ali Mohammed Jabbar, Khalid Haneen Abass, Sami Salman Chiad and Nadir Fadhil Habubi, Synthesis and Characterization of Indium-doped CdO Nanostructured Thin Films: a Study on Optical, orphological, and Structural Properties, J. Nanostruct 10(4): 744-750, Autumn 2020.
[22] Adel H.Omran Alkhayatt1, Imad A. Disher Al-hussainy, Oday A. Chichan Al-rikaby, Annealing Effect on the Structural and Optical Properties of Sol- Gel Deposited Nanocrystalline CdO Thin Films, Advances in Physics Theories and Applications, ISSN 2224-719X, 34 (2014).
[23] Othman, M.S., Mishjil, K.A., Rashid, H.G., Chiad, S.S., Habubi, N.F., Al-Baidhany, I.A., Comparison of the structure, electronic, and optical behaviors of tin-doped CdO alloys and thin films, Journal of Materials Science: Materials in Electronics 31(11), pp. 9037-9043, 2020.
[24] Jandow, N.N., Othman, M.S., Habubi, N.F., Chiad, S.S., Mishjil, K.A., Al-Baidhany, I.A., Theoretical and experimental investigation of structural and optical properties of lithium doped cadmium oxide thin films, Materials Research Express 6(11), 2020.

[25] Hassan, E. S., Qader, K.Y., Hadi, E.H., Chiad, S. S., Habubi, N.F., Abass, K.H., Sensitivity of nanostructured mn-doped cobalt oxide films for gas sensor application, Nano Biomedicine and Engineering, 12(3), pp. 205-213, 2020.
[26] Chiad, S. S., Habubi, N.F., Abass, W.H., Abdul-Allah, M.H., Effect of thickness on the optical and dispersion parameters of Cd0.4Se0.6 thin films, Journal of Optoelectronics and Advanced Materials, 18(9-10), pp. 822-826, 2016.
[27] Habubi, N.F., Abdulmunem, O. M., Shaban, Z.M.,Dawood, M.O., Chiad, S.S. IOP Conference Series: Earth and Environmental Sciencethis link is disabled, Effect of Cu doping ZrO2Thin films on physical properties grown by spray pyrolysis deposition, 2021, 790(1), 012078.
[28] Kim, T., Lee, W., Kim, J., Lee, D., & Kim, D., Annealing effect on the properties of CdO thin films grown by spray pyrolysis for CdTe solar cells. Journal of Korean Physical Society, 74(9), 709-713 (2019).
[29] Vijayalakshmi, V., Ramachandra Reddy, A., & Vijayalakshmi, L., Effect of annealing temperature on optical properties of CdO thin films prepared by spray pyrolysis. Journal of Materials Science: Materials in Electronics, 30(13), 13038-13046 (2019).
[30] Agool, I. R., Dawood, M. O., Hassan, E. S., Abdulmunem, O. M., Chiad, S.S., Influence of Fluorine Content on physical Characterization of Sprayed CdO, IOP Conference Series: Earth and Environmental Sciencethis link is disabled, 2021, 790(1), 012079.
[31] Khadayeir, A. A., Hassan, E. S., Mubarak, T. H., Chiad, S.S., Habubi, N. F., Dawood, M.O., Al-Baidhany, I. A., The effect of substrate temperature on the physical properties of copper oxide films, Journal of Physics: Conference Series, 2019, 1294 (2) 022009.
[32] Senthilkumar, K., & Kumar, G., Influence of annealing temperature on the structural and optical properties of CdO thin films. Journal of Materials Science: Materials in Electronics, 28(8), 6286-6291(2017).
[33] Hadi, E.H., Sabur, D.A., Chiad, S.S., Habubi, N.F., Abass, K.H., Physical properties of nanostructured li-doped zro2 thin films, Journal of Green Engineering, 10(10), pp. 8390-8400, 2020.
[34] Ghazai, A. J., Abdulmunem, O. M., Qader, K.Y., Chiad, S. S., Habubi, N. F., Investigation of some physical properties of Mn doped ZnS nano-thin films, 2020, AIP Conference Proceedings 2213 (1), 020101.
[36] Huang, H., Shen, W., Zhang, J., & Zhao, H., Optical properties and band gap engineering of CdO thin films deposited by spray pyrolysis. Applied Surface Science, 441, 365-371 (2018).
[37] Salloom, H. T., Hadi, E. H., Habubi, N. F., Chiad, S. S., Jadan, M., Addasi, J. S., Characterization of silver content upon properties of nanostructured nickel oxide thin films, Digest Journal of Nanomaterials and Biostructures 15(4), pp. 1189-1195, 2020.
[38] Hussin, H. A., Al-Hasnawy, R.S., Jasim, R. I., Habubi, N. F., Chiad, S. S., Optical and structural properties of nanostructured CuO thin films doped by Mn, Journal of Green Engineering, 10(9), pp. 7018-7028, 2020.
[39] Venkateswarlu, M., Sreedhar, A., & Ramesh Babu, K., Optical properties of annealed CdO thin films deposited by spray pyrolysis technique. Materials Today: Proceedings, 4(2), 1472-1479 (2017).
[40] Abdel-Hady, K., Abdel-Rahim, M. A., & El-Rabaie, S., Optical properties of annealed CdO thin films prepared by spray pyrolysis. Superlattices and Microstructures, 87, 404-413 (2015).

Image Processing Techniques for Iris Eye Detection

Dr. Kadhim Ajeel Obaid[1*], Dr. Ziad M. Abood[2]**
[2]Department of Physics, College of Education, Mustansiriyah University, Iraq
[*]E-mail: kadhim.ajeel@sadiq.edu.iq, ** dr.ziadmabood@uomustansiriyah.edu.iq

Abstract:
Based on unique features possessed by an individual, the biometric system provides automatic identification of the person. There have been various implementations using biometrics، especially for identification and verification cases. In general, typical iris recognition follows the approach of image processing and computer vision. This approach contains various stages-image segmentation, image normalization, feature extraction، and image recognition. Iris Biometry has been proposed as asound measure. In this paper, an iris recognition system is presented with four steps. First, image segmentation is performed using Canny Edge Detector followed by iris Circular Hough transformation (CHT), which is able to localize the iris and pupil regions. The segmented iris is further normalized. Then features are extracted using discrete 2D reverse biorthogonal wavelet. Finally, the iris codes are compared. The proposed system gives a high recognition rate of 75% whereas the FAR and FRR values are calculated the lowest as compared to existing systems. The proposed method is simple and effective. The system is implemented in MATLAB.

Keywords: Iris Recognition, Human eye, Normalization, Segmentation, Wavelet.

المستخلص:
هناك تطبيقات مختلفة باستخدام القياسات الحيوية، خاصةً في حالات تحديد الهوية اعتمادا على الميزات الفريدة التي يمتلكها الفرد مثل التعرف على قزحية العين من خلال استخدام تقنيات نهج معالجة الصور ورؤية الحاسوب.
يحتوي هذا النهج على العديد من تجزئة الصورة بالمراحل، وتطبيع الصورة، واستخراج الميزات والتعرف على الصور. تم اقتراح القياس الحيوي للقزحية كإجراء سليم. في هذا البحث، يتم تقديم نظام التعرف على قزحية العين من أربع خطوات. أولاً، يتم إجراء تجزئة للصورة باستخدام مرشح كاني للحواف متبوعًا بتحويل القزحية الدائري (CHT)، القادر على توطين مناطق القزحية والتلميذ. يتم تطبيع القزحية المجزأة بشكل أكبر. ثم يتم استخلاص السمات باستخدام الموجة المويجة العكسية ثنائية الأبعاد المنفصلة. أخيرًا، تمت مقارنة أكواد قزحية العين. يعطي النظام المقترح معدل التعرف العالي بنسبة 75٪ بينما يتم حساب قيم FAR و FRR الأقل مقارنة بالأنظمة الحالية. الطريقة المقترحة بسيطة وفعالة. يتم تنفيذ النظام في MATLAB.

الكلمات المفتاحية: التعرف على قزحية العين، عين الإنسان، التطبيع، التقسيم، التحويل المويجي.

1.1 Introduction

Biometrics science is the measuring technology of data analyzing biological. It's used to identify unique individuals by their characteristics of physical/ behavior personal and to allow access to employees for areas of certain and general ID purposes. A system of biometrics depended on basic steps:

1. Data of Acquiring.
2. Data of Analysis.
3. Encryption. [1]

In USA, there are lawful issues to consider utilizing the arrangement of biometrics as a part of the livelihood setting. Some of these contemplations incorporate the First and Fourth and Fifth Corrections, common claims, for example, carelessness and break of agreement, and tort claims, for example, attack of protection. This is in no way, shape or form a complete rundown of the considerable number of cases that may be attested by somebody who affirms harms that came about because of the utilization of biometrics. It is additionally essential to comprehend that there is very little case law yet with respect to the utilization of biometrics. [2].

Biometrics is the science and innovation of measuring and examining organic information. It is utilized to particularly recognize people by their physical attributes or individual conduct characteristics. Bosses use biometrics for general ID purposes and to permit access to ensured regions. TheBiometrics framework has three fundamental steps. To start with, it gains information through a suitable scanner/peruses. Second, it encodes the information. Third, it dissects the information. [3]

Crack of assentation I the business has a procedure that states it will keep a specialist's bio-data private the agent may claim abreak of understanding if the bio-data is hacked, stolen, or used as a piece of a raunchy way. Security torts-the business that abuses data acquired through biometrics may be at risk for the tort of attack of protection by the worker.

If it's not too much trouble take note that this is a short rundown of illustrations of legitimate cases that may be stated by workers however it doesn't constitute a full rundown of lawful cases nor is it to be utilized as alawful exhortation.

At the point when a business is utilizing biometrics it is checking its workers and it is utilizing the representatives' natural attributes to distinguish the worker [4].

1.2 Image processing [5]

Some can envision that computerized picture handling means just pictures embellish operations and the presentation of some design and charges for them or erase them to appear later in another appearance varies from the first. In any case, the computerized picture handling past that truth be told, they very nearly couldn't care less about this part of picture preparation by any stretch of the imagination. Where it is here to concentrate on advanced encryption suitable for pictures and discover approaches to address this computerized information so that these pictures or data conveyed by the pictures are usable by a machine that can be a PC or a robot or different machines. Are computerized picture handling of awesome significance in the field of acknowledgment of any pictures, for instance, when attempting to make a PC or robot comprehend its means or the picture as it is likewise essential in the field of example acknowledgment or shapes can envision, for instance, that a robot perceives the human structure (for instance, the human proportionate to a rectangle vast fork to the four little rectangles and circle) and he doesn't welcome the feline home, for instance. Likewise, to recognize examples of awesome significance in the robotized preparation of pictures caught by the vans to the world's surface and the utilization of the military. They are likewise vital in dependence on route maps or pictures starting from the earliest stage.

1.2.1 Image Processing Methods [6, 4]

Linear processing of the file: deals with where the image signal is applied modalities of Digital Signal processing them.

Traditional image processing system consists of six successive stages which respectively:

1) Obtaining the image (image acquisition) by a sensitive optical (e.g. camera, sensitive Liz, etc.)
2) Pretreatment (pre-processing) image of jamming or converted to a binary image.
3) Cutting image (segmentation) to separate the important information (for example, any object in the picture) on the rear.
4) Draw features (features extraction) or qualities.
5) Classification features (classification) and link it back to him that the style and pattern recognition.

6) Understanding of the image (image understanding) and image processing systems are used in many applications, particularly applications of automatic control, robotics, computer vision … etc.

1.2.2 Image processing applications [7]

In image processing source of radiation was important and the sources were Gamma-ray imaging, X-ray imaging, imaging in UV band, imaging in the visible band and IR band, imaging in the Microwave band, and imaging in the Radio band. [7] In agriculture, Remote Sensing (RS) technique was widely used for various applications. [2] Remote Sensing was the science of identification of earth's surface features and estimation of geo-biophysical properties using electromagnetic radiation. Applications with optical and microwave sensors. The author discussed the satellites launched by different countries and their uses in various fields along with spatial, spectral, and temporal variations of data. Analytical techniques using digital image processing, multi-source data fusion, and GIS were also discussed. Applications towards agriculture provide the earth observation data which supports increased area under agriculture, increased crop intensity and productivity, etc. RS data can provide data related to groundwater helping in irrigation, and flood management. Applications like environment assessment and monitoring, disaster monitoring and mitigation, weather climate, village resource center, etc. were also discussed

1.2.3 Digital image

Is a representation of two-dimensional pictures on the PC by zero and one (1, 0). It comprises of an advanced picture of each of the pixels on the PC which is a representation of two-dimensional pictures on the PC by zero and one computerized picture. [9]

Every picture is a lattice containing lines and sections of pixels, and the more noteworthy the quantity of pixels as the picture is clearer and advanced pictures are isolated into: [10]

1- Binary Image: an image that contains black and white only and carries out each pixel is either zero or one.

2 Gray Scale Image: an image that contains black and white with shades of gray representing the intensity of numbers from 0 to 255, where a single white color and intensity when you are 255, the color of the pixel is black, and when the representation of the image on the computer represented by columns of equal and rows of pixels equal each pixel by 8 cells determines the intensity of 0 to 255.

3- Color Image: are digital images that support the colors through the allocation of three boxes per pixel to determine the severity of the three basic colors (red, green, and blue) and each box contains 8 House for writing it, for example, the intensity of the green may be 00100000 i.e., that there is a 24 bit per pixel, but some images may be out 8 house only and contain 256 color only.

There are other ways to represent images such as the image is represented as a function f (x, y), and displays digital images through the files GIF, Bmp, JPEG, PNG**.**

1.3 Human Iris

The iris (or irises) is a dainty, round structure in the eye, in charge of controlling the distance across and size of the understudy and the measure of light coming to the retina. The iris' shade is frequently alluded to as eye shading. [8]

The iris is the blue zone. Alternate structures noticeable are the understudy focus and the white sclera encompassing the iris. The overlying cornea is imagined, yet not unmistakable, as it is straightforward. Likewise, envisioned are the red-hued veins inside of the sclera. These are effortlessly obvious in any individual's eyes. [8]

PC vision-based systems that perceive human components, for example, confronts, finger prints, palms, and eyes have numerous applications in observation and security. The vast majority of the current routines have restricted capacities in perceiving generally complex components in reasonable pragmatic circumstances. The goal of this correspondence is to present another methodology for perceiving people from pictures of the eyes' iris under functional conditions.

The iris has remarkable components and is sufficiently intricate to be utilized as a biometric signature [1]. This implies that the likelihood of finding two individuals with indistinguishable iris examples is right around zero. Accordingly, so as to utilize the iris design for identic.

Wavelet Transforms Results

The transformed wavelets samples father of application. By Matlab program 2012a and from Start, choose the Wave menu to open an application Wavelet Toolboxes.

In the current study was to focus on the use of two-dimensional wavelets for has been applied of 15 images for each group, and applies wavelet type (Biorthogonal, Coiflets, Symlets, Daubechie, Haar).

Then apply again the same six statistical operations (Mean, Std., Var., Energy, Homogeneity, and Entropy) on images extracted after the wavelet transforms.

The results of the application of the wavelet transform on study samples are shown in figures.

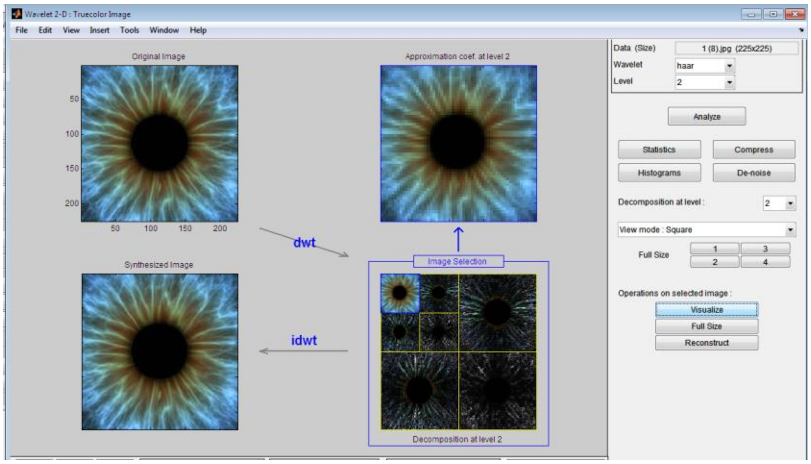

Figure (1) Wavelet transform (Haar type) application on Flower irises

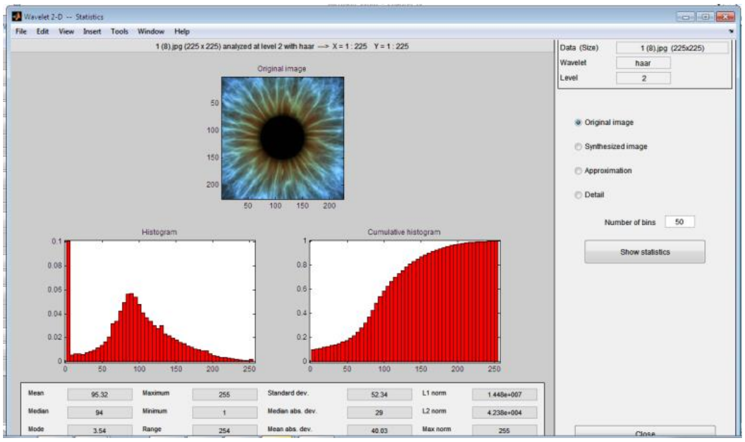

Fig (2) Analyzed with (Haar - level 2) of Flower irises

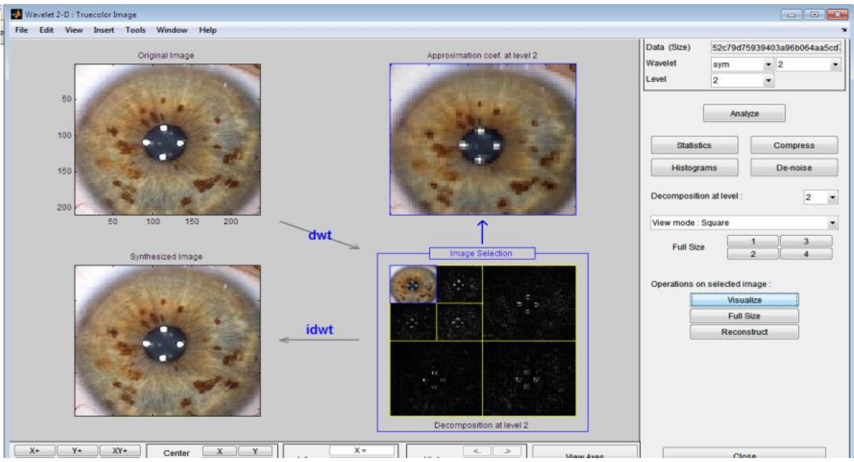

Figure (3) Wavelet transforms (Sym type) application on Jewels irises

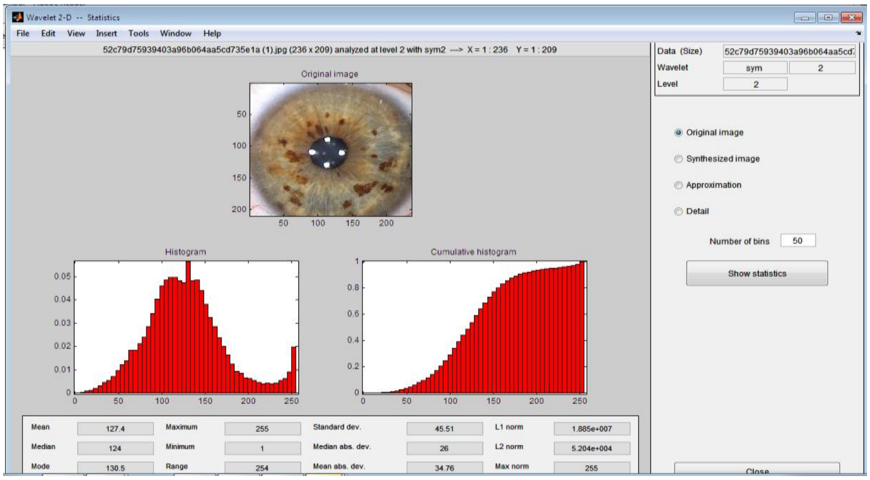

Figure (4 Analyzed at (Sym. Type- level 2) to Jewels Irises

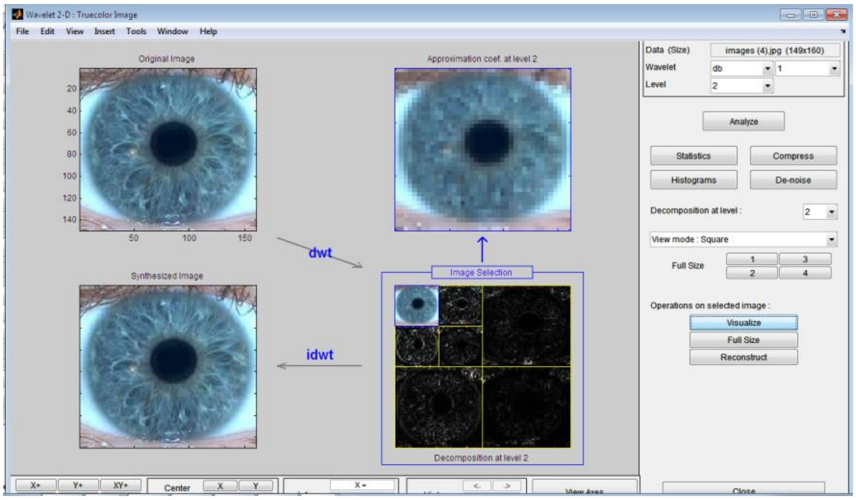

Figure (5 Wavelet transform (Db type) application on Shaker type

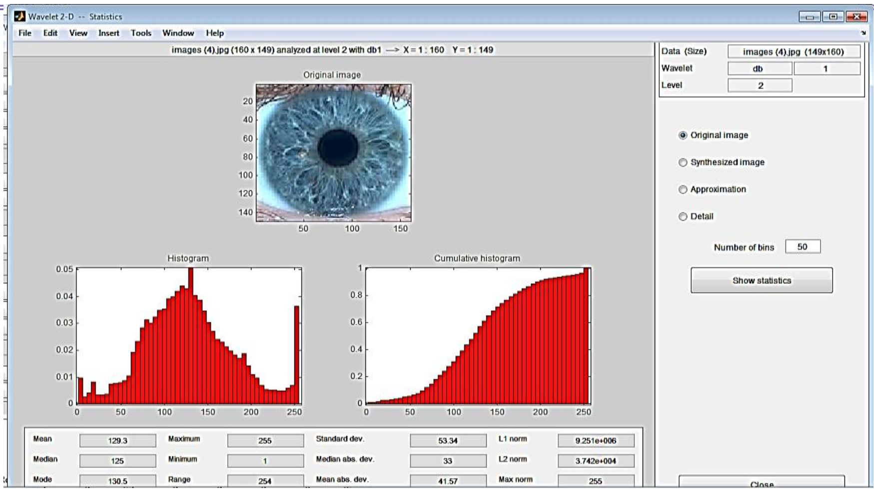

Fig (6) Analyzed at with (Db. level 2) of Shaker irises

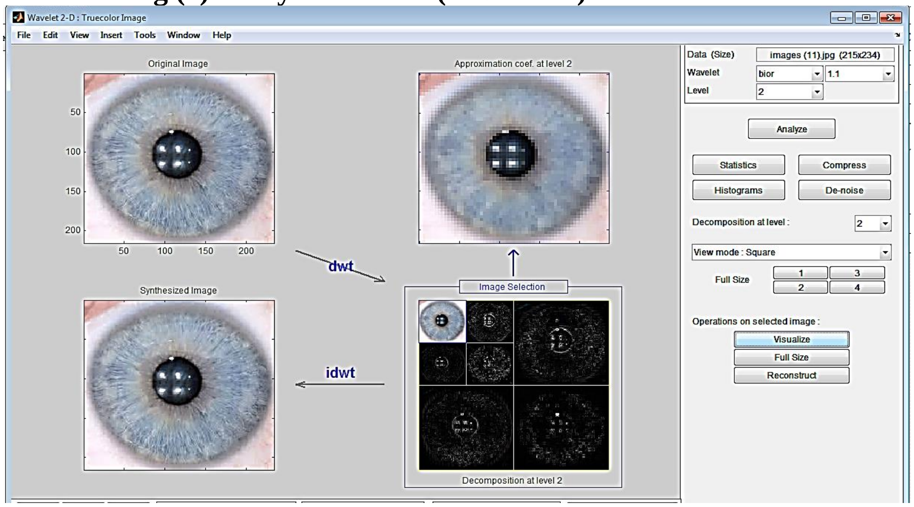

Figure (7) Wavelet transform (Bior type) application on stream irises.

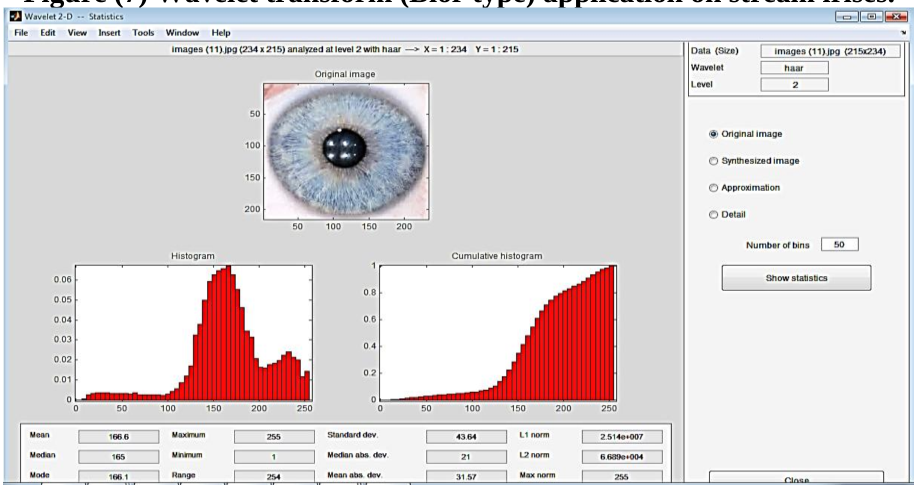

Figure (8) Analyzed at (Haar level 2) to stream irises

Table (1) shows values of mean, Std., energy, homogeneity, and entropy to samples for study, after applying wavelet (Syb type).

Table (1) Statistical operations by wavelet of flower irises

No	Mean	Std.	Var.	Energy	Homogeneity	Entropy
1	111.4	73.59	5.44E+003	1.48E-005	1.21E-004	7.832
2	129.3	53.72	2.87E+003	1.04E-005	1.21E-004	7.5987
3	162.4	58.82	3.46E+003	1.54E-006	2.64E-005	7.6342
4	130.2	45.2	2.03E+003	4.96E-005	5.72E-004	7.4608
5	75.33	38.78	1.48E+003	5.20E-005	4.02E-004	7.181
6	95.32	52.34	2.73E+003	8.56E-006	5.94E-004	7.301
7	125.01	76.24	5.75E+003	6.95E-005	8.27E-004	6.6641
8	109.1	76.26	5.77E+003	5.52E-005	7.00E-004	7.547
9	134.3	48.26	2.30E+003	5.53E-005	5.74E-004	7.5128
10	130.11	45.84	2.10E+003	7.45E-006	1.05E-004	7.4834
11	130.5	51.99	2.68E+003	5.36E-005	5.67E-005	7.514
12	78.74	73.44	5.36E+003	9.35E-005	1.97E-004	6.7889
13	126.91	50.6	2.56E+003	7.68E-006	9.19E-005	7.5341
14	125.11	77.26	5.95E+003	9.13E-006	1.35E-004	6.2766
15	151.30	69.93	4.87E+003	8.04E-006	8.73E-005	7.8353
Min	75.33	38.78	1.48E+003	1.54E-006	2.64E-005	6.2766
Max	162.4	77.26	5.95E+003	9.35E-005	8.27E-004	7.8353
Sum	1814.99	1008.31	6.28E+004	1.54E-006	5.46E-003	124.2758
Ave.	120.9993	59.48466	3.69E+03	3.31E-005	3.07E-004	7.34E+00

cation, it is critical to define a representation that is all-around adjusted for extricating the iris data content from pictures of the human.

Table (2) The accuracy results of four groups with ANNs by wavelet

Cases	Results accuracy convertible wavelet
1	**76.7%**
2	**75%**
3	**75%**
4	**76.7%**

Dissuasion;

1. Selected six statistics operations proved more favorable than the rest of the other Mini.
2. Proven method of high accuracy in the pictures networks classification.
3. Enactment of the image conversion in methods, it gave the best accuracy in the classification.
4. Wavelet and ANN is the best among all groups.

References

1. R. J. Schalko (1989), Digital Image Processing and Computer Vision, John Wiley and Sons.

2. Dictionary of Photography and Digital Imaging, The Essential Reference for the Modern Photographer, comp. Tom Ang. (London: Argentum, 2001), 52-53.

3. Jähne, Bernd, Digital Image Processing: Concepts, Algorithms, and Scientific Applications, 2nd ed., Springer-Verlag. 1993.

4. Jonathan Sachs 1996-1999 Digital Light & Color.

5. R. C. Gonzalez and R. E. Woods “Digital Image Processing”, 2nd edition, Pearson Education, 2004.

6. Trevor Roper, P.D.: The Eye and its Disorders. Oxford London, Blackwell Scientific Publications 1974.

7. Berggren, L.: Acta Ophthalmologica, A critical review. In, 63, 18, 1985.

8. Flom, L., Sar, A.: Iris recognition system. U.S. Patent No. 4, 641, 349. Washington, U.S. Goverment 1987.

9. Daugman, J. G.: Biometric personal identification system based on iris analysis. U.S. Patent No. 5, 291, 560. Washington, U.S. Government 1994.

Structural and Optical Properties of Nickel Oxide Thin Films with Cobalt doping

Nazar Abdulmahdi Jabir[1], Zahraa abdul Mahdi Jaber[2], Esraa Hassn Hadi[3]
[1]Department of Physics, College of Science, Mustansiriyah University.
[2]Department of Chemistry, College of Science for Women, University of Baghdad.
[3]Department of Physics, College of Education, Mustansiriyah University.

Abstract:
The deposition of pure NiO and NiO:Co films was carried out using the spray pyrolysis technique.
The XRD analysis confirmed the presence of the tetragonal phase of NiO in both pure NiO and NiO:Co films, with the (101) peak being the predominant peak. The grain size of the films increased with higher cobalt doping concentration, while the dislocation density decreased. The transmittance spectra showed a gradual decrease in transmittance with increasing cobalt doping concentration. The absorption spectra exhibited an increase in optical absorption as the cobalt doping concentration increased. The absorption coefficient values increased with the addition of cobalt doping. The optical band gap energy values obtained showed a decrease with cobalt doping. The extinction coefficient decreased and the refractive index with increasing cobalt doping concentration.
Keywords: NiO, Co Thin Films, optical and structural properties, E_g.

الخصائص التركيبية والبصرية لأغشية اوكسيد النيكل الرقيقة المشوب بالكوبلت

نزار عبد المهدي جابر[1]، زهراء عبد المهدي جابر[2]، اسراء حسن هادي[3]
[1] قسم الفيزياء، كلية العلوم، الجامعة المستنصرية. [2] قسم الكيمياء/ كلية العلوم للبنات/ جامعة بغداد.
[3] قسم الفيزياء، كلية التربية، الجامعة المستنصرية.

المستخلص
تم ترسيب الأغشية الرقيقة من اوكسيد النيكل النقي واوكسيد النيكل المشوب بالكوبلت باستخدام تقنية التحلل الحراري بالرش. بين تحليل حيود الأشعة السينية أن الأفلام المحضرة ذات بنية رباعية الطور لكل من اغشية اوكسيد النيكل النقي واوكسيد النيكل المشوب بالكوبلت وان الاتجاه الساد هو (101)، ازداد الحجم الحبيبي مع زيادة التشويب بالكوبلت بينما انخفضت كثافة الانخلاعات. أظهرت أطياف النفاذية انخفاضًا تدريجيًا في النفاذية مع زيادة التشويب بالكوبلت. أظهرت أطياف الامتصاص زيادة في الامتصاص البصري مع زيادة التشويب بالكوبلت. ازدادت قيم معامل الامتصاص مع زيادة التشويب بالكوبلت. أظهرت قيم طاقة فجوة البصرية انخفاضًا مع زيادة التشويب بالكوبلت. انخفض معامل الخمود ومعامل الانكسار مع زيادة تركيز شائبة الكوبلت.
الكلمات الافتتاحية: اوكسيد النيكل، كوبلت، أغشية رقيقة، الخصائص البصرية والتركيبية، فجوة الطاقة.

Introduction

Nickel oxide (NiO) exhibits exceptional properties that make it a highly promising material for p-type transparent conducting oxide films [1]. It possesses excellent chemical stability [2], good crystallinity [3], a wide direct energy gap ranging from 3.6 to 4.0 eV [4], broad transparency across a wide spectral range, and is cost-effective [5]. pure NiO films typically demonstrate high resistivity on the order of 10^{13} Ω cm at room temperature [6]. However, this resistivity can be significantly reduced by p-doping NiO through the introduction of Ni vacancies and/or interstitial oxygen into the NiO structure [7]. The behavior and characteristics of NiO strongly depend on its stoichiometric ratio of nickel to oxygen atoms [8]. Nonstoichiometric variations in the nickel oxide films lead to changes in various film properties, with different effects observed in different applications such as electrochromic materials, solar cell electrodes, chemical gas sensors, and organic light-emitting diodes [9-12]. Numerous techniques have been developed for the preparation of nickel oxide thin films, such as sol-gel process [13], CVD [14], electron-beam evaporation [15], chemical bath deposition (CBD) [16], PLD [17], atomic layer deposition (ALD) [18], dc-magnetron sputtering [19], electrodeposition process [20] and spray pyrolysis [21-24]. chemical spray pyrolysis is the most commonly used and cost-effective method for fabricating large-area, homogeneous NiO coatings. It offers advantages such as the elimination of vacuum systems, ease of setup, and uniform size distributions in the resulting thin films [8]. The grain size of the films can be controlled by adjusting various parameters such as preparation conditions, doping type, and concentration. Extensive research has been conducted to investigate the impact of these preparation parameters on the properties of NiO films, including studies on the effect of thickness and substrate temperature [9]. In this work we have explored the influence of different precursors on the structural and optical properties of sprayed NiO thin films on glass substrates. This study aimed to examine the modifications in the properties of NiO thin films, both structurally and optically, following the introduction of cobalt dopant through the spray pyrolysis technique. The research also sought to explore the impact of varying dopant concentrations on the film characteristics.

Experiment

Nickel oxide (NiO) films were fabricated through chemical spray pyrolysis using different precursors, namely nickel nitrate($Ni(NO_3)_2{\cdot}6H_2O$), nickel chloride ($NiCl_2{\cdot}6H_2O$), and nickel acetate ($Ni(OCOCH_3)2{\cdot}4H_2O$). A doping agent of 0.1 M cobalt nitrate ($CoNO_3$) was utilized for doping the nickel oxide films, with two different doping concentrations of 1% and 3%. The deposition process took place on preheated Corning glass substrates at 400 °C. Prior to deposition, the glass substrates were carefully cleaned using an ultrasonic bath with acetone followed by rinsing with distilled water to ensure a clean surface for film nucleation. The spray nozzle-to-substrate distance was maintained at 28 cm to achieve uniform film deposition. A consistent deposition time of 8 minutes and compressed air pressure of 1.5 bar were employed for all samples to ensure similar film characteristics across the substrates. The film thickness was determined to be approximately 330 cm with an uncertainty of ± 20 nm using the weighing method. X-ray diffraction (XRD) analysis was conducted to examine the structural properties of the films, while the optical and transmission spectra were recorded using a double-beam UV/VIS spectrophotometer in the wavelength range of 300-900 nm.

Result and discussion

The XRD results of the Pure NiO and NiO:Co films are shown in Figure 1. The peaks observed at 2θ= 37.79°, 43.81°, and 62.52° correspond to the (101), (012), and (110) spectral peaks, respectively. These peaks are in good agreement with the tetragonal anatase phase of NiO as confirmed by the ICDD (44-1159) database. The (101) peak is found to be the predominant peak.

To determine the grain size, Equation (1) was applied. [25, 26]:

$$D = \frac{0.9\,\lambda}{\beta cos\theta} \qquad (1)$$

where λ is the wavelength of X-rays (λ=1.5406 Å), and β is the full width at half maximum (FWHM) at the position of the peak [22]. The results are presented in Table 1, which shows that the grain size increases with higher doping concentration (3%) compared to pure NiO. It is observed that the grain size ranges from 36.28 nm to 26.64 nm with an increase in cobalt doping concentration up to 3%.

To estimate the dislocation density (δ), Williamson and Smallman's relation given by Equation (2) was utilize [27, 28]:

$$\delta = \frac{1}{D^2} \qquad (2)$$

The results are presented in Table 1. It is observed that the dislocation density (δ) decreases as the cobalt concentration increases, ranging from 109.18 to 88.16. This decrease can be attributed to the improvement in the crystallinity of the films [23].
The strain (ε) in the thin films was estimated using Equation (3), which is given by: [29,30]:

$$\varepsilon = \frac{\beta cos\theta}{4} \qquad (3)$$

Table 1 summarizes the obtained structural results. It can be observed that the value of strain (ε) decreases with increasing cobalt doping concentration.

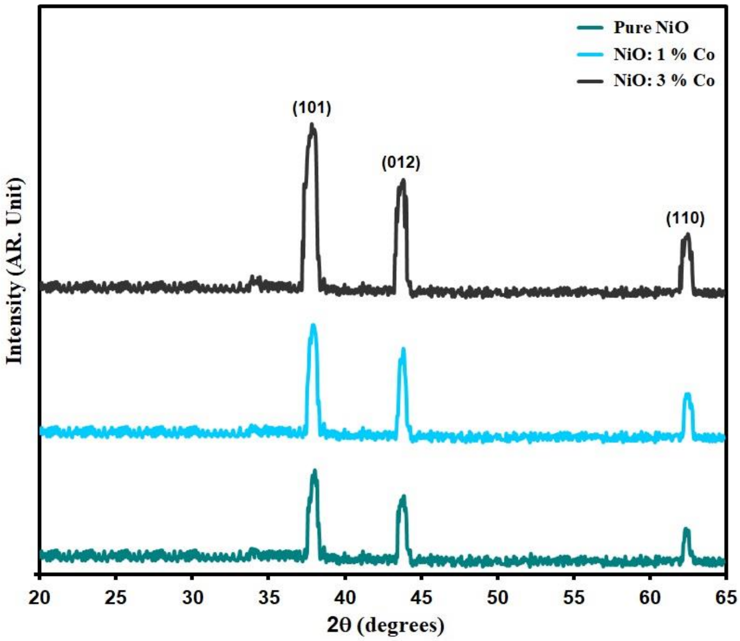

Fig. (1): The XRD patterns of the grown films.

Table 1 The grain size, optical bandgap, and structural parameters of the films.

Samples	2 □ (°)	(hkl) Plane	FWHM (°)	Optical bandgap (eV)	Grain size (nm)	Dislocations density (× 10^{14})(lines/m^2)	Strain (× 10^{-4})
Pure NiO	37.79	101	0.44	3.77	36.28	23.71	17.48
NiO: 1% Co	37.75	101	0.41	3.70	31.95	20.45	15.49
NiO: 3% Co	37.71	101	0.37	3.65	26.64	18.83	14.97

Fig. 2 presents the transmittance spectra of NiO thin films with different concentrations of cobalt doping. It can be observed that the transmittance decreases gradually as the doping concentration of cobalt increases, ranging from 79% to 68%. This decrease in transmittance can be attributed to the presence of lattice defects caused by the introduction of nano cobalt into the NiO lattice. The cobalt particles may occupy interstitial sites within the NiO lattice, thereby reducing the transmission of light through the film [31]. Fig. 3 illustrates the relationship between absorption spectra (A) and wavelength. It is evident that the optical absorption spectra increases as the concentration of cobalt doping increases [32].

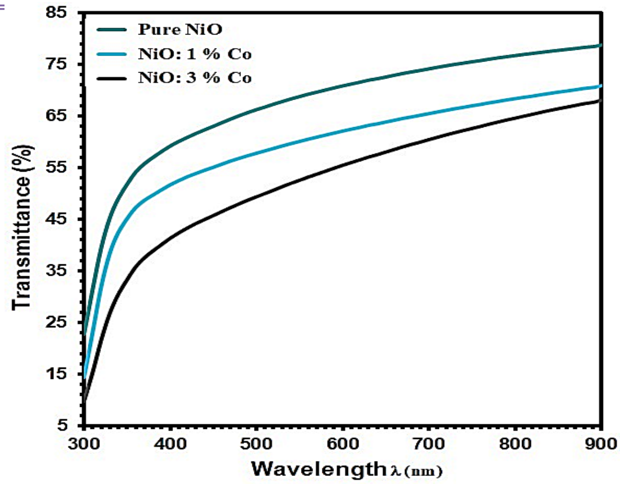

Fig. (2): Transmittance versus wavelength (λ) of NiO and NiO:Co thin films.

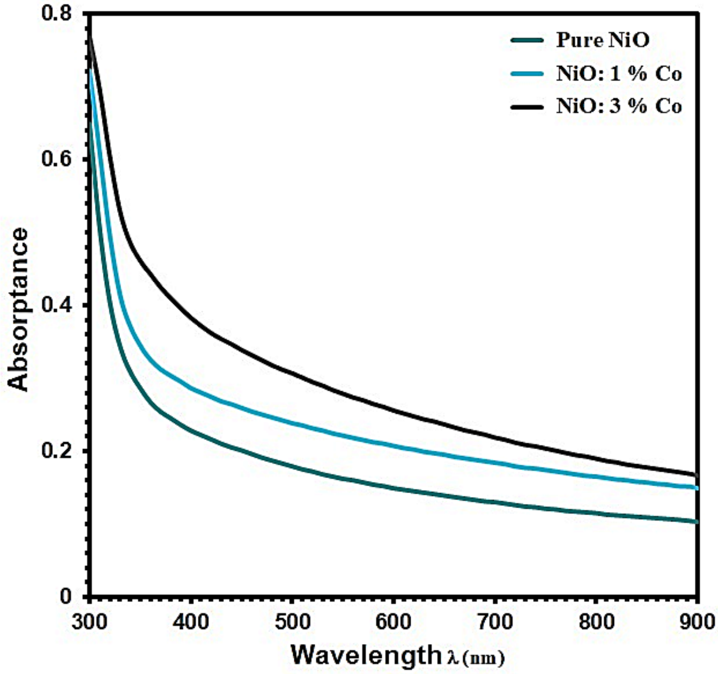

Fig. (3): Absorption versus wavelength (λ) of NiO and NiO:Co thin films.

The absorption coefficient (α) can be determined by utilizing the following relationship, which relates the film's absorbance to the absorption coefficient [33,34]:

$$\alpha = \frac{20303\,A}{t} \qquad (4)$$

Where t is the film thickness and A is the optical absorption.

Figure 4 depicts the variation of the absorption coefficient (α) with photon energy for both pure NiO and NiO: Co films. It is evident that the values of the absorption coefficient increase with the addition of cobalt doping. [35].

Fig. 5 displays the optical band gap energy (Eg) as determined using Tauc's relation [36, 37]:

$$(\alpha h\nu)^{1/2} = A\,(h\nu - Eg)^{1/2} \qquad (5)$$

Where A Constant and (hν) photon energy, The optical band gap energy (Eg) values obtained using Tauc's relation show a decrease from 3.77 eV for pure NiO films to 3.65 eV for NiO: 3% Co thin films. This decrease in E_g values indicates a widening of the band gap with the introduction of cobalt doping in NiO films [38].

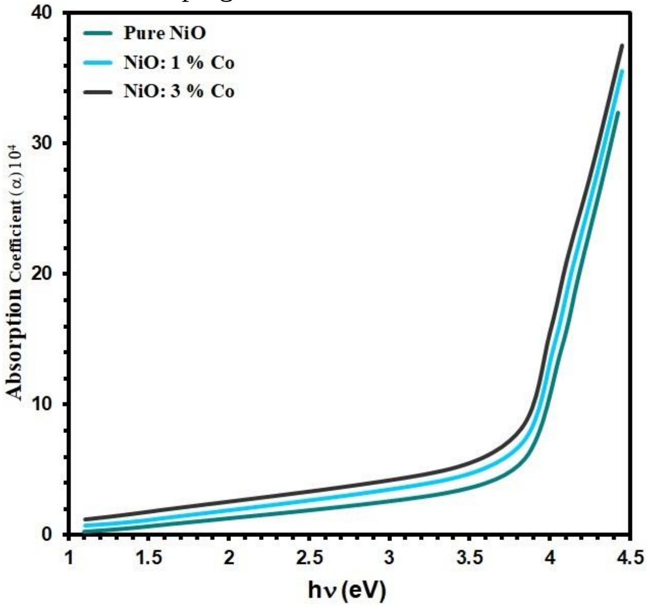

Figure (4): absorption coefficient versus photon energy (hν) of NiO and NiO:Co thin films.

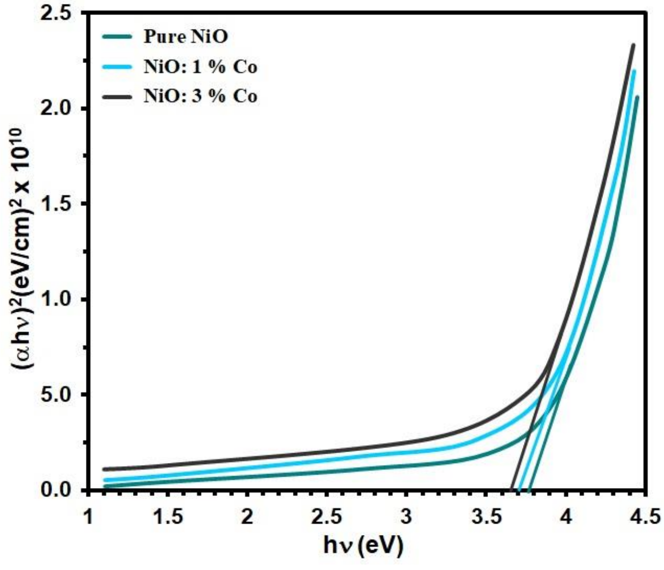

Figure (5): (αhν)2 via hν of NiO and NiO:Co thin films.

The extinction coefficient (k) can be determined using the following equation [39, 40]:

$$k = \frac{\alpha\lambda}{4\pi} \qquad (6)$$

where λ is the wavelength of light. The extinction coefficient of NiOand NiO: 3% Co thin films is plotted in Figure 7. It can be observed that the extinction coefficient decreases with increasing cobalt doping concentration.

The refractive index (n) is obtained from the equation [41, 42]:

$$n = \left(\frac{1+R}{1-R}\right) + \sqrt{\frac{4R}{(1-R)^2} - k^2} \qquad (7)$$

Where the R is the reflectance. Figure 7 illustrates the refractive index of Cadmium oxide thin films. It is evident that the refractive index decreases as the cobalt doping concentration increases. This decrease in refractive index can be attributed to the enhancement in crystal quality and grain size of the films with the higher cobalt doping concentration [43].

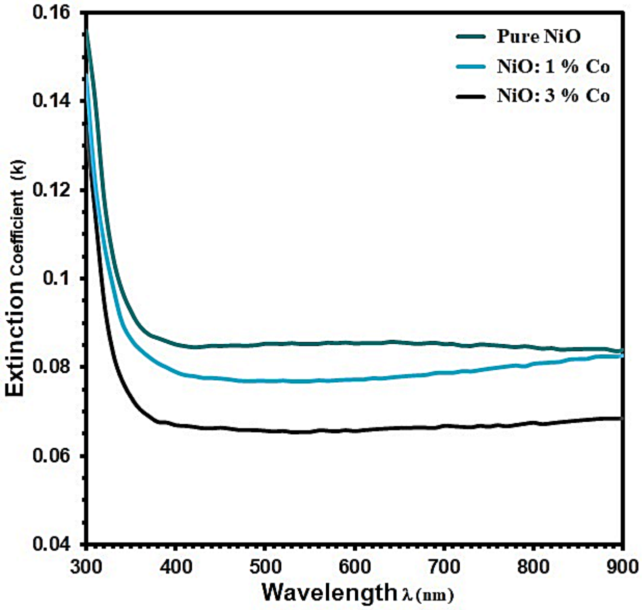

Fig. (6). extinction coefficient versus wavelength of NiO and NiO:Co thin films.

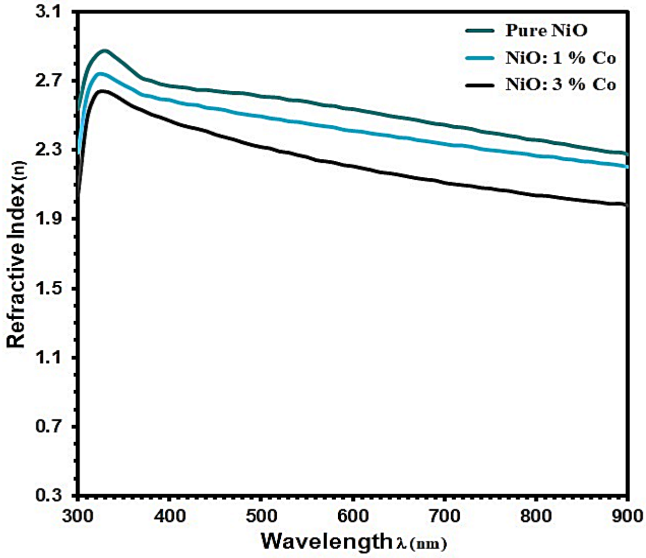

Fig. (7) refractive index versus wavelength of NiO and NiO:Co thin films.

Conclusion

Using the spray pyrolysis technique (CSP), pure NiO and NiO:Co films were successfully deposited. The incorporation of cobalt into NiO thin films exhibited notable influences on their structural and optical properties. X-ray diffraction (XRD) analysis confirmed the presence of the tetragonal anatase phase of NiO in both pure NiO and NiO:Co films. With an increase in cobalt doping concentration, the grain size of the films increased, while the dislocation density decreased. Moreover, the transmittance of the films decreased as the cobalt doping concentration increased. The absorption spectra demonstrated an augmentation in optical absorption as the cobalt doping concentration increased. Additionally, the absorption coefficient displayed an increment with the addition of cobalt doping. Furthermore, the optical band gap energy decreased as cobalt doping was introduced. Lastly, the extinction coefficient and refractive index exhibited a decrease with an increase in cobalt doping concentration.

References

[1] G. S. Gund, C. D. Lokhande, and H. S. Park, “Controlled synthesis of hierarchical nanoflake structure of NiO thin film for supercapacitor application,” Journal of Alloys and Compounds, vol. 741, pp. 549–556, Apr. 2018.

[2] H. Yang, J. H. Yu, H. J. Seo, R. H. Jeong, and J. H. Boo, “Improved electrochromic properties of nanoporous NiO film by NiO flake with thickness

[3] H. Lin et al., “The growth, properties and application of reactively sputtered nickel oxide thin films in all thin film electrochromic devices,” Materials Science and Engineering: B, vol. 270, p. 115196, Aug. 2021.

[4] Hotovy I., Spiess L., Predanocy M., Rehacek V., Racko J., Sputtered nanocrystalline NiO thin films for very low ethanol detection, Vacuum 107 (2014) 129–131.

[5] S. J. Lee, T. G. Lee, S. Nahm, D. H. Kim, D. J. Yang, and S. H. Han, “Investigation of all-solid-state electrochromic devices with durability enhanced
tungsten-doped nickel oxide as a counter electrode,” Journal of Alloys and Compounds, vol. 815, p. 152399, Jan. 2020. controlled by aluminum,” Applied Surface Science, vol. 461, pp. 88–92, Dec. 2018.

[6] Shang Z. W., Hsu H. H., Zheng Z. W., Cheng C. H., Progress and challenges in p-type oxide-based thin film transistors, Nanotechnology Reviews 8 (2019) 422–443.

[7] Gund G. S., Lokhande C. D., Park H. S., Controlled synthesis of hierarchical nanoflake structure of NiO thin film for supercapacitor application, Journal of Alloys and Compounds 741 (2018) 549-556.

[8] Herissi L., Hadjeris L., Aida M. S., Bougdira J., Properties of (NiO)1-x(ZnO)x thin films deposited by spray pyrolysis, Thin Solid Films 605 (2016) 116–120.

[9] Guezzoun H., Benhaoua B., Benramache S., Synthesis and characterizations of nanocrystalline Na and Al codoped NiO thin films, International Journal of Integrated Engineering 12 (1) (2020) 204-209.

[10] IsmailR. A., S. Ghafori, G. A. Kadhim, "Preparation and characterization of nanostructurednickel oxide thin films by spray pyrolysis", Appl. Nanosci., vol. 3, pp. 509-514, 2013.

[11] Raza M. H., Movlaee K., Wu Y., El-Refaei S. M., Karg M., Leonardi S.G., Neri G., Pinna N., Tuning the NiO Thin Film Morphology on Carbon Nanotubes by Atomic Layer Deposition for Enzyme-Free Glucose Sensing, ChemElectroChem 6 (2019) 383–392.

[12] R. O. Ijeh et al., “Magnetic and optical properties of electrodeposited nanospherical copper doped nickel oxide thin films”, Physica E: Low-dimensional Systems and Nanostructures, vol. 113, pp. 233–239, Sep. 2019.

[17] S. Zargouni, S. El Whibi, E. Tessarolo, M. Rigon, A. Martucci, and H. Ezzaouia, "Structural properties and defect related luminescence of Yb-doped NiO sol-gel thin films," Superlattices and Microstructures, vol. 138, p. 106361, Feb. 2020.
[18] A. S. Kondrateva, M. V. Mishin, and S. E.Alexandrov, "TOF MS Investigation of Nickel Oxide CVD," J. Am. Soc. Mass Spectrom., vol. 28, no. 11, pp. 2352–2360, Nov. 2017.
[15] D. R. Sahu, T.-J. Wu, S.-C. Wang, and J.-L. Huang, "Electrochromic behavior of NiO film prepared by e-beam evaporation," Journal of Science: Advanced Materials and Devices, vol. 2, no. 2, pp. 225–232.
[16] J.-H. Yu, S.-H. Nam, Y. E. Gil, and J.-H. Boo, "The effect of ammonia concentration on the microstructure and electrochemical properties of NiO nanoflakes array prepared by chemical bath deposition," Applied Surface Science, vol. 532, p. 147441, Dec. 2020.
[17] M. A. Hameed, O. A. Ali, and S. S. M. Al-Awadi, "Optical properties of Ag-doped nickel oxide thin films prepared by pulsed-laser deposition technique," Optik, vol. 206, p. 164352, Mar. 2020.
[18] M. H. Raza et al., "Tuning the NiO Thin Film Morphology on Carbon Nanotubes by Atomic Layer Deposition for Enzyme-Free Glucose Sensing," ChemElectroChem, vol. 6, no. 2, pp. 383–392, 2019.
[19] P. Salunkhe, M. A. A.V, and D. Kekuda, "Structural, spectroscopic and electrical properties of dc magnetron sputtered NiO thin films and an insight into different defect states," Appl. Phys. A, vol. 127, no. 5, p. 390, Apr. 2021.
[20] B. R. Cruz-Ortiz, M. A. Garcia-Lobato, E. R. Larios-Duran, E. M. Muzquiz-Ramos, and J. C. Ballesteros-Pacheco, "Potentiostatic electrodeposition of nanostructured NiO thin films for their application as electrocatalyst," Journal of Electroanalytical Chemistry, vol. 772, pp. 38–45, Jul. 2016.
[21] K. O. Ukoba, A. C. Eloka-Eboka, and F. L. Inambao, "Review of nanostructured NiO thin film deposition using the spray pyrolysis technique," Renewable and Sustainable Energy Reviews, vol. 82, pp. 2900–2915, Feb. 2018.
[22] Mironova-Ulmane N., Kuzmin A., Sildos I., Puust L., Grabis J., Magnon and Phonon Excitations in Nanosized NiO, Latvian Journal of Physics and Technical Sciences 56 (2019) 726–737.
[23] Dawood, M.O., Chiad, S.S., Ghazai, A.J., Habubi, N.F., Abdulmunem, O.M., Effect of Li doping on structure and optical properties of NiO nano thin-films by SPT, AIP Conference Proceedings 2213, 2020, 020102.
[24] Mohammed, K.G., Agool, I. R., Abdul Ameer, F.S., Habubi, N.F., Chiad, S.S., Investigation of Nanostructured NiO and Au Doped NiO Thin Films by SPT, IOP Conference Series: Earth and Environmental Sciencethis link is disabled, , , 2021, 790(1), 012080.
[25] Othman, M.S., Mishjil, K.A., Rashid, H.G., Chiad, S.S., Habubi, N.F., Al-Baidhany, I.A., Comparison of the structure, electronic, and optical behaviors of tin-doped CdO alloys and thin films, Journal of Materials Science: Materials in Electronics 31(11), pp. 9037-9043, 2020.
[26] Jandow, N.N., Othman, M.S., Habubi, N.F., Chiad, S.S., Mishjil, K. A., Al-Baidhany, I. A., Theoretical and experimental investigation of structural and optical properties of lithium doped cadmium oxide thin films, Materials Research Express 6(11), 2020.
[27] Khadayeir, A. A., Hassan, E. S., Mubarak, T. H., Chiad, S.S., Habubi, N. F., Dawood, M.O., Al-Baidhany, I. A., The effect of substrate temperature on the physical properties of copper oxide films, Journal of Physics: Conference Series, 2019, 1294 (2) 022009.

[28] Muhammad, S. K., Taqi, N.D.M., Chiad, S.S., Abass, K.H., Habubi, N.F., Influence of nanostructured nio thin films doped with chrome by using green chemical spray gyrolysis csp, Journal of Green Engineering, 11(2), pp. 1287-1299, 2021.
[29] E. Fujii, A. Tomozawa, H. Torii, R. Takayama, "Preferred orientations of NiO films prepared by plasma-enhanced metalorganicchemical vapor deposition", Jpn. J. Appl. Phys35(1996) L328–L330.
[30] Hadi, E. H., Sabur, D.A., Chiad, S. S., Habubi, N. F., Abass, K.H., Physical properties of nanostructured li-doped zro_2 thin films, Journal of Green Engineering, 10(10), pp. 8390-8400, 2020.
[31] Ghazai, A. J., Abdulmunem, O. M., Qader, K. Y., Chiad, S. S., Habubi, N. F., Investigation of some physical properties of Mn doped ZnS nano thin films, 2020, AIP Conference Proceedings 2213 (1) , 020101.
[32] R. Paulose, R. Mohan, and V. Parihar, "Nanostructured nickel oxide and its electrochemical behaviour—A brief review," Nano-Structures & Nano-Objects, vol. 11, pp. 102–111, Jul. 2017.
[33] Salloom, H.T., Hadi, E.H., Habubi, N.F., Chiad, S.S., Jadan, M., Addasi, J.S., Characterization of silver content upon properties of nanostructured nickel oxide thin films, Digest Journal of Nanomaterials and Biostructures 15(4), pp. 1189-1195, 2020.
[34] Hussin, H.A., Al-Hasnawy, R.S., Jasim, R.I., Habubi, N.F., Chiad, S.S., Optical and structural properties of nanostructured CuO thin films doped by Mn, Journal of Green Engineering, 10(9), pp. 7018-7028, 2020.
[35] Manouchehri I., Mehrparvar D., Moradiana R., Gholami K., Osati T., Investigation of structural and optical properties of copper doped NiO thin films deposited by RF magnetron reactive sputtering, Optik 127 (2016) 8124–8129.
[36] Chiad, S. S., Alkelaby, A.S., Sharba, K. S., Optical Conduct of Nanostructure Co3O4 rich Highly Doping Co_3O_4: Zn alloys, Journal of Global Pharma Technology, 11(7), pp. 662-665, 2020
[37] Ahmed, N.Y., Bader, B. A., Slewa, M. Y., Habubi, N. F., Chiad, S. S., Effect of boron on structural, optical characterization of nanostructured fe_2O_3 thin films, NeuroQuantology, 18(6), pp. 55-60, 2020.
[38] Jung, D. L. Kim, S. H. Oh, and H. J. Kim, "Stability enhancement of organic solar cells with solution-processed nickel oxide thin films as hole transport layers," Solar Energy Materials and Solar Cells, vol. 102, pp. 103–108, Jul. 2012.
[39] Al Rawas, A. S., Slewa, M. Y., Bader, B. A., Habubi, N. F., Chiad, S. S., Physical characterization of nickel doped nanostructured TiO_2 thin films, Journal of Green Engineering10 (9), pp. 7141-7153, 2020.
[40] Hassan, E. S., Mubarak, T. H., Chiad, S. S., Habubi, N. F., Khadayeir, A.A., Dawood, M. O., Al-Baidhany, I. A., Physical Properties of indium doped Cadmium sulfide thin films prepared by (SPT), Journal of Physics: Conference Series, 1294(2), 2019.
[41] Hassan, E. S., Qader, K. Y., Hadi, E. H., Chiad, S. S., Habubi, N. F., Abass, K. H., Sensitivity of nanostructured mn-doped cobalt oxide films for gas sensor application, Nano Biomedicine and Engineering, 12(3), pp. 205-213, 2020.
[42] Sakhil, M. D., Shaban, Z. M., Sharba, K. S., Habub, N. F., Abass, K. H., Chiad, S.S., Alkelaby, A. S., Influence mgo dopant on structural and optical properties of nanostructured cuo thin films, NeuroQuantology, 18 (5), pp. 56-61, 2020.
[43] H. Lee, Y. T. Huang, M. W. Horn, and S. P. Feng, "Engineered optical and electrical performance of rf– sputtered undoped nickel oxide thin films for inverted perovskite solar cells", Sci Rep, vol. 8, no. 1, p. 5590, Apr. 2018.

Study the Structural and Optical Properties of Nickel Doped Copper Oxide Thin films prepared by Chemical Spray Pyrolysis Technique

Israa Hmood Ibraheem[1], Zahraa Abdul Mahdi Jaber[1], Zina Mahmood Shaban[2]
[1] Department of Chemistry, College of Science for Women, University of Baghdad.
[2]Department of Physics, College of Education, Mustansiriyah University.

Abstract:
CuO and CuO:Ni thin films wad deposit by chemical spray pyrolysis method. X-ray diffraction (XRD) analysis revealed that both pure CuO and CuO:Ni films were polycrystalline, with a preferred orientation of (200). The grain size of the films increased from 16.87 nm to 19.75 nm with increasing Nickel concentration. The films exhibited high transmittance (>78.5%) in the visible region for CuO and CuO:Ni. As the Nickel concentration increased the absorption coefficient decreased, while the energy gap decreased from 2.28 eV to 2.23 eV. The refractive index and extinction coefficient also decreased with increasing Nickel concentration.
Keywords: CuO, Thin Films, Ni, structural and optical properties, E_g.

دراسة الخصائص التركيبية والبصرية لأغشية أوكسيد النحاس الرقيقة المشوب بالنيكل المحضرة بتقنية التحلل الكيميائي الحراري

اسراء حمود ابراهيم[1]، زهراء عبد المهدي جابر[1]، زينة محمود شعبان[2]
[1] قسم الكيمياء / كلية العلوم للبنات/ جامعة بغداد. [2] قسم الفيزياء، كلية التربية، الجامعة المستنصرية.

المستخلص
تم تحضير أغشية رقيقة من اوكسيد النحاس والمشوب بالنيكل باستخدام تقنية التحلل الكيميائي الحراري، اثبت تحليل حيود الاشعة السينية بان أغشية اوكسيد النحاس واوكسيد النحاس المشوب بالنيكل كانت متعددة التبلور وباتجاه سائد (200). ازداد الحجم الحبيبي للأغشية اوكسيد النحاس من 16.87 نانومتر إلى 19.75 نانومتر مع زيادة تركيز النيكل. أظهرت الأفلام نفاذية في المنطقة المرئية للأغشية اوكسيد النحاس واوكسيد النحاس المشوب بالنيكل كانت أعلى من 78.5%، بينما قلت قيمة معامل الامتصاص مع زيادة التشويب بالنيكل في الأغشية. كما تم ملاحظة انخفاض قيمة فجوة الطاقة ومعامل الانكسار ومعامل الخمود مع زيادة تركيز النيكل.
الكلمات الافتتاحية: اوكسيد النحاس، أغشية رقيقة، النيكل، الخصائص التركيبية والبصرية، فجوة الطاقة.

Introduction

Copper oxide (CuO) is a black or dark brown inorganic compound that occurs naturally as the minerals tenorite and paramelaconite. Itis also produced synthetically through various methods, such as thermal decomposition of copper salts and oxidation of copper metal [1]. CuO has several important physical and chemical properties that make iuseful in various applications [2]. CuO is a semiconductor with a narrow bandgap of approximately 1.2 eV, which makes it suitable for use in solar cells, gas sensors, and catalysis. It also has a high melting point of 1326°C, good thermal conductivity, and is resistant to thermal shock and oxidation making it useful in high-temperature applications such as in the production of superconductors and in nuclear reactors [3]. In addition, CuO is used as a pigment in ceramics and glassmaking due to its ability to produce shades of blue and green [4]. It is also used in the production of magnetic storage media and as a fungicide in agriculture. Furthermore, CuO has been found to exhibit antibacterial, antifungal, and anticancer properties, which have led to its use in medicine and biomedical research [5]. Its ability to induce apoptosis, or programmed cell death [6], has been of particular interest in cancer research. Overall, copper oxide is a versatile and important compound that has applications in various fields such as materials science, electronics, medicine, and agriculture [7]. Various methods can be employed to deposit copper oxide films, including the oxidation of copper sheets, Chemical Bath Deposition (CBD) [8], Sol–gel [9], magnetron sputtering [10], thermal oxidation, electrodeposition [11] and chemical spray pyrolysis [12-15]. The spray pyrolysis technique is suitable for fabricating metal oxide films due to the high melting point of metal oxides [16,17]. In this study, pure CuO and CuO: Ni thin films were deposited on glass substrates using CSP at a temperature of 400°C.

Experiment

Utilizing the spray pyrolysis technique, pure CuO and CuO:Ni films were produced. A laboratory-designed glass atomizer with a 1 mm output nozzle was used to spray the films onto preheated glass substrates at a temperature of 400°C and 0.1 M of Cu [$C_4H_6CuO_4$]. The doping process involved resolving (NiCl3) in re-distilled water and adding drops of HCl to obtain a clear solution. The optimized conditions for spray pyrolysis included a 10second spray time followed by a two-minute interval to prevent excessive cooling, a constant spray interval of 1.5 minutes, a carrier gas pressure of 105 Nm^{-2}, a nozzle-to-substrate distance of approximately 31 cm ± 1 cm, and a solution flow rate of 5 ml/min. The film's mass was determined by weighing the samples before and after spraying, and the film thickness was measured gravimetrically with a value of 325 ± 35 nm. The XRD technique was used to evaluate the films' structural properties, while double-beam UV/VIS (Shimadzu Corporation Japan) was employed to record the optical and transition spectra in the wavelength range of 300-900 nm.

Result and discussion

Fig. (1) depicts the XRD patterns of CuO and undoped Ni thin films (1). The (111), (200) and (020) diffraction peaks are seen to be aligned along these lines at angles of 35.37°, 38.47° and 53.37°, respectively. These angles match to the card number (48-1548) of the International Centre for Diffraction Data (ICDD) [18]. Other studies have also recorded similar behavior. The peak's substantially larger intensity suggests preferred (200) plane indicates a substantial peak expansion along that plane [19, 20].

Using Scherrer's formula [21,22], we were able to determine crystallite size as follows:

$$D = \frac{0.9\,\lambda}{\beta cos\theta} \quad (1)$$

where (FWHM), the diffraction angle, and the active X-ray wavelength are the proper units. Table 1's findings reveal that, compared to pure CuO, the crystallite size rises for higher doping concentrations (Ni 4%) and reduces for lower doping concentrations (Ni = 2%).

Using the relation, the dislocation density (δ) was computed. [23, 24],

$$\delta = \frac{1}{D^2} \quad (2)$$

As the Ni content is raised from 0% to 4%, the dislocation density drops from 62.76 to 28.14. This trend is similar to CuO films made using sol-gel, spray pyrolysis [9], and ultrasonic spray pyrolysis techniques [14].

The strain (ε) showed by the formula [25, 26]:

$$\varepsilon = \frac{\beta cos\theta}{4} \quad (3)$$

As the content is raised from 0% to 4%, the strain value falls from 28.14 to 23.85. The derived structural coefficients Sc are displayed in Table 1, and figure 1 represents the content of Sc versus Nickel.

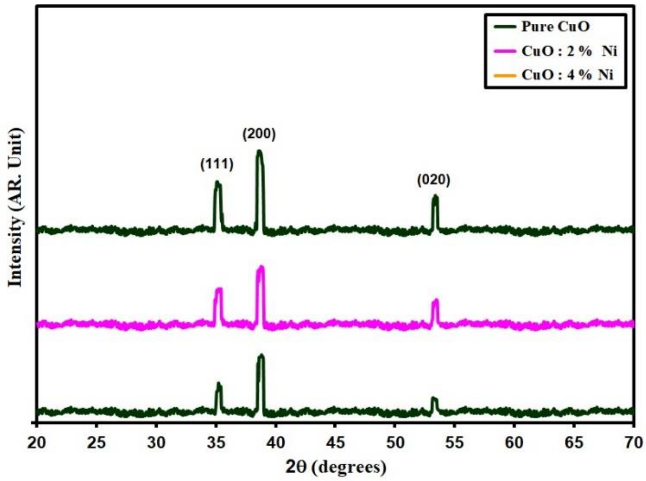

Fig. (1): XRD styles of grown samples.

Table 1. Grain size, optical bandgap and structural parameters of the films.

Samples	2 q (º)	(hkl) Plane	FWHM (º)	Optical bandgap (eV)	Grain size (nm)	Dislocations density ($\times 10^{14}$)(lines/m^2)	Strain ($\times 10^{-4}$)
CuO	38.47	200	0.58	2.28	16.87	62.76	28.14
CuO: 2% Ni	38.43	200	0.56	2.23	17.32	56.31	26.06
CuO: 4% Ni	38.40	200	0.53	2.17	19.75	49.84	23.85

In Figure 2, the transmittance (T) of CuO and CuO:Ni nanoparticles is shown as a function of wavelength. As the concentration of CuO:Ni increases, there is a reduction in transmittance. This is because the added nanoparticles contain electrons that can absorb electromagnetic energy and move to a higher energy level. The pure film has high transmittance due to the absence of particles. It lacks free electrons and requires a high energy transition to break the bonds. This is consistent with previous research [27].

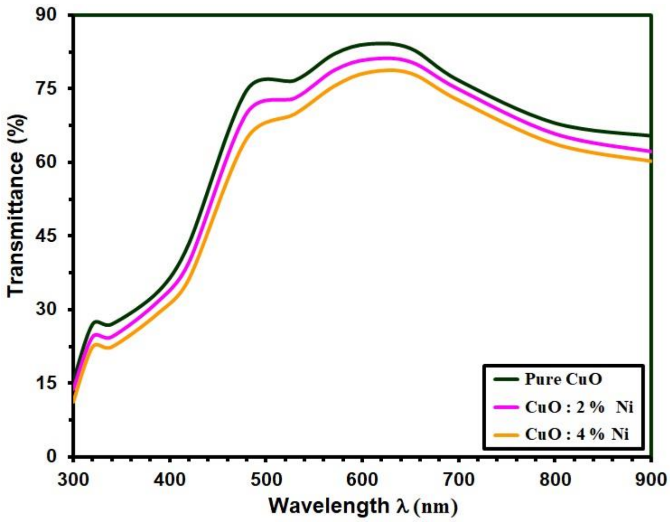

Fig. (2): T of the intended films.

The absorption coefficient (α) was calculated by employing the following formula [25]:

$$\alpha = \frac{20303A}{t} \qquad (4)$$

Where A is the optical absorption and t is the film thickness. Figure (3) as show the absorption coefficient α as a function of wavelength for (CuO and CuO:Ni) nanoparticles', has a high value of (10^4 cm^{-1}), stating direct electronic transitions. It can be seen that by increasing the doping, increases very slightly and the absorption coefficient travels toward to low energies.

Tauc's relationship was used to calculate the l band gap (Eg) and type of transit [28, 29]:

$$(\alpha h\nu)^{1/2} = A_s (h\nu - Eg)^{1/2} \qquad (4)$$

Where A_s Constant and (hv) photon energy The photon energy, which rapidly rises between (2.28-2.17) eV. The formation of new localized levels that invade the basic levels that absorb the reduced photons has caused values to rise. [30].

In Figure 4, the relationship between the absorption edge of CuO and CuO:Ni nanoparticles and photon energy is illustrated. The pure CuO has an Eg of 2.28 eV, and as the concentration of Ni increases, we can observe that the E_g also decreased. This phenomenon is caused by the emergence of site levels in the forbidden energy gap. In this case, the transition occurs in two steps, with the electron initially moving from the valence band to the local levels and then to the conduction band. This observation is consistent with previous research [31].

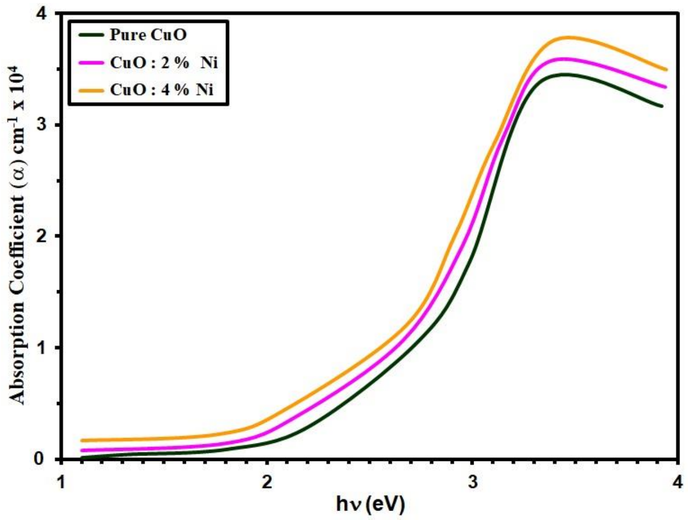

Fig. (3): The absorption coefficient spectra as a function of wavelength.

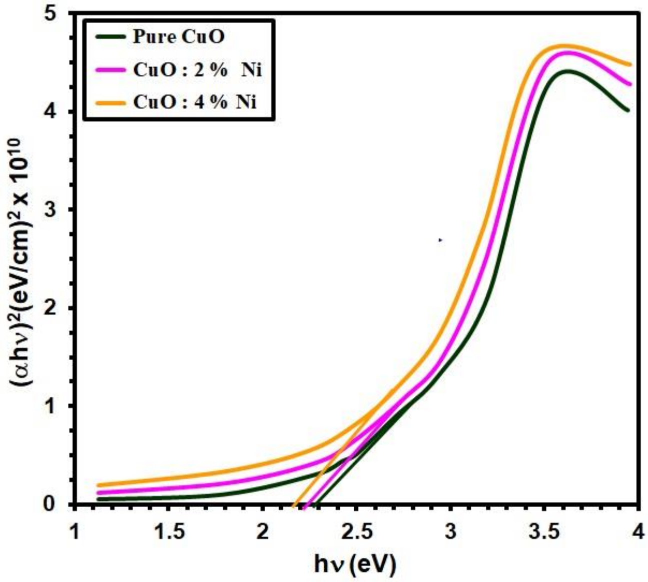

Fig. (4): Direct transition of the intended films.

Figure (4) showe variation of extinction coefficient of (CuO and CuO:Ni) nanoparticales with wavelength .The extinction coefficient (k) (CuO-Ni)nanoparticles' has indeed been determined via equation (5) [13]. The extinction coefficient versus wavelength variation for CuO pure and Ni NPs composites was demonstrated as in This figure shows that the extinction coefficient increases with increasing (Ni) constriatio and decreases with increasing wavelength due to the extinction coefficient's dependence on the values of the absorption coefficient [32, 33].

$$K=\alpha\lambda/4\pi \quad \ldots (5)$$

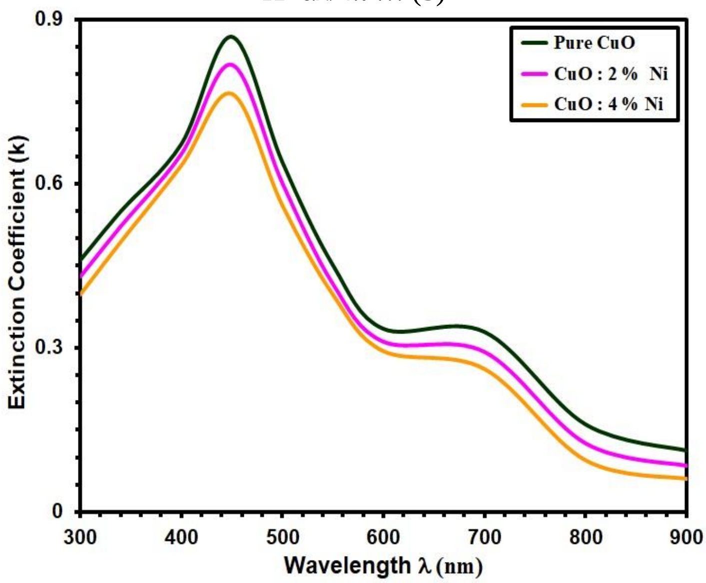

Fig. (5). Variation of extinction coefficient of (CuO andCuO:-Ni) with wavelength

The refractive index is calculated using the following formulas (6) [34, 35]:

$$n = \left(\frac{1+R}{1-R}\right) + \sqrt{\frac{4R}{(1-R)^2} - k^2} \qquad (6)$$

The refractive index of (CuO and CuO:Ni) nanoparticles as a function of wavelength is shown in Figure(5). The refractive index increases as the weight ratios of the concentration of CuO, Ni nanoparticles increase but decrease as the wavelength increases. This behavior is explained by the increasing density of nanocomposites. When incident light interacts with a sample with high refractivity in the UV region, the refractive index values increase. This behavior is consistent with research findings [36].

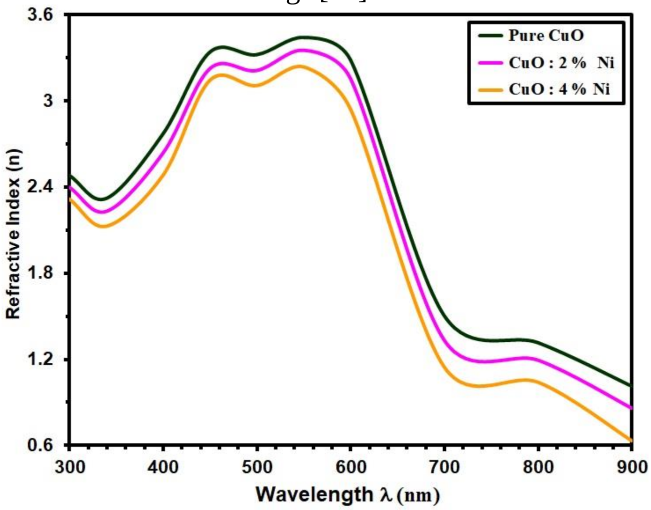

Fig. (6) Variation of refractive index of (CuO and CuO:Ni) with wavelength.

Conclusion

The CuO-doped Ni films were created by modifying doping through the spray pyrolysis technique. XRD patterns indicated that the films exhibited a predominant (200) peak. The size of CuO:4% Ag grains ranged from 16.87-19.75 nm, while the strain (%) parameter increased from 28.14-23.85. The transmittance in the UV-VIS region decreased with an increase in titanium concentration, reaching 78.5% for undoped Ni films. More dopant CuO in the visible region resulted in a higher absorption coefficient. The band gap value of the Ni thin film was 2.28 eV, while doped CuO at 2% and 4% reported 2.23 and 2.17 eV, respectively. As Copper oxide concentration increased, the examined optical constants decreased.

References

[1] Tripathi, A.; Dixit, T.; Agrawal, J.; Singh, V. Bandgap engineering in CuO nanostructures: Dual-band, broadband, and UV-C photodetectors. Appl. Phys. Lett. 2020, 116, 111102.

[2] Editorial Feature of AEO Nano. Copper (Cu) Nanoparticles-Properties, Applications. Available online: https://www.azonano. com/article.aspx?ArticleID=3271 (accessed on 9 May 2021).

[3] Kesarwani, R.; Khare, A. Surface plasmon resonance and nonlinear optical behavior of pulsed laser-deposited semitransparent nanostructured copper thin films. Appl. Phys. B 2018, 124, 116.

[4] M. Kaur, K. Muthe, S. Despande et al., "Growth and branching of CuO nanowires by thermal oxidation of copper," Journal of Crystal Growth, vol. 289, no. 2, pp. 670–675, 2006.

[5] M. F. Al-Kuhaili, "Characterization of copper oxide thin flms deposited by the thermal evaporation of cuprous oxide (Cu2O)," Vacuum, vol. 82, no. 6, pp. 623–629, 2008.

[6] I. Lyubinetsky, S. Tevuthasan, D. E. McCready, and D. R. Baer, "Formation of single-phase oxide nanoclusters: Cu [sub 2]O on SrTiO[sub 3](100)," Journal of Applied Physics, vol. 94, no. 12, 2003.
[7] C. A. N. Fernando and S. K. Wetthasinghe, "Investigation of photoelectrochemical characteristics of n-type Cu2O flms," Solar Energy Materials and Solar Cells, vol. 63, no. 3, pp. 299–308, 2000.
[8] Nasser Saadaldin, M.N.Alsloum, and N.Hussain, preparing of copper oxides thin Films by Chemical Bath Deposition (CBD) for Using in Environmental Application, Volume 74, 1 2015, Pages 1459-1465.
[9] Korošec, R. C., & Bukovec, P. (2006). Sol–gel prepared NiO thin films for electrochromic applications. Acta Chim. Slov, 53(53), 136-147.
[10] Ogwu A.A., Darma T.H. and Bouquerel E., (2007). Electrical resistivity of copper oxide thin films prepared by reactive magnetron sputtering. Journal of Achievements in Materials and Manufacturing Engineering 24:172-177.
[11] Ristov, M., Sinadinovski G. I., and I. Grozdanov, I., (1985). Chemical deposition of Cu_2O thin films, Thin solid films, 123:63-67.
[12] 1attin, L., Reguig, B. A., Khelil, A., Morsli, M., Benchouk, K., & Bernede, J. C. (2008). Properties of NiO thin films deposited by chemical spray pyrolysis using different precursor solutions. Applied Surface Science, 254(18), 5814-5821.
[13] Alver, U., Yaykaşlı, H., Kerli, S., & Tanrıverdi, A. (2013). Synthesis and characterization of boron-doped NiO thin films produced by spray pyrolysis. International Journal of Minerals, Metallurgy, and Materials, 20(11), 1097-1101.
[14] Qader, K.Y., Ghazi, R.A., Jabbar, A.M., Abass, K.H., Chiad, S.S., Reduce of energy gap of CuO nano structure film by Ag doping, Journal of Green Engineering, 10(10), pp. 7387-7398, 2020.
[15] Hussin, H.A., Al-Hasnawy, R.S., Jasim, R.I., Habubi, N.F., Chiad, S.S., Optical and structural properties of nanostructured CuO thin films doped by Mn, Journal of Green Engineering, 10(9), pp. 7018-7028, 2020.
[16 Habubi, N.F., Oboudi, S.F., Chiad, S.S., Study of some optical properties of mixed SnO2-CuO Thin Films, 2012, Journal of Nano- and Electronic Physics 4(4) ,04008 (4).
[17] Sakhil, M.D., Shaban, Z.M., Sharba, K.S., Habub, N.F., Abass, K.H., Chiad, S.S., Alkelaby, A.S., Influence mgo dopant on structural and optical properties of nanostructured cuo thin films, NeuroQuantology, 18 (5), pp. 56-61, 2020.
[18] Aydin, H., Mansour, S. A., Aydin, C., Al-Ghamdi, A. A., Al-Hartomy, O. A., El-Tantawy, F., & Yakuphanoglu, F. (2012). Optical properties of nanostructure boron doped NiO thin films. Journal of sol-gel science and technology, 64(3), 728-733.
[19] Powell, R. J., & Spicer, W. E. (1970). Optical properties of NiO and CoO. Physical Review B, 2(6), 2182.
[20] Salloom, H.T., Jasim, R.I., Habubi, N.F., Chiad, S.S.Jadan, M., Addasi, J.S. Gas sensor using gold doped copper oxide nanostructured thin films as modified cladding fiber, Chinese Physics Bthis link is disabled, 2021, 30(6), 068505.
[21] Khadayeir, A. A., Hassan, E. S., Mubarak, T. H., Chiad, S.S., Habubi, N. F., Dawood, M.O., Al-Baidhany, I. A., The effect of substrate temperature on the physical properties of copper oxide films, Journal of Physics: Conference Series, 2019, 1294 (2) 022009.
[22] Chiad, S.S., Noor, H.A., Abdulmunem, O.M., Habubi, N.F., Optical and structural properties of Ni-doped Co3O4Nanostructure thin films via CSPM, Journal of Physics: Conference Series 1362(1), 2019.
[23] Othman, M.S., Mishjil, K.A., Rashid, H.G., Chiad, S.S., Habubi, N.F., Al-Baidhany, I.A., Comparison of the structure, electronic, and optical behaviors of tin-doped CdO alloys and thin films, Journal of Materials Science: Materials in Electronics 31(11), pp. 9037-9043, 2020.

[24] Jandow, N.N., Othman, M.S., Habubi, N.F., Chiad, S.S., Mishjil, K.A., Al-Baidhany, I.A., Theoretical and experimental investigation of structural and optical properties of lithium doped cadmium oxide thin films, Materials Research Express 6(11), 2020.

[25] Hadi, E.H., Sabur, D.A., Chiad, S.S., Habubi, N.F., Abass, K.H., Physical properties of nanostructured li-doped zro_2 thin films, Journal of Green Engineering, 10(10), pp. 8390-8400, 2020.

[23] Ghazai, A.J., Abdulmunem, O.M., Qader, K.Y., Chiad, S.S., Habubi, N.F., Investigation of some physical properties of Mn doped ZnS nano thin films, 2020, AIP Conference Proceedings 2213 (1) , 020101.

[26] Hassan, E.S., Qader, K.Y., Hadi, E.H., Chiad, S. S., Habubi, N.F., Abass, K.H., Sensitivity of nanostructured mn-doped cobalt oxide films for gas sensor application, Nano Biomedicine and Engineering, 12(3), pp. 205-213, 2020.

[27] Abakaliki, Nigeria, "Optical and Solid State Characterization of Optimized Manganese Sulphide Thin Films and Their Possible Applications in Solar Energy", the Pacific Journal of Science and Technology 7(2006).

[28] Sakhil, M.D., Shaban, Z.M., Sharba, K.S., Habub, N.F., Abass, K.H., Chiad, S.S., Alkelaby, A.S., Influence mgo dopant on structural and optical properties of nanostructured cuo thin films, NeuroQuantology, 18 (5), pp. 56-61, 2020.

[29] Chiad, S.S., Noor, H.A., Abdulmunem, O.M., Habubi, N.F., Jadan, M., Addasi, J.S., Optical and structural performance of nanostructured Te thin films by (CSP) with various thicknesses, Journal of Ovonic Research, 16 (1), pp. 35-40, 2020.

[30] O. G. Abdullah, B. K. Aziz, and S. A. Hussen, “Optical characterization ofpolyvinyl alcohol-ammonium Nitrate polymer electrolytes films,” Chem. Mater. Res., vol. 3, no. 9, pp. 84–90, 2013.

[31] A. Hashim, I. R. Agool, and K. J. Kadhim, “Novel of (polymer blend- Fe3O4) magnetic nanocomposites: preparation and characterization for thermal energy storage and release, gamma ray shielding, antibacterial activity and humidity sensors applications,” J. Mater. Sci. Mater. Electron.,vol. 29, no. 12, pp. 10369–10394, 2018, doi: 10.1007/s10854-018-9095-z.

[32] Salloom, H.T., Hadi, E.H., Habubi, N.F., Chiad, S.S., Jadan, M., Addasi, J.S., Characterization of silver content upon properties of nanostructured nickel oxide thin films, Digest Journal of Nanomaterials and Biostructures 15(4), pp. 1189-1195, 2020.

[33] Chiad, S. S., Alkelaby, A.S., Sharba, K.S., Optical Conduct of Nanostructure Co3O4 rich Highly Doping Co_3O_4: Zn alloys, Journal of Global Pharma Technology, 11(7), pp. 662-665, 2020

[34] Ahmed, N.Y., Bader, B. A., Slewa, M. Y., Habubi, N.F., Chiad, S. S., Effect of boron on structural, optical characterization of nanostructured fe2o3 thin films, NeuroQuantology, 18(6), pp. 55-60, 2020.4

[35] Khadayeir, A. A., Jasim, R. I., Jumaah, S. H., Habubi, N.F., Chiad, S. S., Influence of Substrate Temperature on Physical Properties of Nanostructured ZnS Thin Films, Journal of Physics: Conference Series1664 (1), 2020.

[36] Armelao Lidia, Davide Barreca, Manuel Bertapelle, Gregorio Bottaro and Cinzia Sada and Eugenio Tondello, Sol-gel synthesis and characterization of CuO-based nanosystems, Materials Research Society Symposium Proceedings. (Materials Research Society) 737: 27 (2003).